Gamma decay of analog resonances

Yu. V. Naumov and O. E. Kraft

A. A. Zhdanov Leningrad State University
Fiz. Elem. Chastits. At. Yadra **6**, 892–970 (October–December 1975)

The problems which arise in study of the γ decay of analog resonances are reviewed. The experimental data are compared for analog β and γ transitions and analog-antianalog transitions. Data on the population of states of the core-polarization type are collected and analyzed. The problems relating to the γ decay of fine-structure components of analogs are described. The $E1$ decay of analogs is discussed.

PACS numbers: 23.20.−g

INTRODUCTION

Study of the γ decay of analog resonances has proved to be an informative and fruitful field of nuclear research. Apart from purely spectroscopic information about low-lying states of nuclei such as their energies and quantum numbers, the mixing of the multipolarities of transitions, and the values of branching ratios, information can be extracted about effects due to the nature of analog states. An analog state differs by unity in isospin from neighboring states. Its wave function is fairly well known despite the large excitation energy of about 6–20 MeV in medium and in heavy nuclei. Data on the γ decay of analogs are widely used as a test for the wave functions of low-lying states. Analysis shows that the information obtained about nuclear structure from the γ decay of analogs is qualitatively similar to the information obtained from β decay. However, the range of excitation energies achieved in γ decay (3–6 MeV) is appreciably greater than in β decay. Study of analog–antianalog transitions in different regions of nuclei enable one to obtain new data about the properties of one-particle states. Charge-exchange nuclear excitations of collective type can also be investigated by γ decay of analogs. In many nuclei, states that can be interpreted as core-polarization states are strongly populated. A search for direct and indirect proofs that a giant Gamow–Teller resonance exists is one of the most interesting problems.

A new field is the study of the γ decay of the components of the fine structure of analogs. Correlation analysis is used to obtain interesting data about the structure of the $T_<$ component of an analog.

The γ decay of analogs has attracted attention only recently. One of the first reviews of this question is Hanna's,[1] and a brief review of the main problem can be found in Refs. 2 and 3.

1. BASIC IDEAS ABOUT THE γ DECAY OF ANALOG STATES

The wave function of an analog state can be written in the form

$$\Psi^{as}_{T_0+1,\,T_0}=\frac{1}{\sqrt{2(T_0+1)}}\,T_-\Psi^{ps}_{T_0+1,\,T_0+1}. \tag{1}$$

Here, $\Psi^{ps}_{T_0+1,\,T_0+1}$ is the wave function of the parent state with isospin T_0+1 and isospin projection T_0+1. The operator T_- carries a neutron into a proton without changing the state in which the particle is:

$$T_-=\sum_i a_p^+(i)\,a_n(i). \tag{2}$$

By virtue of the Pauli principle, the summation is restricted to states populated by excess neutrons.

An analog state has a definite isospin T_0+1, equal to the isospin of the parent state, and is in a nucleus with isospin projection T_0. In this nucleus, the low-lying states usually have isospin equal to the projection, i.e., T_0. As a rule, an analog state is at high excitation energies (from a few MeV to 20 MeV in medium and heavy nuclei). At these excitation energies, the density of states with ordinary isospin is much greater than the density of analog states. An analog state is sharply distinguished by many of its properties. The experimental and theoretical data indicate that the mixing of states with different isospins is small, and the individual character of analog states is clearly manifested in many experiments.

In the γ decay of an analog state, $\Delta T=1$, so that only the isovector part of the operator of the γ transition contributes to the transition. The information which can then be extracted is in principle different from that obtained from transitions between low-lying states with $\Delta T=0$ (which are particularly sensitive to the isoscalar part). The hope is that the γ decay of a isobaric analog resonance could yield information about the parts of the wave functions that are sensitive to the isovector part of the operator of the electromagnetic transition.

The electromagnetic transition operator $\mathfrak{M}(\lambda,\mu)$ is the operator of the interaction between the currents in the nucleus and the radiation field:

$$\mathfrak{M}(\lambda,\,\mu)=\frac{1}{c}\int \mathbf{j}(r)\,A^*_{\lambda\mu}(kr)\,dr. \tag{3}$$

An isospin dependence is contained in the factor $\mathbf{j}(r)$. The expression for the current includes terms of the so-called convection current for protons, and spin currents (or magnetization currents) for protons and neutrons:

$$\begin{aligned}\mathbf{j}(r)=&\sum_p e_p\left[\frac{\mathbf{p}_M}{2M_p}\delta(\mathbf{r}-\mathbf{r}_p)+\delta(\mathbf{r}-\mathbf{r}_p)\frac{\mathbf{p}_M}{2M_p}\right]\\&+c\sum_p\mu_p\left(\frac{e\hbar}{2M_pc}\right)\nabla\times\sigma_p\delta(\mathbf{r}-\mathbf{r}_p)\\&+c\sum_n\mu_n\left(\frac{e\hbar}{2M_pc}\right)\nabla\times\sigma_n\delta(\mathbf{r}-\mathbf{r}_n),\end{aligned} \tag{4}$$

where μ_p and μ_n are the magnetic moments of the proton

TABLE 1. Data on double analogs.

Nucleus	T_z, T	Excitation energy, MeV	Literature
$^{12}_{6}C_6$	0, 2	27.50 ±0.10	[4]
$^{16}_{8}O_8$	0, 2	22.717±0.008	[5]
	0, 2	(24.70 ±0.10)	[4]
$^{20}_{10}Ne_{10}$	0, 2	16.732±0.0024	[1, 4, 6]
	0, 2	(18.430±0.0050)	[4]
$^{24}_{12}Mg_{12}$	0, 2	15.434±0.003	[7]
$^{28}_{14}Si_{14}$	0, 2	15.223±0.003	[8—10]
$^{32}_{16}S_{16}$	0, 2	12.050±0.004	[11, 12]
$^{36}_{18}Ar_{18}$	0, 2	10.858±0.035	[4]
$^{38}_{18}Ar_{20}$	1, 3	18.784±0.030	[4]
$^{40}_{20}Ca_{20}$	0, 2	11.978±0.025	[8, 13]
$^{44}_{22}Ti_{22}$	0, 2	9.338 ±0.002	[14]
$^{52}_{26}Fe_{26}$	0, 2	8.54 ±0.10	[4]
$^{56}_{28}Ni_{28}$	0, 2	9.90±0.10	[4]
$^{210}_{84}Po_{126}$	21, 23	37.36	[15]

and neutron. Using the isospin operators, we can rewrite this expression in the form

$$\mathbf{j}(r) = \frac{e}{2}\sum_i (1-\tau_3^{(i)})\left[\frac{\mathbf{p}_i}{2M_p}\delta(\mathbf{r}-\mathbf{r}_i)+\delta(\mathbf{r}-\mathbf{r}_i)\frac{\mathbf{p}_i}{2M_p}\right] + \frac{c}{2}\left(\frac{e\hbar}{2M_pc}\right)\sum_i [\mu_+ + \mu'_-\tau_3^{(i)}]\nabla\times\sigma_i\delta(\mathbf{r}-\mathbf{r}_i); \quad (5)$$

here $\mu_+ = \mu_n + \mu_p$ and $\mu'_- = \mu_n - \mu_p = -\mu_-$.

We obtain for the current the isoscalar part

$$\mathbf{j}^{(0)}(r) = \frac{e}{2}\sum_i\left[\frac{\mathbf{p}_i}{2M_p}\delta(\mathbf{r}-\mathbf{r}_i)+\delta(\mathbf{r}-\mathbf{r}_i)\frac{\mathbf{p}_i}{2M_p}\right] + \frac{c}{2}\left(\frac{e\hbar}{2M_pc}\right)\sum_i \mu_+\nabla\times\sigma_i\delta(\mathbf{r}-\mathbf{r}_i), \quad (6)$$

and also the isovector part

$$\mathbf{j}^{(1)}(r) = -\frac{e}{2}\sum_i \tau_3^{(i)}[\nabla\delta(\mathbf{r}-\mathbf{r}_i)]_{\text{sym}} + \frac{c\mu'}{2}\left(\frac{e\hbar}{2M_pc}\right)\sum_i \tau_3^{(i)}\nabla\times\sigma_i\delta(\mathbf{r}-\mathbf{r}_i). \quad (7)$$

Accordingly, one can separate the isoscalar and isovector parts in the transition operator:

$$\mathfrak{M}(\lambda,\mu) = \mathfrak{M}_0(\lambda,\mu) + \mathfrak{M}_1(\lambda,\mu)\,t_z. \quad (8)$$

We give the expressions for the isovector part of the operator for $M1$, $E2$, and $E1$ transitions:

$$\mathfrak{M}_1(M1) = \sqrt{\frac{3}{4\pi}}\frac{e\hbar}{2M_pc}(4.70\sigma_\mu + l_\mu); \quad (9)$$

$$\mathfrak{M}_1(E2) = (e_p - e_n)\,r^2Y^2_\mu(r); \quad (10)$$

$$\mathfrak{M}_1(E1) = (e_p - e_n)\,rY^1_\mu(r). \quad (11)$$

The separation of the electromagnetic transition operator into isovector and isoscalar parts determines the main isospin selection rule for γ transitions: γ transitions of any multiplet must satisfy the condition $\Delta T = 0, \pm 1$.

Important information about the fulfilment of this rule can be deduced from γ transitions between states with $\Delta T = 2$, i.e., study of the γ decay of double analog states. At the present time, states have been discovered in nuclei for which the isospin is two units greater than the isospin projection: $T = |T_z| + 2$. These states in nuclei with isospin projection T_z are double analogs of states of nuclei with isospin projection $|T_z| + 2$.

Double analog states are at high excitation energies and appear as resonances in reactions of various kinds. Table 1 gives the nuclei with established double analog states and their excitation energies. As a rule, the states found are double analogs of the ground states of the nuclei. However, one can sometimes also observe double analogs of some excited states. The energies of these states are enclosed in brackets in Table 1.

Apart from the nuclei given in Table 1, double analogs are apparently observed in the nuclei ^{48}Cr and ^{60}Zn (Ref. 4) and ^{59}Ni and ^{90}Nb (Ref. 16), and also as resonances in the ^{59}Cu compound nucleus in the reaction ^{58}Ni$(p,n)^{58}$Cu (Ref. 17).

Gamma emission accompanying the excitation of double analogs has been studied for nuclei with $A = 4n$: ^{20}Ne (Refs. 1, 18, 19); ^{24}Mg (Refs. 1, 7), ^{28}Si (Refs. 9, 10), ^{32}S (Refs. 12, 20, 21), and ^{44}Ti (Ref. 14). It was established that these states decay by a two-step γ cascade through levels with $T = 1$ to levels with $T = 0$. Direct transitions from $T = 2$ to levels with $T = 0$ were not found. For the intensities of $E2$ transitions with $\Delta T = 2$ upper limits have been given for ^{24}Mg (Ref. 7), ^{28}Si (Ref. 9), ^{32}S (Ref. 12), and ^{44}Ti (Ref. 14). These limits for the values of $B(E2)$ lie in the range 0.06–0.004 Weisskopf units, which is about 10–100 times less than the mean strength of isospin-allowed $E2$ transitions for nuclei in the range $20 \le A \le 40$ (Ref. 22).

Data on the probabilities of γ transitions with $\Delta T = 2$ can be used to analyze the isospin purity of double analog states. The same information can be obtained by analyzing the decay of double analog states with emission of heavy particles: α particles, deuterons, and protons. Such decays are isospin-forbidden, but are observed with high probability. The isospin-forbidden (α,γ) reactions serve to excite double analog states. Gamma transitions to states with $T = 1$ are isospin-allowed, so that for the analysis one can use isospin-forbidden and isospin-allowed processes. Note that the admixtures of states with $T = 0$ to a double analog state in nuclei with $T_z = 0$ do not contribute to the γ transitions from double analogs to analogs, since for transitions with $\Delta T = 0$

$$\langle J'M'T'T_z|\mathfrak{M}_1|JMTT_z\rangle = \frac{T_z}{[T(T+1)(2T+1)]^{1/2}}\langle J'M'||\mathfrak{M}_1||JM\rangle.$$

Here, we have written out the isospin-reduced matrix element and used the explicit form of the Clebsch–Gordan coefficients.

One can also give a further relation which shows that the probabilities of transitions for the γ decay of double analogs and the corresponding analogs differ only by a numerical factor:

$$\langle J'M'T'T_z|\mathfrak{M}_1|JMTT_z\rangle = (-)^{T'-T}\left[\frac{T_>^2 - T_z^2}{T_>(2T_>-1)(2T_>+1)}\right]^{1/2}\langle J'M'||\mathfrak{M}_1||JM\rangle. \quad (12)$$

Here, $T_>$ is the larger of T and T'.

In Table 2, we give data on the γ decay of double analogs in the ^{24}Mg, ^{28}Si, and ^{32}S nuclei and of the analogs

TABLE 2. Decay of $T=2$ levels in nuclei with $T_z=0$ and $T_z=1$.

$T_z=0$				$T_z=1$			
Nucleus	E_i-E_f, MeV	$J_i^\pi, T_i - J_f^\pi, T_f$	Decay %	Nucleus	E_i-E_f, MeV	$J_i^\pi, T_i - J_f^\pi, T_f$	Decay %
$^{24}_{12}Mg_{12}$	15.43—9.97	$0^+, 2 - 1^+, 1$	83 } [7]	$^{24}_{11}Na_{13}$	5.97—0.47	$0^+, 2 - 1^+, 1$	76 } [23]
	15.43—10.71	$0^+, 2 - 1^+, 1$	17 }		5.97—1.35	$0^+, 2 - 1^+, 1$	14 }
					5.97—3.59	$0^+, 2 - (1^+), 1$	10 }
$^{28}_{14}Si_{14}$	15.22—10.60	$0^+, 2 - 1^+, 1$	8 } [10]	$^{28}_{13}Al_{15}$	5.99—1.37	$0^+, 2 - 1^+, 1$	14 } [23]
	15.22—10.72	$0^+, 2 - 1^+, 1$	9 }		—	—	— }
	15.22—10.90	$0^+, 2 - 1^+, 1$	43 }		5.99—1.62	$0^+, 2 - 1^+, 1$	34 }
	15.22—11.44	$0^+, 2 - 1^+, 1$	40 }		5.99—2.20	$0^+, 2 - 1^+, 1$	43 }
					5.99—3.10	$0^+, 2 - 1^+, 1$	<6 }
					5.99—3.54	$0^+, 2 - (1^+), 1$	9 }
$^{32}_{16}S_{16}$	12.05—7.00	$0^+, 2 - 1^+, 1$	6 } [12]	$^{32}_{15}P_{17}$	5.07—0	$0^+, 2 - 1^+, 1$	7,8 } [11]
	12.05—8.13	$0^+, 2 - 1^+, 1$	83 }		5.07—1.15	$0^+, 2 - 1^+, 1$	85,6 }
	12.05—9.21	$0^+, 2 - 1^+, 1$	11 }		5.07—2.23	$0^+, 2 - (1^+), 1$	6,6 }

corresponding to them in the ^{24}Na, ^{28}Al, and ^{32}P nuclei. Note the great similarity between the γ decay of levels with $T=2$ in nuclei with $T_z=0$ and $T_z=1$.

Gamma decay of double analogs is characterized by strong transitions to $T=1$ states. The γ decay schemes now known for double analog states are given in Fig. 1. It can be seen that these states decay in all cases by a two-step γ decay through levels with $T=1$ to levels with $T=0$. Without exception, all γ transitions from double analogs are strong $M1$ transitions of the type 0^+, $2-1^+$, 1.

In the ^{44}Ti nucleus there are two levels with $T=1$ next to each other: 6.60 MeV, 2^+ and 7.22 MeV, 1^+. The double analog decays only to a level with $J^\pi=1^+$ ($M1$ transition), and an $E2$ transition to a level with $J^\pi=2^+$ is not observed. The experimental strengths of the $M1$ transitions from double analogs are given in Table 3 together with the theoretical values of $B(M1)$.

The theoretical values of $B(M1)$ were obtained in a many-particle shell model with effective interaction. In all cases, the calculations give a good explanation of the relative intensities of the transitions from $T=2$ levels to $T=1$ levels and of the absolute intensities of transitions from $T=1$ to $T=0$ levels. The situation is more complicated for $B(M1)$ for the transitions $T=2\to T=1$. In Refs. 7, 10, and 14 it is noted that the theoretical value is approximately an order of magnitude higher than the experimental for the nuclei ^{24}Mg, ^{28}Si, and ^{44}Ti. At the same time, the calculations of Ref. 6 give values that agree with the experimental ones.

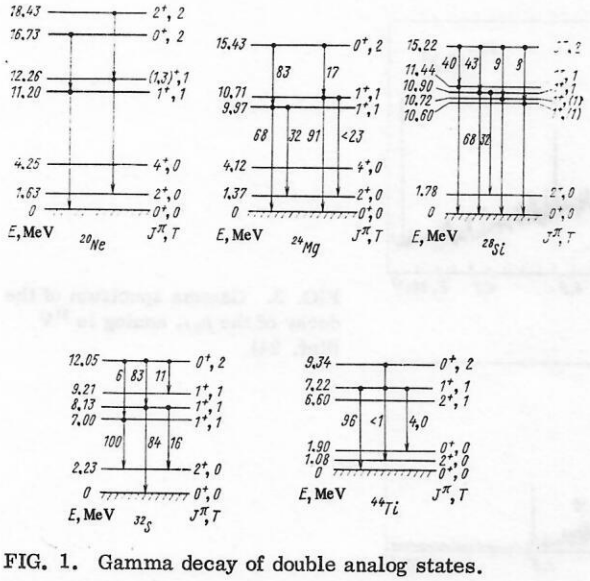

FIG. 1. Gamma decay of double analog states.

2. GAMMA DECAY OF ANALOG RESONANCES AND THE STRUCTURE OF LOW-LYING STATES

The transition operator in the γ decay of analog resonances is the isovector part of the electromagnetic transition operator. One can therefore expect the study

TABLE 3. Experimental and theoretical values of $B(M1)$ for the γ transitions $T=2\to T=1$.

Nucleus	Transition		$B(M1)$, W. units	
	E_i-E_f, MeV	$J_i^\pi, T_i - J_f^\pi, T_f$	Experiment	Theory
$^{20}_{10}Ne_{10}$	16.73—11.20	$0^+,2 - 1^+, 1$	1.40±0.25 [6]	1.33 [6]
$^{24}_{12}Mg_{12}$	15.43—9.97	$0^+,2 - 1^+, 1$	0.8±0.3	0.99
	15.43—10.71	$0^+,2 - 1^+, 1$	0.27±0.09 [7]	1.34 [7]
$^{28}_{14}Si_{14}$	15.22—11.44	$0^+, 2-1^+, 1$	0.54	3.94
	15.22—10.90	$0^+, 2-1^+, 1$	0.39	5.62
	15.22—10.72	$0^+, 2-1^+, 1$	0.07 }	1.85
	15.22—10.60	$0^+, 2-1^+, 1$	0.06 } [10]	[10]
$^{32}_{16}S_{16}$	12.05—7.00	$0^+, 2-1^+, 1$	0.053±0.011*	0.038
	12.05—8.13	$0^+, 2-1^+, 1$	1.57±0.31	0.89
	12.05—9.21	$0^+, 2-1^+, 1$	0.55±0.11 [12]	0.33 [6]
$^{44}_{22}Ti_{22}$	9.34—7.22	$0^+, 2-1^+, 1$	0.6 [14]	4.2 [14]

*Under the assumption $\Gamma_p=\Gamma$.

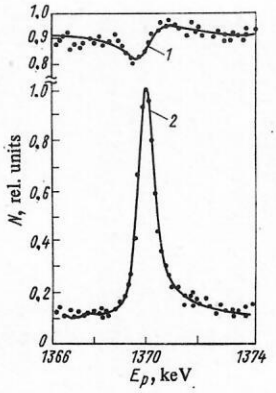

FIG. 2. Excitation function near the $p_{3/2}$ analog in ^{51}V (Ref. 24): 1) pp_0 reaction; 2) $p\gamma$ reaction.

of γ decay of analogs to give information of a qualitatively new type that is not similar to the information obtained by studying γ transitions with $\Delta T = 0$ between low-lying states of nuclei.

Data on the γ decay of analogs can be used as a test of wave functions of low-lying states. It is important that in calculations of the probabilities of transitions from an analog it is unnecessary to write out the analog's wave function explicitly. It is sufficient to know the wave function $\Psi^{ps}_{T_0+1, T_0+1}$ of the parent state and the function $\Psi^{f}_{T_0, T_0}$ of the final state.

The reduced matrix element for a γ transition from the analog state $\Psi^{as}_{T_0+1, T_0}$ to the final state $\Psi^{f}_{T_0, T_0}$ can be expressed as follows:

$$\left.\begin{aligned} &\left\langle \Psi^{f}_{T_0, T_0} \left\| \sum_i \mathfrak{M}_1(i)\, t_z(i) \right\| \Psi^{as}_{T_0+1, T_0} \right\rangle \\ &= \frac{1}{\sqrt{2(T_0+1)}} \left\langle \Psi^{f}_{T_0, T_0} \left\| \sum_i \mathfrak{M}_1(i)\, [T_-, t_z(i)] \right\| \Psi^{ps}_{T_0+1, T_0+1} \right\rangle \\ &= \frac{1}{\sqrt{2(T_0+1)}} \left\langle \Psi^{f}_{T_0, T_0} \left\| \sum_i \mathfrak{M}_1(i)\, t_-(i) \right\| \Psi^{ps}_{T_0+1, T_0+1} \right\rangle . \end{aligned}\right\} \quad (13)$$

The probability of the γ transition is determined by the parent, $\Psi^{ps}_{T_0+1, T_0+1}$, and final, $\Psi^{f}_{T_0, T_0}$, wave functions. The γ decay of the analog state can be regarded as a charge-exchange process.

In the majority of cases, one studies analogs of low-lying states whose wave functions are fairly well known. One can then compare experiment and the results of calculations with model functions $\Psi^{f}_{T_0, T_0}$. On the other hand, if Ψ^{f} is known well, data on the γ decay can give information about the function $\Psi^{ps}_{T_0+1, T_0+1}$. Note that in these calculations the assumption of purity of the analog state is important: An analog is a pure $T_> = T_0 + 1$ state and the mixing with $T_< = T_0$ states can be ignored.

In recent years, many experimental data have been published about the γ decay of analogs. However, few theoretical calculations have been made. One of the nuclei studied in most detail is ^{51}V, for which the γ decay of the $p_{3/2}$ analog state was studied.[24-26] The experimental values of the transition probabilities were used in Ref. 27 to study the structure of low-lying states.

The excitation function in pp_0 and $p\gamma$ reactions and the γ spectrum of the decay of the $p_{3/2}$ analog to the ground state of ^{51}Ti are shown in Figs. 2 and 3 (Ref. 24). The ground state of ^{51}Ti is assumed to consist of two protons and a neutron above the ^{48}Ca core. The protons in the $f_{7/2}$ state are coupled to angular momentum $J_p = 0$, and the neutron is at the level $p_{3/2}$. However, one cannot exclude a configuration in which the protons are coupled to angular momentum $J_p = 2$. In this case, the wave function of the ^{51}Ti ground state has the form

$$\Psi(^{51}\mathrm{Ti}_{gs}\ J^\pi = 3/2^-) = \sum_{J_p} a_{gs}(J)\, [(f^p_{7/2})^2_{J_p}\, p^n_{3/2}]_{J=3/2}\, {}^{48}\mathrm{Ca}). \quad (14)$$

For the low-lying states of ^{51}V the following configuration is assumed: three protons in the $f_{7/2}$ shell outside the ^{48}Ca core. The next step is to take into account the $p_{3/2}$ shell, i.e., two protons in the $f_{7/2}$ shell and one in the $p_{3/2}$ shell: $[(f^p_{7/2})^2 p^p_{3/2}]_J$. The energies of the low-lying states can be fairly well described by the simplest configuration $(f_{7/2})^3$, although it is then not possible to reproduce all the experimental levels. Inclusion of the

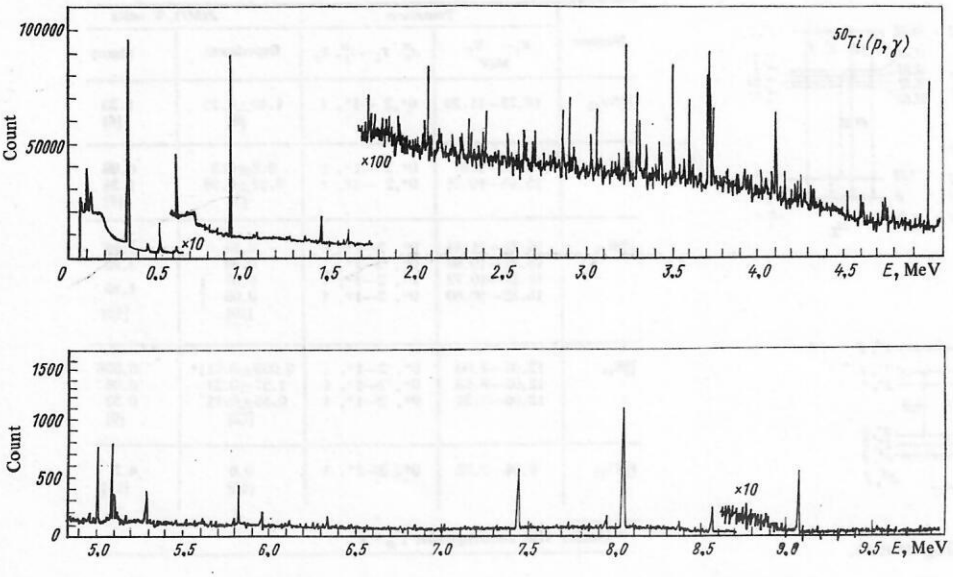

FIG. 3. Gamma spectrum of the decay of the $p_{3/2}$ analog in ^{51}V (Ref. 24).

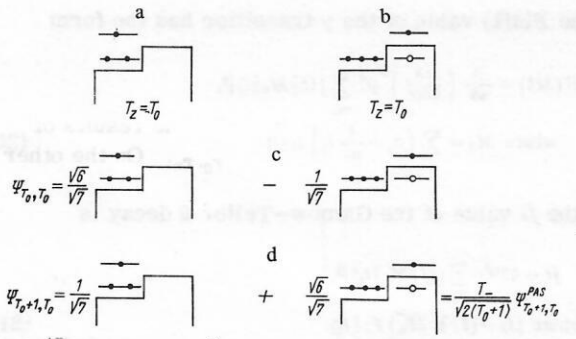

FIG. 4. Scheme of ^{51}V states with definite isospin $T=T_0$ (c) and $T=T_0+1$ (d) from the configurations a and b (Ref. 27): c – $\langle T_0+1/2,\ T_0+1/2,\ 1/2,\ -1/2 \mid T_0,\ T_0\rangle \mid T_0+1/2,\ T_0+1/2\rangle \mid 1/2,\ -1/2\rangle + \langle T_0+1/2,\ T_0-1/2,\ 1/2,\ 1/2 \mid T_0,\ T_0\rangle \mid T_0+1/2,\ T_0-1/2\rangle \mid 1/2,\ 1/2\rangle$; d – $\langle T_0+1/2,\ T_0+1/2,\ 1/2,\ -1/2 \mid T_0+1,\ T_0\rangle \mid T_0+1/2,\ T_0+1/2\rangle \mid 1/2,\ -1/2\rangle + \langle T_0+1/2,\ T_0-1/2,\ 1/2,\ 1/2 \mid T_0+1,\ T_0\rangle \mid T_0+1/2,\ T_0-1/2\rangle \mid 1/2,\ 1/2\rangle$.

$p_{3/2}$ configuration significantly improves the agreement between the calculated and experimental energy levels.

A serious shortcoming of this description is that the $(f_{7/2})^2 p_{3/2}$ configuration does not have a definite isospin. To obtain a state with definite isospin, it is necessary to form linear combinations of the two configurations shown in Fig. 4. For this, one can use the method of projection operators[28] or the method of Clebsch–Gordan coefficients.[29]

If one considers the probabilities of transitions between low-lying states with $\Delta T=0$, they are not greatly changed by the use of functions with definite isospin. This conclusion can be drawn on the basis of the fact that the correction from the (p, n^{-1}) configurations is small. However, in the calculation of the probabilities of transitions from an analog state the result is very sensitive to the functions used for the low-lying states. The reduced probabilities of transitions from an analog resonance to low levels of ^{51}V may change by an order of magnitude, and in some cases by more, when the calculations are made with functions with definite isospin rather than by the ordinary method.

In the simple model for the configurations of the low-lying states $^{51}\mathrm{V}(f^p_{7/2})^3$ the wave functions Ψ^f of the final state have definite isospin. If the $p_{3/2}$ shell is also taken into account, then in (13) one must use functions Ψ^f with definite isospin:

$$\Psi_{T_0,\ T_0}=N_{T_0}P_{T_0}\Psi_{T_z=T_0}, \tag{15}$$

where N_{T_0} is a normalizing factor; P_{T_0} is the projection operator which separates the components with definite isospin; $\Psi_{T_z=T_0}$ is a function with the two isospin values $T=T_0$ and $T=T_0+1$.

The operator P_{T_0} has the form

$$P_{T_0}=1-\frac{1}{2(T_0+1)}T_-T_+\equiv 1+\mathcal{P}. \tag{16}$$

Then for the matrix element (13) we obtain

$$\langle P_{T_0}\Psi_{T_z=T_0}\|\sum_i m^\lambda(x_i)\,t_-(i)\|\Psi^{ps}_{T_0+1,\ T_0+1}\rangle = \langle\Psi_{T_z=T_0}\|\sum_i m^\lambda(x_i)\,t_-(i)\|\Psi^{ps}_{T_0+1,\ T_0+1}\rangle + \Psi_{T_z=T_0}\|\sum_i m^\lambda(x_i)\,[\mathcal{P},\ t_-(i)]\|\Psi^{ps}_{T_0+1,\ T_0+1}. \tag{17}$$

Calculating the commutator in the second term, we find

$$\langle P_{T_0}\Psi_{T_z=T_0}\|\sum_i m^\lambda(x_i)\,t_-(i)\| \times\Psi^{ps}_{T_0+1,\ T_0+1}\rangle = \frac{T_0}{T_0+1}\langle\Psi_{T_z=T_0} \times\|\sum_i m^\lambda(x_i)\,t_-(i)\|\Psi^{ps}_{T_0+1,\ T_0+1}\rangle - \frac{1}{\sqrt{2(T_0+1)}}\langle\Psi_{T_z=T_0} \times\|\sum_i m^\lambda(x_i)\,2t_z(i)\|\Psi^{ps}_{T_0+1,\ T_0+1}\rangle. \tag{18}$$

We now turn to actual calculations of the probabilities of γ transitions from the analog state in ^{51}V (Ref. 27). In Table 4, we give the transition probabilities calculated in different approximations.

Note first that the simplest $(f_{7/2})^3$ approximation gives only one γ transition to the ground state (first column). To see this, note, first, that in this model only $2p_{3/2}-1f_{7/2}$ transitions are possible. This excludes all $M1$ transitions. Second, in order to obtain nonzero E_2 transitions to $(f^3_{7/2})_{J_f}$ configurations, these last must include the structure $[(f^3_{7/2})_{J_p}f_{7/2}]_{J_f}$, where J_p is the angular momentum of the pair of protons in the ^{51}Ti state. For the approximation I, $J_p=0$ and all $E2$ transitions to states with spin $J_f\neq 7/2$ are excluded. Inclusion of the $(f_{7/2})^2_2 p_{3/2}$ configuration in the ^{51}Ti state enables one to obtain $E2$ transitions to the ^{51}V states with spins 5/2 and 3/2 (second column). In the third column, we give the results for the approximation in which allowance is made for the $p_{3/2}$ configuration for ^{51}V. A serious shortcoming of these calculations is the use of functions with indefinite isospin. In the fourth column, this shortcoming is rectified. It can be seen that to calculate the probabilities of transitions from the analog state it is essential to use functions with definite

TABLE 4. Probabilities of transitions in different approximations. I–III denote differing approximations for the initial, $|i\rangle$ $(\Psi^{ps}_{T_0}+1,\ T_0+1)$ and final $|f\rangle$ states; I) the configuration $(f_{7/2})$ for ^{51}V and $(f_{7/2})^2_0 p_{3/2}$ for ^{51}Ti. The approximation II entails allowance for the $p_{3/2}$ configuration for ^{51}V using functions with definite isospin; II′) without construction of functions with definite isospin. For ^{51}Ti the approximation II entails allowance for the configuration $(f_{7/2})^2_2 p_{3/2}$; III) further complexification of the ^{51}Ti configuration.

Level of ^{51}V	$B(E2,\ i\to f)\,e^2,\ \mathrm{F}^4$ / $B(M1,\ i\to f)$, $10^{-2}\ \mu_0^2$				
$\lvert i\rangle$	I	II	II	II	III
$\lvert f\rangle$	I	I	II′	II	II
7/2⁻, ground state	1.23	0.76	0.76	0.76	0.73
5/2⁻ (1)	0 0	0.13 0	1.93 0.093	0.19 0.52	0.20 4.8
3/2⁻ (1)	0 0	0.018 0	0.39 0.53	0.029 0.0052	0.03 0.86
3/2⁻ (2)	—	—	0.91 22	0.34 57	0.38 67
5/2⁻ (2)	—	—	10.4 0.36	0.17 5.3	0.29 9.8
3/2⁻ (3)	—	—	10.0 56	0.44 86	0.39 75

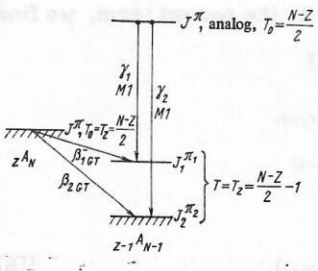

FIG. 5. Connection between β and γ transitions.

isospin. In the last column of Table 4, we give calculations with an even more complicated ^{51}Ti state (approximation III). To the ^{51}Ti wave function we have added 29% of the $f^2_{7/2}(J_p=2)p_{1/2}(n)$ configuration and 0.9% of the $f^2_{7/2}(J_p=2)f_{5/2}(n)$ configuration.

This admixture reproduces the ft values for β transitions from the ^{51}Ti ground state to the $5/2^-$ and $3/2^-$ levels of ^{51}V. This admixture will also strongly influence the $M1$ transitions from the analog state since it introduces transitions between members of the spin-orbit doublets $2p_{1/2}$-$2p_{3/2}$ and $1f_{5/2}$-$1f_{7/2}$.

In recent years, experimental data on the γ decay of analogs in nuclei of the sd shell have been widely used as one further test of nuclear models. For nuclei with $A=19-24$, calculations have been made of the probabilities of γ transitions from analogs to low-lying states in the many-particle shell model with different effective residual interactions.[6,7,23,30-33] Nilsson's model was used to calculate the probabilities of transitions from analogs for nuclei with $A=21-31$ (Refs. 34–37). For nuclei of the region $A\approx 30$, extensive calculations, including the decay of analog states, were made in the framework of the many-particle shell model with surface δ forces.[38,39]

3. GAMMA DECAY OF ANALOG STATES AND β DECAY

There is a fundamental relation between the probability of a γ decay from an analog state to any level and the ft value for the β transition from the parent state to the same level. This relation is based on the similarity of the isovector part of the operator of a γ transition of definite multipolarity and the operator of the β transition of corresponding type. It has frequently been used to analyze transitions in light nuclei, and has recently been used to study medium and heavy nuclei.

Most frequently, one uses the connection between the reduced probability of an $M1$ γ transition from the analog state and the ft value of the corresponding Gamow–Teller β transition. The β-transition operator is

$$Y_-=\sum_i \sigma_i\tau_-(i). \tag{19}$$

Comparing this expression with Eq. (9) for the operator of the $M1$ transition, we note that they have a similar structure. If the contribution of the l part to the operator of the $M1$ transition from the analog state is ignored, we can obtain a connection between the probabilities of β and γ transitions.

The $B(M1)$ value of the γ transition has the form

$$B(M1)=\frac{3}{4\pi}\left(\frac{e\hbar}{2Mc}\right)^2\mu_-^2\sum_{m_f}|\langle f|M_0|i\rangle|^2,$$
$$\text{where } M_0=\sum_i\left(\sigma_i+\frac{1}{\mu_-}l_i\right)t_z(i). \tag{20}$$

and the ft value of the Gamow–Teller β decay is

$$ft=4390/\sum_{m_f}|\langle f|Y_-|i_0\rangle|^2,$$
$$\text{where } |i\rangle=(1/\sqrt{2T_0})\,T_-|i_0\rangle. \tag{21}$$

Using a relation analogous to

$$\langle f|\sum_i\sigma_i\tau_-(i)|i_0\rangle=-\langle f|\,[\sum_i\sigma_i{}^1\!/_2\tau_z(i)\,T_-]\,|i_0\rangle$$
$$=-f|\sum_i\sigma_i{}^1\!/_2\tau_z(i)\,T_-|i_0\rangle$$
$$=-\sqrt{2T_0}\langle f|\sum_i\sigma_i t_z(i)|i\rangle,$$

we obtain the following relation between the ft value and the spin part of the operator of the $M1$ transition:

$$ft=11\,530/[T_0B(M1,\sigma)]. \tag{22}$$

Here, T_0 is the isospin of the analog and $B(M1,\sigma)$ is expressed in units of

$$\mu_0^2=[e\hbar/(2Mc)]^2.$$

Gamma transitions from an analog with isospin T_0 to low-lying states of a nucleus with isospin T_0-1 and the corresponding β transitions, which are called analog β transitions, are shown in Fig. 5.

The intensities of the β and γ transitions can be compared in different ways. In what follows, we shall compare the value of $B(M1,\sigma)$ obtained from the experimental ft value of the β transition in accordance with (22) with the experimental $B(M1)$ value for the corresponding γ transition from the analog.

Since the value of $B(M1,\sigma)$ characterizes the contribution to the γ transition of only the spin part of the operator, comparison of $B(M1,\sigma)$ and $B(M1)$ enables one to draw a conclusion about the applicability of the relation (22), which is based on neglect of the orbital part of the γ-transition operator.

In the literature, one frequently uses an association of other quantities to compare the probabilities of β and γ transitions of this type. The probability of the $M1$ γ transition is characterized by $\Lambda(M1)$:

$$\Lambda(M1)=4\pi[2Mc/(e\hbar)]^2B(M1)/3, \tag{23}$$

and the probability of the β transition by $\Lambda(GT)$:

$$\Lambda(GT)=4390/(ft). \tag{24}$$

The relationship between $\Lambda(M1)$ and $\Lambda(GT)$ may be different for different cases of β and γ decays encountered in practice. For the β and γ transitions shown in Fig. 5 it is

$$\Lambda(M1)=11.1\Lambda(GT)/T_0. \tag{25}$$

TABLE 5. Values of the factor $(1+g_l k/\mu_-)$ in Eq. (29) for different transitions.

Transition	Factor	Transition	Factor
$s_{1/2}-s_{1/2}$	1.000	$f_{7/2}-f_{7/2}$	1.636
$p_{3/2}-p_{3/2}$	1.212	$f_{7/2}-f_{5/2}$	0.894
$p_{1/2}-p_{3/2}$	0.894	$f_{5/2}-f_{5/2}$	0.152
$p_{1/2}-p_{1/2}$	0.576	$g_{9/2}-g_{9/2}$	1.848
$d_{5/2}-d_{5/2}$	1.424	$g_{9/2}-g_{7/2}$	0.894
$d_{5/2}-d_{3/2}$	0.894	$g_{7/2}-g_{7/2}$	0.060
$d_{3/2}-d_{3/2}$	0.364		

In the general case one can, using the matrix elements for the β and γ transitions reduced with respect to the isospin and the total angular momentum, write

$$\Lambda(M1)=\frac{\mu^2}{2}\frac{\langle T_f T_{f_z} 10 \mid T_i T_{i_z}\rangle^2_\gamma}{\langle T_f T_{f_z} 1\varkappa \mid T_i T_{i_z}\rangle^2_\beta} \times \frac{(2T_i+1)_\beta}{(2T_i+1)_\gamma}\frac{(2J_i+1)_\beta}{(2J_i+1)_\gamma}\left[1+\frac{1}{2\mu_-}\frac{\langle f\|l\tau\|i\rangle}{\langle f\|\sigma\tau\|i\rangle}\right]^2\Lambda(GT), \quad (26)$$

where $\varkappa=\pm1$ for $\beta^{\mp}$ decays.

In the general case, the expression for $B(M1,\sigma)$ has the form

$$B(M1,\sigma)=\frac{3}{4\pi}\frac{\mu^2}{2}\frac{4390}{ft}\frac{\langle T_f T_{f_z} 10 \mid T_i T_{i_z}\rangle^2_\gamma}{\langle T_f T_{f_z} 1\varkappa \mid T_i T_{i_z}\rangle^2_\beta} \times \frac{(2T_i+1)_\beta}{(2T_i+1)_\gamma}\frac{(2J_i+1)_\beta}{(2J_i+1)_\gamma}. \quad (27)$$

The ratio of $B(M1)$ and $B(M1,\sigma)$, which characterizes the contribution of the l part to the γ transition, can be expressed by

$$\frac{B(M1)}{B(M1,\sigma)}=\left[1+\frac{1}{2\mu_-}\frac{\langle f\|l\tau\|i\rangle}{\langle f\|\sigma\tau\|i\rangle}\right]^2. \quad (28)$$

In deriving (22) and (25)–(27), we have used two assumptions: 1) the possibility of ignoring the l part in the operator of the $M1$ transition; 2) that the analog state is a pure $T_>$ state. The first assumption seems reasonable on the basis of a one-particle estimate of the contribution of the l part to the transition.

One can show that for transitions between the one-particle states $j_>-j_>$, $j_>-j_<$, and $j_<-j_<$, where $j_>=l+1/2$, and $j_<=l-1/2$, the reduced matrix element has the form

$$\left.\begin{aligned}\left\langle j_>\left\|\sigma+\frac{g_l}{\mu_-}l\right\|j_>\right\rangle&=\left\langle j_>\|\sigma\|j_>\right\rangle\left(1+\frac{g_l}{\mu_-}l\right);\\ \left\langle j_>\left\|\sigma+\frac{g_l}{\mu_-}l\right\|j_<\right\rangle&=\left\langle j_>\|\sigma\|j_<\right\rangle\left(1-\frac{g_l}{2\mu_-}\right);\\ \left\langle j_<\left\|\sigma+\frac{g_l}{\mu_-}l\right\|j_<\right\rangle&=\left\langle j_<\|\sigma\|j_<\right\rangle\left[1-\frac{g_l}{\mu_-}(l+1)\right].\end{aligned}\right\} \quad (29)$$

The values of the second factor, which determine the contribution of the l part, are given in Table 5 for different transitions.

Data on $M1$ transitions from analogs and information about the Gamow–Teller β transitions corresponding to them in the region of nuclei with $19\le A\le 70$ are given in Table 6. The $B(M1)$ values are determined from the experimental γ widths, the $B(M1,\sigma)$ values are calculated in accordance with Eq. (27), and in the last column we give the ratio $B(M1)/B(M1,\sigma)$. In Fig. 6, this ratio is given as a function of A.

The error in determination of $B(M1)/B(M1,\sigma)$ includes the error in determination of the reduced probabilities of $M1$ γ transitions and the values of lg ft. In some cases, the authors of the papers cited in Table 6 do not give the errors of the measured $B(M1)$ values. This is explained by the following factors. To calculate $B(M1)$, it is necessary to know the radiative width Γ_γ and to determine the mixture of the multipoles in the investigated transition. The radiative widths are most frequently determined in the $(p\gamma)$ reaction. To extract Γ_γ from the experimental value of the integrated reaction cross section it is necessary to determine independently the proton width Γ_p of the level. In many cases, this is known from measurements of the proton elastic-scattering cross section. For some nuclei, however, such measurements have not been made. To determine Γ_γ in these cases it is assumed that $\Gamma_p\gg\Gamma_\gamma$. This assumption is reasonable for medium and heavy nuclei, for proton energies 1–3 MeV, and for small values of l_p.

The measurements of Γ_p and Γ_γ, which have been made for analog resonances in the nuclei ^{45}Sc (Ref. 55), ^{47}V (Refs. 56, 57), ^{49}Sc (Ref. 49), ^{51}V (Ref. 24), ^{55}Mn (Ref. 50), ^{55}Co (Refs. 58, 59), and ^{59}Co (Ref. 60) at proton energies in the range 1.25–2.3 MeV, have shown that the ratio Γ_p/Γ_γ for the different resonances formed by the capture of protons with $l_p=1$ fluctuates from 7 to 700.

However, when, for example, $lp\ge2$ the assumption $\Gamma_p\gg\Gamma_\gamma$ is not so obvious and justified. Thus, in the cases when Γ_p is not measured independently, measurement of the $p\gamma$ reaction cross section gives only a lower limit for Γ_γ. In these cases, the authors of papers giving the value of Γ_γ do not always indicate the error of the measurements.

To determine the mixtures of multipoles in a transition, it is necessary to measure the angular distribution of the γ's. In many cases such measurements are made, and $B(M1)$ is determined with allowance for the measured δ. However, in some investigations there

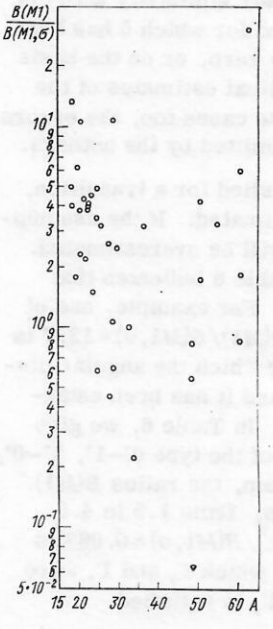

FIG. 6. The ratio $B(M1)/B(M1,\sigma)$ for analog γ and β transitions as a function of A.

TABLE 6. Comparison of analog β and γ transitions.

	beta decay				gamma decay			
A	$Z_iA(E_i)-Z_fA(E_f)$	$J_i^\pi,\ T_i - J_f^\pi,\ T_f$	lg ft	$B(M1,\sigma)$, μ_0^2	$Z_iA(E_i-E_f)$	$J_i^\pi,\ T_i - J_f^\pi,\ T_f$	$B(M1)\,\mu_0^2$	$\frac{B(M1)}{B(M1,\sigma)}$
19	$^{19}_{8}$O (0) — $^{19}_{9}$F (0.19)	5/2+, 3/2—5/2+, 1/2	5.42	0.029	$^{19}_{9}$F (7.54—0.19)	5/2+, 3/2—5/2+, 1/2	0.40 [30]	13.7±4.2
19	$^{19}_{8}$O (0) — $^{19}_{9}$F (1.55)	5/2+, 3/2—3/2+, 1/2	4.59	0.20	$^{19}_{9}$F (7.54—1.55)	5/2+, 3/2—3/2+, 1/2	1.0 [30]	5.1±1.4
19	$^{19}_{8}$O (0) — $^{19}_{9}$F (4.38)	5/2+, 3/2—7/2+, 1/2	3.60	1.1	$^{19}_{9}$F (7.54—4.38)	5/2+, 3/2—7/2+, 1/2	4.6 [30]	4.0
20	$^{20}_{8}$O (0) — $^{20}_{9}$F (1.06)	0+, 2 —1+, 1	3.73 [40]	1.43	$^{20}_{10}$Ne (16.73—11.2)	0+, 2 —1+, 1	2.55 [1]	1.80
20	$^{20}_{9}$F (0) —$^{20}_{10}$Ne (1.63)	2+, 1 —2+, 0	4.98 [40]	0.12	$^{20}_{10}$Ne (10.26—1.63)	2+, 1 —2+, 0	0.73 [41]	6.23
21	$^{21}_{9}$F (0) —$^{21}_{10}$Ne (0)	5/2+, 3/2—3/2+, 1/2	5.21	0.047	$^{21}_{11}$Na (8.97—0)	5/2+, 3/2—3/2+, 1/2	0.11 [34]	2.3±1.6
21	$^{21}_{9}$F (0) —$^{21}_{10}$Ne (0.35)	5/2+, 3/2—5/2+, 1/2	4.74	0.14	$^{21}_{11}$Na (8.97—0.34)	5/2+, 3/2—5/2+, 1/2	0.55 [34]	3.9±1.2
21	$^{21}_{9}$F (0) —$^{21}_{10}$Ne (1.75)	5/2+, 3/2—7/2+, 1/2	5.06	0.066	$^{21}_{11}$Na (8.97—1.72)	5/2+, 3/2—7/2+, 1/2	0.70 [34]	10.6±3.2
22	$^{22}_{12}$Mg(0)—$^{22}_{11}$Na(0.58)	0+, 1 —1+, 0	3.66	2.97	$^{22}_{11}$Na (0.66—0.58)	0+, 1 —1+, 0	6,6 [1]	2.2±0.8
22	$^{22}_{12}$Mg(0)—$^{22}_{11}$Na(1.94)	0+, 1 —1+, 0	3.43	1.43	$^{22}_{11}$Na (1.94—0.66)	1+, 0 —0+, 1	6,2 [1]	4.4±4.0
23	$^{23}_{10}$Ne (0)—$^{23}_{11}$Na (0)	5/2+, 3/2—3/2+, 1/2	5.27	0.041	$^{23}_{11}$Na (7.89—0)	5/2+, 3/2—3/2+, 1/2	0.17 [42]	4.1±1.4
23	$^{23}_{10}$Ne (0)—$^{23}_{11}$Na(0.44)	5/2+, 3/2—5/2+, 1/2	5.39	0.031	$^{23}_{11}$Na (7.89—0.44)	5/2+, 3/2—5/2+, 1/2	0.12 [42]	4.0±1.4
24	$^{24}_{10}$Ne (0)—$^{24}_{11}$Na(0.47)	0+, 2 —1+, 1	4.38	0.32	$^{24}_{12}$Mg (15.43—9.97)	0+, 2 —1+, 1	1.43 [7]	4.5±1.8
24	$^{24}_{10}$Ne (0)—$^{24}_{11}$Na(1.34)	0+, 2 —1+, 1	4.37	0.33	$^{24}_{12}$Mg (15.43—10.7)	0+, 2 —1+, 1	0.48 [7]	1.5±0.7
25	$^{25}_{11}$Na (0)—$^{25}_{12}$Mg (0)	5/2+, 3/2—5/2+, 1/2	5.25	0.043	$^{25}_{13}$Al (7.90—0)	5/2+, 3/2—5/2+, 1/2	0.15 [36]	3.5±2.4
25	$^{25}_{11}$Na (0)—$^{25}_{12}$Mg(0.97)	5/2+, 3/2—3/2+, 1/2	5.05	0.069	$^{25}_{13}$Al (7.90—0.94)	5/2+, 3/2—3/2+, 1/2	0.04 [36]	0.6±0.6
25	$^{25}_{11}$Na (0)—$^{25}_{12}$Mg(1.61)	5/2+, 3/2—7/2+, 1/2	5.03	0.072	$^{25}_{13}$Al (7.90—1.61)	5/2+, 3/2—7/2+, 1/2	0.35 [36]	4.9±3.4
26	$^{26}_{14}$Si (0) —$^{26}_{13}$Al (1.06)	0+, 1 —1+, 0	3.53	1.13	$^{26}_{13}$Al (1.06—0.23)	1+, 0 —0+, 1	3.7 [1, 43. 44]	3.3±1.2
28	$^{28}_{12}$Mg(0)—$^{28}_{13}$Al (1.37)	0+, 2 —1+, 1	4.46	0.27	$^{28}_{14}$Si (15.22—10.72)	0+, 2 —1+, 1	0.12 [10]	0.45±0.23
28	$^{28}_{12}$Mg(0)—$^{28}_{13}$Al (1.62)	0+, 2—1+, 1	4,56	0.27	$^{28}_{14}$Si (15.22—10.90)	0+, 2—1+, 1	0.70 [10]	2.6±1.6
29	$^{29}_{13}$Al (0)—$^{29}_{14}$Si (1.23)	5/2+, 3/2—3/2+, 1/2	5,05	0.069	$^{29}_{15}$P (8.37—1.38)	5/2+, 3/2—3/2+, 1/2	0.043 [36]	0.62±0.40
29	$^{29}_{13}$Al (0)—$^{29}_{14}$Si (2.03)	5/2+, 3/2—5/2+, 1/2	5,72	0.015	$^{29}_{15}$P (8.37—1.96)	5/2+, 3/2—5/2+, 1/2	0.16 [36]	10.6±6.4
29	$^{29}_{13}$Al (0)—$^{29}_{14}$Si (2.43)	5/2+, 3/2—3/2+, 1/2	4,97	0.082	$^{29}_{15}$P (8.37—2.40)	5/2+, 3/2—3/2+, 1/2	0.10 [36]	1.2±0.8
30	$^{30}_{16}$S (0) —$^{30}_{15}$P (0)	0+, 1—1+, 0	4,38	0.47	$^{30}_{15}$P (0.68—0)	0+, 1—1+, 0	1.2 [1. 45]	2.5±0.6
31	$^{31}_{14}$Si (0) —$^{31}_{15}$P (0)	3/2+, 3/2—1/2+, 1/2	5,52	0.023	$^{31}_{15}$P (6.38—0)	3/2+, 3/2—1/2+, 1/2	$\leqslant$0.036 [42]	$\leqslant$1.56
33	$^{33}_{18}$Ar (0)—$^{33}_{17}$Cl (0.81)	1/2+, 3/2—1/2+, 1/2	4,44	0.27	$^{33}_{17}$Cl (5.50—0.81)	1/2+, 3/2—1/2+, 1/2	0.27 [46]	1.0±0.3
34	$^{34}_{18}$Ar (0)—$^{34}_{17}$Cl (0.66)	0+, 1—1+, 0	4,78	0.063	$^{34}_{17}$Cl (0.66—0)	1+, 0—0+, 1	0.014 [47]	0.22±0.17
37	$^{37}_{16}$S (0) —$^{37}_{17}$Cl (3.11)	7/2−, 5/2—7/2−, 3/2	4,37	0.20	$^{37}_{17}$Cl (10.22—3.11)	7/2−, 5/2—7/2−, 3/2	1.40 [48]	3.2±0.8
49	$^{49}_{20}$Ca (0)—$^{49}_{21}$Sc (3.08)	3/2−, 9/2—3/2−, 7/2	4,9	0.032	$^{49}_{21}$Sc (11.56—3.08)	3/2−, 9/2—3/2−, 7/2	0.002 [49]	0.063
49	$^{49}_{20}$Ca (0)—$^{49}_{21}$Sc (4.07)	3/2−, 9/2—5/2−, 7/2	4,7	0.051	$^{49}_{21}$Sc (11.56—4.07)	3/2−, 9/2—5/2−, 7/2	0.044 [49]	0.86
49	$^{49}_{20}$Ca (0)—$^{49}_{21}$Sc (4.74)	3/2−, 9/2—5/2−, 7/2	4,5	0.081	$^{49}_{21}$Sc (11.56—4.74)	3/2−, 9/2—5/2−, 7/2	0.045 [49]	0.55
51	$^{51}_{22}$Ti (0)—$^{51}_{23}$V (0.32)	3/2−, 7/2—5/2−, 5/2	4,82 [24]	0.049	$^{51}_{23}$V (9.40—0.32)	3/2−, 7/2—5/2−, 5/2	0.084 [24]	1.7±0.5
51	$^{51}_{22}$Ti (0)—$^{51}_{23}$V (0.93)	3/2−, 7/2—3/2−, 5/2	5,45 [24]	0.012	$^{51}_{23}$V (9.40—0.93)	3/2−, 7/2—3/2−, 5/2	0.051 [24]	4.3±1.3
55	$^{55}_{24}$Cr(0)—$^{55}_{25}$Mn (0)	3/2−, 7/2—5/2−, 5/2	4,95	0.037	$^{55}_{25}$Mn (10.0—0)	3/2−, 7/2—5/2−, 5/2	0.12 [50]	3.2
61	$^{61}_{29}$Cu(0)—$^{61}_{28}$Ni (0)	3/2−, 3/2—3/2−, 5/2	5,1	0.036	$^{61}_{29}$Cu (6.40—0)	3/2−, 5/2—3/2−, 3/2	0.24 [51]	6.0
61	$^{61}_{29}$Cu(0)—$^{61}_{28}$Ni(0.067)	3/2−, 3/2—5/2−, 5/2	6,3	0.0015	$^{61}_{29}$Cu (6.45—0)	5/2−, 5/2—3/2−, 3/2	0.0027 [52]	1.8
61	$^{61}_{29}$Cu(0)—$^{61}_{28}$Ni(0.28)	3/2−, 3/2—1/2−, 5/2	5,5	0.028	$^{61}_{29}$Cu (6.63—0)	1/2−, 5/2—3/2−, 3/2	0.024 [52]	0.85
63.	$^{63}_{28}$Ni(0)—$^{63}_{29}$Cu (0)	1/2−, 7/2—3/2−, 5/2	6,5	0.0010	$^{63}_{29}$Cu (8.57—0)	1/2−, 7/2—3/2−, 5/2	0.030 [53]	30

Note: Unless otherwise indicated, the values of lg ft are taken from Ref. 54. The values of E_i and E_f are given in MeV.

are no measurements of δ. The authors of the corresponding papers assume that the transitions from analog resonances are pure magnetic dipole transitions, this being justified on the basis of their similarity with the γ transitions for which $\Delta T=1$ and for which δ has been measured and found to be nearly zero, or on the basis of a comparison with the theoretical estimates of the transition probabilities. In these cases too, the errors for $B(M1)$ are also sometimes omitted by the authors.

Note that if $\Gamma_p \gg \Gamma_\gamma$ is not satisfied for a transition, $B(M1)/B(M1,\sigma)$ will be underestimated. If the assumption $\delta \approx 0$ is not true, the ratio will be overestimated. Analysis of the data shown in Table 6 indicates that there are no such correlations. For example, one of the largest values of the ratio $B(M1)/B(M1,\sigma)=13.7$ is obtained for the ^{19}F nucleus, for which the angular distributions have been measured and it has been established experimentally that $\delta \approx 0$. In Table 6, we give data on ten pure $M1$ transitions of the type 0^+-1^+, 1^+-0^+, and $1/2^+-1/2^+$. For seven of them, the ratios $B(M1)/B(M1,\sigma)$ have fairly large values: from 1.5 to 4.5. Finally, the smallest ratio $B(M1)/B(M1,\sigma)=0.063$ is obtained for the ^{49}Sc nucleus, in which Γ_p and Γ_γ were measured and the relation $\Gamma_p \gg \Gamma_\gamma$ is satisfied.

We also mention that information about the values of Γ_γ can be obtained from measurements of the resonance fluorescence cross sections and from study of inelastic scattering of electrons through large angles and the $\alpha\gamma$ reaction. For low-lying levels in odd–odd nuclei information about Γ_γ has been obtained from a determination of the lifetimes.

In Table 6 we give the more reliable experimental values. The details of the experiment can be found in the literature quoted in the table. Information about some of the less reliable transitions not included in the table will be discussed below.

The majority of the collected values refer to transitions in nuclei of the *sd* shell. A great many theoretical studies have been made of these nuclei, and the probabilities of γ transitions with $\Delta T=1$ have been calculated, i.e., the decay of analogs. In some of the investigations, the probabilities of the analog β transitions were also calculated. Usually, one compares the theoretical and experimental data on the relative and absolute probabilities of β and γ transitions. However, on some occasions use has also been made of a comparison of the theoretical ratios $B(M1)/B(M1,\sigma)$, or other ratios

that characterize the contribution of the orbital part to the γ transition, with the experimental values. Ratios of this type can serve as an additional criterion for evaluating the model. Below, we give a brief review of the papers in which β and γ transitions have been calculated simultaneously.

A=19. One compares β transitions from the ground state $^{19}O(5/2^+)$ to the states $^{19}F(5/2^+, 3/2^+, 7/2^+)$. To other states of ^{19}F sufficiently strong β transitions are not observed. The analog of the ^{19}O ground state is at a height of 7.539 MeV $(5/2^+)$. Fairly strong γ transitions are detected only to levels that are also populated as a result of β decay. For $5/2^+-5/2^+$ transitions one observes one of the largest values of the ratio $B(M1)/B(M1, \sigma)$ in Table 6. Theoretical calculations and a comparison of the probabilities of β and γ transitions from the analog have been made in several papers.

The shell model with effective residual interactions of different types was used in Refs. 30 and 31. Fair agreement with the experimental values of lg *ft* and $B(M1)$ was obtained for the transitions $5/2^+-5/2^+$ and $5/2^+-3/2^+$. For the transition $5/2^+-7/2^+$ the situation was more complicated. It was noted by Aitken *et al.*[30] that the theory gives much too small (by an order of magnitude) values for the probabilities of both β and γ transitions. However, Arima *et al.*[31] obtained values that, although smaller than the experimental, were fairly near them. In Ref. 32, Gunye and Warke made calculations in the Hartree–Fock formalism. The results were found to lie between the calculations of Ref. 30, on the one hand, and those of Ref. 31, on the other. It should be pointed out that in Refs. 30–32 the ratio $B(M1)/B(M1, \sigma)$ was not analyzed. It was only noted in Ref. 32 that the contribution of the l part to the operator of the $M1$ γ transition cannot be ignored in all cases. It would seem that the $5/2^+-5/2^+$ transition is just such a case when the l part is important in the γ transition from the analog.

A=20. Data on the γ decay of double analogs and analogs in ^{20}Ne enable one to make a comparison with β decay. Gamma decay from the double analog ($T=2$, $J^\pi=0^+$) to the state $T=1$, $J^\pi=1^+$ in ^{20}Ne can be compared with the β decay $^{20}O-^{20}F$. Beta and gamma transitions were calculated simultaneously in Refs. 31 and 33. The calculations were made in the framework of the many-particle shell model with residual interactions. In Ref. 31, Arima *et al.* obtained approximate agreement with experiment, although the calculated probabilities of β and γ transitions were found to be somewhat greater than the experimental ones. In Ref. 33, the agreement with experiment was much worse. The energies of the $T=2$ and 1 states and the probabilities of γ transitions between them differed strongly from the experiment. The $T=2-T=1$ transition probability was approximately ten times larger than the experimental. The $^{20}O-^{20}F$ β decay was hindered relative to the experimental.

One can also compare the β transition of $^{20}F-^{20}Ne$ with the corresponding γ transition in ^{20}Ne (see Table 6). The probability of this γ transition was calculated in Ref. 31. The transition was found to be hindered. The probabilities of β and γ transitions were not calculated simultaneously.

A=21. The existing experimental data enable one to compare the probabilities of β transitions from the ^{21}F ground state to ^{21}Ne levels and the probabilities of $M1$ γ transitions with $\Delta T=1$ in the ^{21}Na nucleus, which is conjugate to ^{21}Ne. We do not know of any simultaneous calculations for these β and γ transitions. However, there is a rule that γ transitions with $\Delta T=1$ must be the same in conjugate nuclei. In Ref. 31, Arima *et al.* calculated simultaneously $^{21}F-^{21}Ne$ β transitions and γ transitions for the decay of the $5/2^+$ analog in ^{21}Ne. For the γ transitions, the order of the absolute probabilities and the relative intensities of the transitions can be reproduced if a comparison is made with the experimental values for the γ decay of the $5/2^+$ analog in ^{21}Na. However, the β transitions are hindered by one or two orders of magnitude.

A=23. For this A, one can compare β transitions from the ^{23}Ne ground state to ^{23}Na levels and γ transitions to ^{23}Na. In Ref. 42, Shikazono and Kawarasaki calculated the probabilities of β and γ transitions in Nilsson's model. This model satisfactorily describes the absolute and relative intensities of the transitions. The contribution of the l part was analyzed. The experimental ratio of the reduced matrix element of the l part to the reduced matrix element of the σ part is 5.5 ± 1.2 and 4.8 ± 1.1 for transitions to the ground and first excited state of ^{23}Na, respectively. The theoretical value, which is the same for the two cases, is 3.76.

A=24. Data on the γ decay of the double analog in ^{24}Mg enable one to make a comparison with the β decay $^{24}Ne-^{24}Na$. In Refs. 7 and 23, data are given on calculations of β and γ transitions in the shell model with residual interactions, and the results of the calculation describe both β and γ transitions well.

A=25. One can compare β transitions from the ground state of ^{25}Na ($T=3/2$) to the ^{25}Mg levels with energies 0, 0.97, and 1.61 MeV ($T=1/2$) and the corresponding $M1$ γ transitions with $\Delta T=1$ in the ^{25}Al nucleus, which is a mirror nucleus of ^{25}Mg (in the nucleus ^{25}Mg itself the radiative widths for the $M1$ transitions with $\Delta T=1$ are unknown). As we have already said, the possibility of such comparison follows from the well known rule that γ transitions of any multipolarity with $\Delta T=1$ have identical properties in the conjugate nuclei.

In Ref. 36, Morrison *et al.* calculated the radiative widths and lg *ft* of β transitions in Nilsson's model. Calculations were made for the allowed transitions $T_iJ_iK_i = 3/2,\ 5/2^+,\ 3/2^+ - T_fJ_fK_f = 1/2,\ 5/2^+,\ 5/2^+$ (ground state) and $1/2,\ 7/2^+,\ 5/2^+$ (1.61 MeV). Agreement is observed between the calculations and experiment for the absolute values of the probabilities of γ and β transitions and for the $B(M1)$ ratio for γ transitions from the analog to low-lying levels that are members of the rotational band with $K=5/2^+$. The calculated value $B(M1) \times (5/2-5/2)/B(M1)\,(5/2-7/2) = 0.40$ agrees well with the experimental value 0.41 ± 0.07.

The transition $3/2,\ 5/2^+,\ 3/2^+ - 1/2,\ 3/2^+,\ 1/2^+$ (0.97 MeV) is forbidden in this model, and to explain the observed probabilities it is necessary to introduce an ad-

mixture of a certain configuration to states with $T = 3/2$.

In Ref. 37, Jones *et al.* made a quantitative comparison of the absolute probabilities of β and γ analog decays in ^{25}Na and ^{25}Al nuclei and of the ratio of these probabilities with calculations made in Nilsson's model. They showed that the experimental data can be reproduced well by the model. In particular, in the framework of this model one obtains an explanation of the experimental fact that the ratio $B(M1)/B(M1, \sigma)$ for allowed transitions to the levels of ^{25}Mg (0 and 1.61 MeV) is approximately six to eight times greater than for the transition to the 0.97-MeV level. The calculated excess in Nilsson's model is about 3–4, whereas for a spherical potential this ratio is the same for all transitions.

A = 28. The γ decay of the double analog in ^{28}Si can be compared with the ^{28}Mg–^{28}Al β transitions. The probabilities of β and γ processes were calculated simultaneously by Jelley *et al.*[10] The branching ratio was reproduced quite well but the absolute probabilities of transitions were much larger than the experimental. In the calculations, a shell model (valence nucleons in the *sd* shell) with residual interaction was used. The contribution of the l part to the γ transition was not analyzed.

A = 29. One can compare the experimental values of β transitions from the ground state of ^{29}Al ($T = 3/2$) to levels of ^{29}Si ($T = 1/2$) and the probabilities of $M1$ γ transitions with $\Delta T = 1$ in the nucleus ^{29}P, which is a mirror nucleus for ^{29}Si (in the nucleus ^{29}Si itself the radiative widths of the corresponding γ transitions are unknown). Attempts to explain the relative probabilities of β decay in the framework of Nilsson's model were unsuccessful. A qualitative explanation of the relative probabilities of β and γ decay can be obtained by using the shell model (spherical potential) with jj coupling.[37]

A = 31. For this A, one can compare the β transitions from the ground state of ^{31}Si to the levels of ^{31}P. However, the probabilities of γ transitions from the analog of the ground state of ^{31}Si to ^{31}P are not known. In Table 6, the value of the upper limit for the transition to the ground state has been used. Nevertheless, there exist theoretical estimates of the contribution of the orbital part. In Ref. 42, Shikazono and Kawarasaki made this estimate in Nilsson's model; in Ref. 32, Gunye and Warke used the shell model and Hartree–Fock calculations.

A = 34. For this A, one can compare the γ decay from the 0.66-MeV state in ^{34}Cl ($T = 0$) to the ground state of this nucleus, which has isospin 1, and the analog β decay from the ground state of ^{34}Ar ($T = 1$) to the 0.66-MeV level of ^{34}Cl. In Ref. 47, Evers and Stocker calculated the probabilities of these β and γ transitions in a shell model with different interactions. They indicate that the best agreement with experiment is obtained when tensor forces are taken into account.

A = 37. The measured radiative width of the γ transition from the analog at 10.22 MeV to the 3.11-MeV level in ^{37}Cl was compared with the calculated value in Refs. 48 and 61. The calculations were made in the shell model. A simultaneous calculation was made of the probability of the analog β decay from the ground state of ^{37}S to the same 3.11-MeV level in ^{37}Cl. Very good agreement with experiment was observed for β and γ processes.

Table 6 does not include a comparison of the intensities of β and γ processes in the ^{24m}Al and ^{24}Mg nuclei. It is known experimentally[62,63] that there is a γ decay of the ^{24}Mg state with $E_x = 10.0$ MeV, which is an analog of the isomer level ^{24m}Al ($J^\pi = 1^+$). It is also known that there is a β decay of the isomer to the ^{24}Mg levels. If the experimental data for $B(M1)$ and $B(M1, \sigma)$ are used, for the ratio of these quantities one obtains very large values: 100 for transition to the ground state of ^{24}Mg and 77 for the transition to the 1.37-MeV level. These large values may arise from an incorrect determination of lg ft for the β transitions; for the transition to the ground state lg $ft = 6.0$; to the 1.37-MeV level, it is 6.2. These values are clearly too large for allowed β decay in light nuclei.

In some of the quoted papers, attention is drawn to the role of the orbital part in an $M1$ transition from analogs. In Ref. 31, for example, Arima *et al.* assert that in nuclei of the *sd* shell $M1$ transitions from an analog are basically determined by the spin part of the operator. In Ref. 32, Gunye and Warke note a similarity between analog β and γ transitions but say that in some cases the l part is important. Quantitative analysis of the experimental data leads to a different conclusion. Comparing the values of $B(M1, \sigma)$ and $B(M1)$ in Table 6, we can conclude that, as a rule, the l part's contribution to the $M1$ transition exceeds the contribution of the spin part or is comparable with it. Nevertheless, one can show that the majority of the $B(M1)/B(M1, \sigma)$ ratio values lie in the range 1 to 5 and one does not encounter very large or very small values.

Attention should be drawn to a circumstance that is not reflected in Table 6 or Fig. 6. Fairly often, one cannot observe a γ transition from an analog or the corresponding analog β transition, although the quantum numbers do not forbid it.

This means that analog β and γ transitions are correlated although the contribution of the l part may be greater than the σ part's. These data can be explained by the selection rules for the matrix elements of the l and σ parts being the same, so that the matrix element of the l part is small in the cases when the σ part's is.

It is to be expected that the contribution of the l part is more important when the β transition is hindered. Indeed, large values of $B(M1)/B(M1, \sigma)$ are observed for β transitions with lg $ft \approx 5$–5.5. These are β decays of nuclei with $A = 19$, 21, 29. However, in other cases when lg ft has the same value, the ratio $B(M1)/B(M1, \sigma)$ has normal values. It should be noted that in cases when β as well as γ transitions are hindered, experimental difficulties generally arise in determination of their absolute intensities. In addition, for weak γ transitions one must take into account the possibility of a contribution from the $T_<$ component of the analog. In nuclei of the $f_{7/2}$ shell there are not many data that enable one to compare analog β and γ transitions.

A=49. Gamma decay transitions of the $p_{3/2}$ analog in ^{49}Sc can be compared with β transitions from the ground state of ^{49}Ca. This case is characterized by the fact that all the ratios $B(M1)/B(M1, \sigma)$ are less than unity. It is obviously difficult to explain the small value of this ratio (for example, 0.063 for transitions to the 3.08-MeV level of ^{49}Sc) by the contribution of the l part. In ^{49}Sc, the neutrons completely fill the $f_{7/2}$ shell, so that the transitions which could contribute to the total value of $B(M1)$ are $f_{7/2}$–$f_{7/2}$, $f_{7/2}$–$f_{5/2}$, $p_{1/2}$–$p_{1/2}$, and $p_{1/2}$–$p_{3/2}$, and the l part for these transitions cannot strongly reduce the ratio $B(M1)/B(M1, \sigma)$. In Ref. 49, Gaarde *et al.* show that the small value of this ratio can be explained by a contribution to the γ transition of the $T_<$ component of the analog and interference between this contribution and the $T_>$ component's. The $p_{3/2}$ analog of ^{49}Sc is split into several fine-structure components. It is known that γ transitions to the 3.08-MeV level of ^{49}Sc take place from at least three components. However, the intensity of these transitions is not correlated with Γ_p for every resonance, this width being a measure of the contribution made to the resonance by the $T_>$ component of the analog. This also means that in the γ transition to the 3.08-MeV level the $T_<$ component makes the main contribution, which can interfere with the contribution of the $T_>$ component. The estimates made in Ref. 49 by Gaarde *et al.* show that the intensity of the transition from the $T_<$ component may be comparable with the intensity of the hindered transition from the $T_>$ component. The contribution of the $T_<$ component to the other two transitions (to the 4.07- and 4.74-MeV levels of ^{49}Sc) is smaller and the ratio $B(M1)/B(M1,\sigma)$ is near unity.

A=51. The γ decay of the $p_{3/2}$ analog in ^{51}V was analyzed in Ref. 27 by Osnes and Warke. They also calculated lg ft of the analog β transitions. The intensities of the β and γ transitions can be reproduced if allowance is made for a small admixture of $p_{1/2}$ and $f_{5/2}$ states to the ^{51}Ti ground state and an admixture of a collective Gamow–Teller state to the low-lying states of ^{51}V.

A=61. Analog β and γ transitions were compared in Ref. 64 by Kraft *et al.*, who pointed out the normal values of the ratio $B(M1)/B(M1, \sigma)$ despite the fact that the probabilities of different γ and β transitions differ strongly.

A=63. The ratio $B(M1)/B(M1, \sigma)$ for this case is the largest in Table 6. Note that the β transition is strongly hindered: lg ft=6.5. In this case, one can expect a large contribution of the l part. On the other hand, since one is studying a γ transition from an analog $p_{1/2}$ state, it is difficult to determine the $E2/M1$ mixing in this transition (the spin 1/2 of the initial state leads to isotropy of the γ's). The possibility cannot be excluded that the observed γ transition is to a considerable extent an $E2$ transition.

4. CONFIGURATION STATES

A detailed study of the γ decay of analogs in medium and heavy nuclei entails a consideration of collective charge-exchange degrees of freedom of the nucleus. Charge-exchange nuclear excitations are characterized by isospin $\tau=1$ and projection $\mu_\tau=-1, 0, +1$. Excitations with $\mu_\tau=0$ correspond to excitations (with isospin 0 or 1) that do not change the isospin projection of the nucleus, i.e., are in the nucleus whose ground state is being considered. Excitations with $\mu_\tau=\pm 1$ are charge-exchange excitations and are in the other nucleus; in these excitations, the isospin projection of the state changes. An analog state is an example of this excitation.

It has been shown above that the γ decay of analogs can be regarded as a charge-exchange process analogous, for example, to β^- decay. The experimental data on the lg ft of Gamow–Teller β decay are explained by the idea of a collective Gamow–Teller state, which is a coherent superposition of $p\bar{n}$ excitations coupled into angular momentum 1^+ (see Refs. 65 and 66). Configurations of this type are also important in analysis of the γ decay of analogs.

Collective charge-exchange excitations appear when residual interactions are taken into account. Before we turn to the study of collective states, we must construct basis functions, i.e. eigenfunctions of the Hamiltonian without interaction. As was noted by Vergados and Kuo,[67] diagonalization of the isoscalar Hamiltonian on an arbitrary but fairly large basis will lead to wave functions having good isospin. However, if one chooses a basis of functions with definite isospin, a number of advantages result, particularly in the cases when the isospin structure of the investigated phenomenon is important. To study the γ decay of analog states, it is evidently expedient to use basis functions with definite isospin. These functions will be constructed in the form of a superposition of particle–hole excitations.

It is not easy to construct functions with a definite isospin, especially when complicated configurations are considered. In Ref. 28, Fujita and Ikeda proposed a method that uses projection operators in order to construct states with definite isospin. In Refs. 67 and 68, states with definite isospin were constructed in order to study the isospin structure of a giant $E1$ resonance. In Ref. 69, Mekjian and MacDonald used functions with definite isospin to construct a theory of analog resonances.

Aleshin[29] has discussed in detail the construction of functions with definite isospin to apply to the study of analog decay. In the construction of states with definite isospin one encounters an analog and an antianalog state, configuration states, core polarization states, and spin-flip states. In different investigations different states have been considered, and there is no unified terminology. Here, we shall give definitions of all these states.

In the many-particle shell model, analog, antianalog, and configuration states are defined as follows. Suppose that above a closed inert core with isospin and spin equal to zero there is a group of nucleons (even number) at level j_1 with total spin $J=0$ and isospin T_0. Consider also an odd particle at level j_2. Then the wave function of the analog corresponds to coupling of the odd particle and the core with J_0 and T_0 to total angular momentum $J=j_2$ and isospin $T=T_0+1/2$:

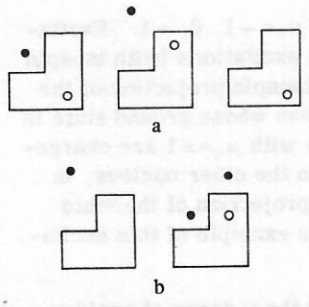

FIG. 7. Simple configurations for odd–odd (a) and odd (b) nuclei that do not have definite isospin.

$|(j_1^n)_{J_0,\,T_0},\,j_2\rangle_{J,\,T_0+1/2}$.

The antianalog state corresponds to the same coupling to angular momentum $J=j_2$ but with isospin $T_0-1/2$: $|(j_1^n)_{J_0,T_0},j_2\rangle_{J,T_0-1/2}$.

All the other states that appear as a result of recoupling of the spin J_0 and isospin T_0 are called configuration states in Lane's terminology.[70] Occasionally, the antianalog state is also included in the concept of configuration states. In what follows, we shall apply the name configuration states to a smaller class of states, separating the antianalog state, core-polarization states, and spin-flip states.

Let us consider first the ground state of an even–even nucleus (N, Z):

$$|0\rangle = |T=T_0,\ T_z=T_0,\ I=0,\ M=0\rangle. \tag{30}$$

The analog state and the other states are found in the nucleus $(Z+1,\ N-1)$, i.e., in an odd–odd nucleus. These states can be obtained in different ways, one of them being by diagonalizing the operator T^2 in the space of excitations[29]:

$$a^+_{\beta p}a_{\beta n}|0\rangle \qquad \beta=1, 2, \ldots, 2T_0. \tag{31}$$

As a result, it is found that there exists only one state belonging to isospin $T=T_0$; this is called the analog state:

$$A(0)=\sum_{\beta}(2T_0)^{-1/2}a^+_{\beta p}a_{\beta n}|0\rangle. \tag{32}$$

The remaining states, of which there are $2T_0-1$, have isospin $T=T_0-1$ and wave functions

$$C(i)=\sum_{\beta}Q^i_{\beta}a^+_{\beta p}a_{\beta n}|0\rangle, \qquad i=1, 2, \ldots, 2T_0, \tag{33}$$

where the coefficients Q^i_β satisfy the condition

$$\sum_{\beta}Q^i_{\beta}=0, \qquad i=1, 2, \ldots, 2T_0-1. \tag{34}$$

These states were first introduced by Lane[70] and are frequently called Lane configuration states. The coefficients Q_β can be chosen in different ways.

An analog state has a definite total angular momentum $I=0$, and its wave function can be represented in the form

$$A(0)=\sum_{b=1}^{F}\left(\frac{n_b}{n_F}\right)^{1/2}(a^+_{bp}a_{bn})_{0^+}|0\rangle. \tag{35}$$

Here, n_b is the number of particles in subshell b; n_F is the total number of particles in the neutron excess; and F is the number of subshells filled by the neutron excess.

The states (33) do not have definite total angular momentum. One can show that the space (33) is equivalent to the space of states with wave functions $C(b, I=0)$ and $K(b, I\neq 0)$:

$$C(b, I=0)=\left\{\left(\frac{N_b-1}{N_b}\right)^{1/2}(a^+_{bp}a_{bn})_{0^+} - \sum_{b_0<b}\left(\frac{n_b n_{b_0}}{N_{b-1}N_b}\right)^{1/2}(a^+_{b_0p}a_{b_0n})_{0^+}\right\}|0\rangle, \tag{36}$$

where $b=1, 2, \ldots, F$ and $N_b=\sum_{b_0=1}^{b}N_b$;

$$K(b, I\neq 0)=(a^+_{bp}a_{bn})_{I\neq 0}|0\rangle. \tag{37}$$

We shall say that the states (36) are configuration states and the states (37) for $I=1^+$ are core-polarization states.

The states (36) and (37) have the definite isospin T_0-1. Other states with definite isospin are obtained as a superposition of particle–hole $(1p-1h)$ and $(2p-2h)$ configurations, which do not have definite isospin. The simplest configurations are shown in Fig. 7. Examples of states $(T=T_0-1)$ for an odd–odd nucleus in which the contribution of the $(1p-1h)$ components is largest are shown in Fig. 8 (Ref. 29). Excitations of this type can be distributed over states with isospin T_0-1, T_0, and T_0+1. The excitations which become the most important in the functions Ψ_{K_1} and Ψ_{K_2} are distributed over the states with $T=T_0-1$ and $T=T_0$. In the third case, a T_0+1 component is possible.

In the study of the γ decay of analogs, the most important particle–hole configurations are those in which the proton and the neutron hole occupy states that are members of a spin–orbit doublet: $j_n=l\pm 1/2$ and $j_p=l\mp 1/2$. We shall say that states with definite isospin in

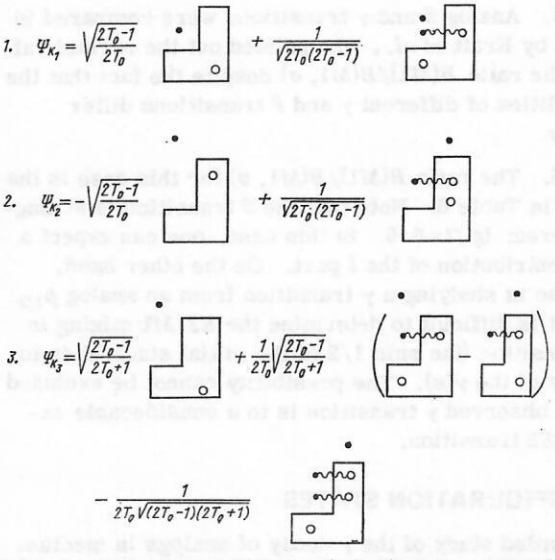

FIG. 8. Examples of different (1, 2, 3) states with definite isospin for odd–odd nuclei. The wavy line denotes summation over the excess neutrons.[29]

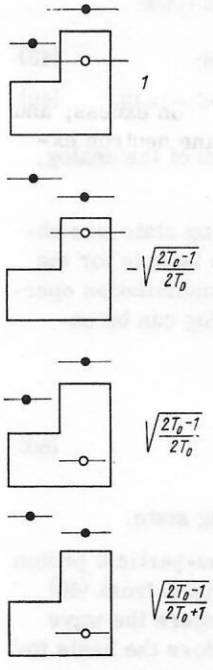

FIG. 9. Three-quasiparticle configurations and their amplitudes in states with definite isospin for an odd nucleus.[29]

which these configurations make the main contribution are spin-flip states.

Let us now consider states of the nucleus $(Z+1, N)$. This case corresponds to the excitation of analogs in the $p\gamma$ reaction on the even–even nucleus (Z, N). The main configuration is the $(Z, N+1)$ nucleus. The analog state and the other states will contain a one-particle component. In the notation of Ref. 69, the analog state can be written in the form

$$\Phi_a = (N-Z+1)^{-1/2} \sum_{\alpha=Z+1}^{N+1} \Phi_{\alpha\alpha},$$
$$\text{where } \Phi_{\alpha\alpha} = a^+_{\alpha p} a_{\alpha n} |\Phi(Z, N+1)\rangle. \quad (38)$$

There is a group of states Φ_l orthogonal to the analog state; these are configuration states, including the antianalog state:

$$\Phi_l = \frac{(l-Z-1)\Phi_{ll} - \sum_{\mu=Z+1}^{l=1} \Phi_{\mu\mu}}{\sqrt{(l-Z)(l-Z+1)}}, \quad (39)$$
$$l = Z+2, \ldots, N+1.$$

Making a comparison with the case of an odd–odd nucleus [the state (33)], we note that there is a new state corresponding to $l = N+1$:

$$\Phi_{N+1} = [(N-Z)\Phi_{N+1,\,N+1} - \sum_{\mu=Z+1}^{N} \Phi_{\mu\mu}] \Big/ \sqrt{(N-Z+1)(N-Z+2)}. \quad (40)$$

This state is called the antianalog state because of its structural similarity to the analog state.

For states that are analogous to (37) an odd neutron is added:

$$K(b, I \neq 0) = a^+_n (a^+_{bp} a_{bn})_{I=0} |0\rangle. \quad (41)$$

The states (38)–(41) have definite isospin. They are made up from configurations that do not (see Fig. 7b).

As in the case of an odd–odd nucleus, other states with definite isospin can be obtained from the configurations of Fig. 7a plus an odd neutron and many-particle configurations. In the study of the γ decays of analogs, the most important states are those that have a large contribution of three-quasiparticle components of the type of Fig. 7a plus a neutron. These states have isospin $T_0 - 1$. In the majority of physical problems and, in particular, in the study of the γ decay of analogs, only the three-quasiparticle components are important. The coefficients of these configurations[29] are given in Fig. 9. Eigenstates (with definite isospin) of the Hamiltonian of independent particles are constructed. For the nucleus $(Z+1, N)$ they include, besides the analog state with isospin $T_0 + 1/2$, configuration states , the antianalog state, core-polarization states, and spin-flip states with isospin $T_0 - 1/2$.

Let us now consider the energy of these states (without allowance for residual interactions). We shall measure the energy from the energy of the analog state (Fig. 10).

The difference between the energies of the analog and the antianalog state is well known and is

$$E_{\bar{a}} - E_a = -(T_0 + 1/2) V_1/A, \quad (42)$$

where $V_1 \approx 100$ MeV. This is a symmetry energy, and can be determined in different experiments. The configuration states lie in the same energy region as the analog state.

A core-polarization state lies higher than the antianalog state by an amount Δ equal to the pairing energy of the neutron:

$$E_c - E_{\bar{a}} = -(T_0 + 1/2) V_1/A + \Delta. \quad (43)$$

The spin-flip states lie even higher: the difference between the energy of a spin-flip state and a core-polarization state is equal to the spin-orbit splitting:

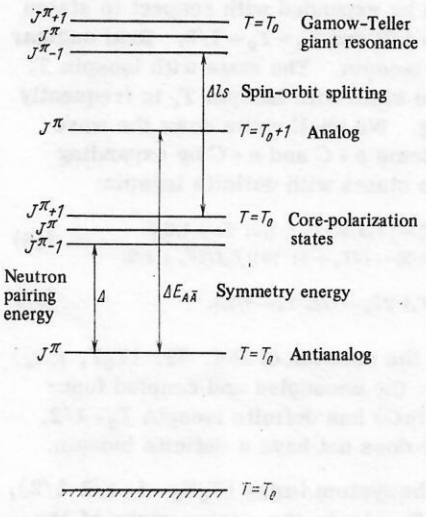

FIG. 10. Energy relations between the analog state, the antianalog state, configuration states, and core-polarization states.

$$E_s - E_c = \Delta_{ls} = \varepsilon(j = l - 1/2) - \varepsilon(j = l + 1/2), \quad (44)$$

so that

$$E_s - E_a = -(T_0 + 1/2) V_1/A + \Delta + \Delta_{ls}. \quad (45)$$

5. ANALOG-ANTIANALOG TRANSITIONS

In investigations into the γ decay of analogs, much attention has been devoted to analog–antianalog transitions. From the experimental point of view, this is because in nuclei with $A < 40$ one observes as a rule one strong transition to the lowest-lying state with the same spin and parity as the analog's. Some years ago, when data on the γ decay of analogs was known only for light nuclei, it appeared that decay by a strong $M1$ transition to the antianalog was the main characteristic feature of the γ decay of analogs. It was also noted that the intensity of analog–antianalog transitions is fairly large: the $B(M1)$ values were of the order of a Weisskopf unit. In recent years, data have become available on the decay of analogs in nuclei of the $f_{7/2}$ shell that have required the introduction of new ideas and have shown that in analysis of the γ decay of analogs one cannot restrict the treatment to only antianalogs. However, in this section we shall analyze the data for only analog–antianalog transitions.

Let us consider the decay of analogs with a clearly expressed one-particle nature. The parent state of such an analog is a fairly good one-particle (one-neutron) state and has a large spectroscopic factor in the (dp) reaction. The analog state must also have a large spectroscopic factor, which can be determined by elastic scattering of protons through the analog and from (^{3}He, d) proton-transfer reactions.[2] In this case, the antianalog state will also have a large spectroscopic factor in the (^{3}He, d) reaction.

Generally, when speaking of antianalogs, one uses ideas on the isospin splitting of one-particle states. When a proton hits a target nucleus C, the resulting system $p + C$ has a wave function without definite isospin. If the isospin of the target nucleus is T_0, the function of the $p + C$ system can be expanded with respect to states with isospin $T_> = T_0 + 1/2$ and $T_< = T_0 - 1/2$. Real nuclear states have definite isospin. The state with isospin $T_>$ is an analog, and the state with isospin $T_<$ is frequently called the antianalog. We shall write down the wave functions of the systems $p + C$ and $n + C$ by expanding them with respect to states with definite isospin:

$$\begin{aligned} |nC\rangle &= |T_0 T_0;\ 1/2 1/2\rangle = |T_0 1/2,\ T_0 + 1/2;\ T_0 + 1/2\rangle; \\ |pC\rangle &= |T_0 T_0;\ 1/2 - 1/2\rangle = (2T_0+1)^{-1/2} [|T_0 1/2 T_0 + 1/2; \end{aligned} \quad (46)$$

$$T_0 - 1/2\rangle + (2T_0)^{1/2} |T_0 1/2 T_0 - 1/2;\ T_0 - 1/2\rangle]. \quad (47)$$

Here, we have used the notation of Ref. 71: $|T_0 T,\ t;\ t_z\rangle$ and $|T_0 1/2 T;\ T_z\rangle$ for the uncoupled and coupled functions. The system $|nC\rangle$ has definite isospin $T_0 + 1/2$, and the system $|pC\rangle$ does not have a definite isospin.

We now introduce the system $|nA\rangle = |T_0 T_0 - 1;\ 1/2\ 1/2\rangle$, in which $|A\rangle = |T_0,\ T_0 - 1\rangle$ is the analog state of the target nucleus $|C\rangle = |T_0,\ T_0\rangle$. Then the $T_>$ and $T_<$ states can be expanded with respect to uncoupled functions:

$$\begin{aligned} |T_0 1/2 T_>;\ T_0 - 1/2\rangle &= (2T_0+1)^{-1/2} [|T_0 T_0;\ 1/2 - 1/2\rangle \\ &+ (2T_0)^{1/2} |T_0 T_0 - 1; 1/2\ 1/2\rangle] \\ &= (2T_0+1)^{-1/2} [|pC\rangle + (2T_0)^{1/2} |nA\rangle]; \end{aligned} \quad (48)$$

$$|T_0 1/2 T_<;\ T_0 - 1/2\rangle = (2T_0+1)^{-1/2} [(2T_0)^{1/2} |pC\rangle - |nA\rangle]. \quad (49)$$

The expression (48) is the wave function of the analog, and (49) is the antianalog's.

In the foregoing section, the antianalog state was obtained as one of the states with definite isospin for the odd system. In terms of creation and annihilation operators, the wave function of the antianalog can be expressed in the form

$$\Psi_{\bar{a}} = \sqrt{\frac{2T_0+1}{2T_0+2}} a^+_{jp1} |0\rangle - \sqrt{\frac{1}{(2T_0+1)(2T_0+2)}} \times \sum_s a^+_{jn1} (a^+_{jps} a_{jns})_{0^+} |0\rangle. \quad (50)$$

Here, T_0 is the isospin of the antianalog state.

Actually, the antianalog state is a one-particle proton state with definite isospin. As can be seen from (49) and (50), the one-particle component enters the wave function with a large weight, and therefore the basis for the identification of the antianalog state is a large spectroscopic factor in proton-transfer reactions.

The position of the antianalog state is approximately determined by the isospin splitting:

$$E_a - E_{\bar{a}} = 2T_0 V_1/A, \quad (51)$$

where T_0 is the isospin of the analog, $V_1 \approx 50$ MeV.

The probability of an analog–antianalog transition is determined solely by the one-particle component of the antianalog. One can show that if the final state contains a three-particle component of the type $a^+_{jni}(a^+_{jp} a_{jn})_I |0\rangle$, a contribution to the $M1$ transition from the analog is made only by the component with $I = 1^+$.

Assuming that the state $\Psi^{ps} |j_{n1}\rangle$ of the parent nucleus is a pure one-neutron state, we obtain the following expression for the probability of an $M1$ analog–antianalog transition:

$$B(M1) = \frac{3}{4\pi} \mu^2 \frac{2T_0+1}{(2T_0+2)^2} \frac{1}{2j_{n1}+1} (j'_{p1} \| \sigma \| j_{n1})^2 (1 + g_l/\mu k)^2, \quad (52)$$

where $B(M1)$ is expressed in units of μ_0^2; T_0 is the isospin of the antianalog; $g_l = 1$;

$$k = \begin{cases} +l \text{ for transitions of the type } j_> - j_>; \\ -(l+1) \text{ for transitions of the type } j_< - j_<. \end{cases}$$

For transitions of the type $j_> = l + 1/2 - j_> = l + 1/2$ the contributions of the orbital and the spin parts are coherent, whereas for transitions of the type $j_< = l - 1/2 - j_< = l - 1/2$ the orbital and the spin parts make contributions of opposite signs. Therefore, $j_> - j_>$ transitions will be enhanced by an order of magnitude compared with transitions of the type $j_< - j_<$.

This effect was analyzed by Maripuu,[72] who obtained the following expression for the probability of the $M1$ analog–antianalog transition:

$$B(M1) = \frac{9}{8\pi} (2T_i + 1) \langle T_i M_T 10 | T_f M_T \rangle^2$$

TABLE 7. Values of $B(M1)$ for analog–antianalog transitions (in W. units) in accordance with the one-particle estimate.

$T_>$	$T_<$	$s_{1/2}$	$p_{3/2}$	$p_{1/2}$	$d_{5/2}$	$d_{3/2}$	$f_{7/2}$	$f_{5/2}$	$g_{9/2}$
3/2	1/2	1.95	1.59	0.071	1.85	0.051	2.24	0.0105	2.75
5/2	3/2	1.40	1.15	0.052	1.36	0.037	1.62	0.0076	1.97
7/2	5/2	1.07	0.88	0.039	1.02	0.028	1.24	0.0058	1.51
9/2	7/2	0.87	0.71	0.032	0.82	0.023	1.00	0.0047	1.22
11/2	9/2	0.72	0.59	0.027	0.69	0.019	0.84	0.0039	1.02
$(g_p-g_n)^2$		88.5	14.5	3.25	7.20	0.465	4.86	0.0408	3.74

$$\times j(j+1)\begin{Bmatrix} 1/2 & 1/2 & 1 \\ T_f & T_i & T_0 \end{Bmatrix}^2 (g_p-g_n)^2. \qquad (53)$$

Here, T_0 is the isospin of the core and g_p and g_n are the gyromagnetic ratios for the proton and the neutron. In the case of transitions between $j_> = l+1/2$ states, the orbital and the spin magnetic moments of the proton and the spin magnetic moment of the neutron are added in such a way that the maximal value is obtained. For $j_<-j_<$ transitions this quantity has minimal value.

The probabilities of one-particle $M1$ analog–antianalog transitions for different types of transitions and different values of the isospin of the analog are given in Table 7. It also includes the values of $(g_p-g_n)^2$. The experimental data that were available some years ago agreed well with the estimates of Ref. 7.

The data now available are given in Table 8 and are illustrated in Fig. 11.

In Table 8, we have collected the experimental data on one-particle transitions of analog–antianalog type. The criterion for selecting analogs was a fairly large spectroscopic factor of the parent state. The antianalogs were also identified by the spectroscopic factor and the

TABLE 8. Analog–Antianalog transitions.

Nucleus (T_Z)	$E_A-E_{\bar{A}}$, MeV	$J^\pi_A, T_A - J^\pi_{\bar{A}}, T_{\bar{A}}$	Parent level: nucleus (T_Z); E, MeV	$B(M1)$, μ_0^2	Literature
^{19}F (1/2)	7.54–0.19	5/2+, 3/2–5/2+, 1/2	^{19}O (3/2); 0	0.40±0.08	[30]
^{21}Na (–1/2)	8.97–0.34	5/2+, 3/2–5/2+, 1/2	^{21}F (3/2); 0	0.55±0.11	[34]
			^{21}Mg (–3/2); 0		
^{21}Na (–1/2)	9.22–2.41	1/2+, 3/2–1/2+, 1/2	^{21}F (3/2); 0.28	<0.30	[34]
^{23}Na (1/2)	7.89–0.44	5/2+, 3/2–5/2+, 1/2	^{23}Ne (3/2); 0	0.12±0.04	[42]
^{25}Al (–1/2)	7.90–0	5/2+, 3/2–5/2+, 1/2	^{25}Na (3/2); 0	0.15±0.09	[36]
			^{25}Si (–3/2); 0		
^{27}Al (1/2)	10.50–6.48	7/2–, 3/2–7/2–, 1/2	^{27}Mg (3/2); 3.76	1.43	[73]
^{29}P (–1/2)	8.37–1.96	5/2+, 3/2–5/2+, 1/2	^{29}Al (3/2); 0	0.16±0.08	[36]
			^{29}S (–3,2); 0		
^{31}P (1/2)	7.14–0	1/2+, 3/2–1/2+, 1/2	^{31}Si (3/2); 0.75	0.30±0.03	[39]
^{31}P (1/2)	9.40–4.43	7/2–, 3/2–7/2–, 1/2	^{31}Si (3/2); 3.14	0.9	[1]
^{33}Cl (–1/2)	5.50–0.81	1/2+, 3/2–1/2+, 1/2	^{33}P (3/2); 0	0.27±0.07	[46]
			^{33}Ar (–3/2); 0		
^{35}Cl (1/2)	7.54–3.16	7/2–, 3/2–7/2–, 1/2	^{35}S (3/2); 1.99	4.0±1.0	[74]
^{35}Cl (1/2)	7.84–4.17	3/2–, 3/2–3/2–, 1/2	^{35}S (3/2); 2.35	1.70±0.30	[61]
^{37}Cl (3/2)	10.22–3.11	7/2–, 5/2–7/2–, 3/2	^{37}S (5/2); 0	1.40±0.23	[48]
^{39}K (1/2)	7.74–4.08	3/2–, 3/2–3/2–, 1/2	^{39}Ar (3/2); 1.27	0.15±0.05	[61, 75]
^{41}K (3/2)	~9.62–2.15*	3/2–, 5/2–(3/2)–, 3/2	^{41}Ar (5/2); 1.35	0.97±0.20	[76]
^{43}Sc (1/2)	6.14–1.18	3/2–, 3/2–3/2–, 1/2	^{43}Ca (3/2); 2.05	0.012±0.005	[77]
^{45}Sc (3/2)	~8.12–1.43 1.90	3/2–, 5/2–3/2–, 3/2	^{45}Ca (5/2); 1.43	Not observed	[55]
^{47}Sc (5/2)	~10.31–2.81 2.83 3.21 3.26	3/2–, 7/2–(3/2–), 5/2	^{47}Ca (7/2); 2.01	0.012	[78]
^{47}V (1/2)	~6.69–2.08	3/2–, 3/2–3/2–, 1/2	^{47}Ti (3/2); 2,54	0.017±0.04	[56]
^{49}Sc (7/2)	~11.56–3.08	3/2–, 9/2–3/2–, 7/2	^{49}Ca (9/2); 0	0.0020±0.0006	[49]
^{49}V (3/2)	~7.75–2.30	3/2–, 5/2–3/2–, 3/2	^{49}Ti (5/2); 1.39	0.032	[79]
^{51}V (5/2)	9.40–2.41	3/2–, 7/2–3/2–, 5/2	^{51}Ti (7/2); 0	0.015±0.006	[24]
^{51}V (5/2)	11.62–3.08	5/2–, 7/2–5/2–, 5/2	^{51}Ti (7/2); 2.14	0.0052	[80]
^{51}Mn (1/2)	~6.31–2.14	3/2–, 3/2–3/2–, 1/2	^{51}Cr (3/2); 1.90*2	0.0016	[81]
^{53}Mn (3/2)	7.55–2.67 3.48	(1/2–), 5/2–1/2–, 5/2	^{53}Cr (5/2); 0.56	0.14	[82]
^{55}Mn (3/2)	~10.0–1.53 2.25 0.56 3.04	3/2–, 7/2–3/2–, 5/2	^{55}Cr (7/2); 0	0.32	[50]
^{55}Co (1/2)	6.92–4.18	5/2–, 3/2–5/2–, 1/2	^{55}Fe (3/2); 2.14*3	0.030±0.007	[58]
^{57}Co (3/2)	~7.26–1.38	3/2–, 5/2–3/2–, 3/2	^{57}Fe (5/2); 0.014*4	0.046±0.014	[83]
^{59}Cu (1/2)	6.90–3.04	9/2+, 3/2–9/2+, 1/2	^{59}Ni (3/2); 3.06	1.48	[84]
^{61}Cu (3/2)	~6.40–0	3/2–, 5/2–3/2–, 3/2	^{61}Ni (5/2); 0	0.24	[51]
^{61}Cu (3/2)	6.45–0.97	5/2–, 5/2–5/2–, 3/2	^{61}Ni (5/2); 0.067	0.0047	[52]
^{61}Cu (3/2)	~6.63–0.47	1/2–, 5/2–1/2–, 3/2	^{61}Ni (5/2); 0.28	0.057	[52]
^{61}Cu (3/2)	~8.47–2.71	9/2+, 5/2–9,2+, 3/2	^{61}Ni (5/2); 2.13	0.80	[84]
^{63}Cu (5/2)	8.57–0.67	1/2–, 7/2–1/2–, 5/2	^{63}Ni (7/2); 0	0.019	[53]
^{63}Cu (5/2)	~8.64–0.96 1.41	5/2–, 7/2–5/2–, 5/2	^{63}Ni (7/2); 0.088	0.019	[53]
^{63}Cu (5/2)	8.74–0	3/2–, 7/2–3/2–, 5/2	^{63}Ni (7/2); 0.158	0.0077	[53]
^{63}Cu (5/2)	~9.86–2.51	9/2+, 7/2–9/2+, 5/2	^{63}Ni (7/2); 1.29	0.36	[84]
^{65}Ga (3/2)	~6.83–2.03	9/2+, 5/2–9,2+, 3/2	^{63}Zn (5/2); 1.06	0.36	[84]
^{67}Ga (5/2)	8.56–2.06	9/2+, 7/2–9/2+, 5/2	^{67}Zn (7/2); 0.60	0.10	[84]

*There is spectroscopic information about the 2.15-MeV level in the ^{41}K nucleus.

*[2]In the parent nucleus ^{51}Cr there are two levels that carry the main $p_{3/2}$ strength: 0.75 and 1.90 MeV.

*[3]In the parent nucleus ^{55}Fe the $f_{5/2}$ strength is distributed over two levels: 0.93 and 2.14 MeV.

*[4]In the parent nucleus ^{57}Fe the main $p_{3/2}$ strength is carried by two levels: 0.014 and 0.37 MeV.

Note. The tilde in front of the energy E_A indicates splitting of the analog into several components.

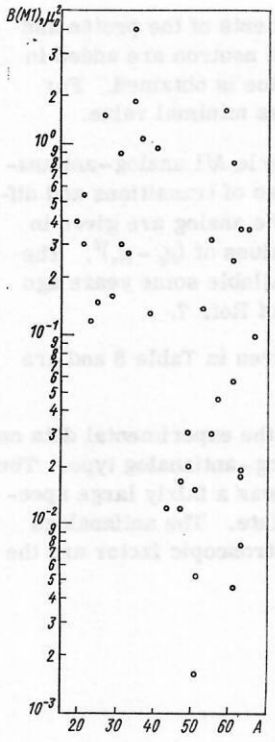

FIG. 11. Dependence of $B(M1)$ on A for one-particle analog–antianalog transitions.

approximate correspondence of the position of the antianalog to Eq. (51). For comparison with the theoretical predictions, we use the ideas of the one-particle shell model. In Table 8, we give transitions for nuclei of the *sd* and *fp* shells. In these nuclei, the nucleons occupy the states $d_{5/2}$, $s_{1/2}$, $d_{3/2}$, $f_{7/2}$, $p_{3/2}$, $f_{5/2}$, $p_{1/2}$, $g_{9/2}$. In the majority of cases, the identification of these one-particle states does not present difficulties. A certain indeterminacy exists for the nuclei from ^{21}Na to ^{29}P, which are in the deformation region. These nuclei are described either by the many-particle shell model or by Nilsson's model.

Analogs with spin $5/2^+$ whose parent states have a large spectroscopic factor in (dp) reactions are found in ^{19}F, ^{21}Na, ^{25}Al, and ^{29}P. We shall call them $d_{5/2}$ analogs. The corresponding antianalogs can also be readily identified by their large spectroscopic factor in the dn or (^{3}He, d) reactions. The $B(M1)$ value of these transitions is 0.10–0.40. Estimates in accordance with Eq. (53) give 1.85 Weisskopf units, i.e., $3.3\mu_0^2$. Thus, in absolute magnitude the $(d_{5/2}-d_{5/2})$ transitions are hindered by about an order of magnitude compared with the estimate (53). The nature of the decay of the $d_{5/2}$ analogs in these nuclei is about the same: Low-lying states with $T=1/2$ and $J^\pi=5/2^+$ (antianalog), $3/2^+$, and $7/2^+$ are populated with comparable intensities.

There are very few data on the γ decay of $d_{3/2}$ analogs. The analog–antianalog $d_{3/2}-d_{3/2}$ $(j_<-j_<)$ transition must be about 40 times weaker than the $d_{5/2}-d_{5/2}$ $(j_>-j_>)$ transition. The $d_{3/2}$ analog has been identified in ^{31}P (Ref. 54). The nature of its decay confirms the assumption that the analog–antianalog transition is weak: The level decays by two transitions, to the states $1/2^+$ (18%) and $5/2^+$ (82%). However, there is no estimate for the limit of the $B(M1)$ value of the γ transition to the $3/2^+$ level, since the radiative width of this level is unknown.

Observations were made of $s_{1/2}$ analogs in the nuclei ^{21}Na, ^{23}Na, ^{27}Al, ^{31}P, and ^{33}Cl. Their parent states in the corresponding nuclei have large spectroscopic factors. In the case of ^{21}Na and ^{23}Na (Ref. 42) the nature of the decay of the $1/2^+$ analogs is the same: One strong transition to a $3/2^+$ state is observed. In neither nucleus does one observe a transition to $1/2^+$, level which could be regarded as an antianalog. For ^{21}Na there exists an estimate of the upper limit for the $1/2^+$–$1/2^+$ transition: $B(M1)\leq 0.30\mu_0^2$. In the ^{27}Al nucleus the $1/2^+$ analog decays by two γ transitions. The strongest decay (70%) is to the $3/2^+$ level; 30% of the decays are to the antianalog level $1/2^+$ (Ref. 54). The radiative widths for this analog are unknown, and therefore data on it are not included in the table. In the ^{31}P nucleus, 84% of the decays of the $1/2^+$ analog take place to the antianalog level, and 16% to the $3/2^+$ level.

The value of $B(M1)$ for the analog–antianalog transition in this nucleus is $0.3\mu_0^2$. In the ^{33}Cl nucleus the $1/2^+$ analog decays principally into the antianalog state, and for the transition to the $3/2^+$ level only the upper limit 12% is given. The $B(M1)$ value of the analog–antianalog transition is approximately $0.3\mu_0^2$. Estimates in accordance with (53) give $B(M1)=3.9\mu_0^2$ for the $s_{1/2}$ analog–antianalog transition.

The smooth manner in which the nature of the decay of the $s_{1/2}$ analog changes is noteworthy: There is an increase in the relative intensity of the population of the antianalog compared with the $3/2^+$ level with increasing A.

Analog–antianalog transitions of type $f_{7/2}-f_{7/2}$ are observed in ^{27}Al, ^{31}P, ^{35}Cl, ^{39}Cl. In all the nuclei, the analogs and antianalogs can be readily identified. In all cases, the analogs decay in the same way: One observes one strong transition to the antianalog, and also weaker $E1$ or even weaker $M1$ transitions to other states. The intensity of the $f_{7/2}-f_{7/2}$ analog-antianalog transitions is large. The value $B(M1)\approx 1-2\mu_0^2$ agrees well with estimates in accordance with (53); Theoretically, $B(M1)=3.2$ and $4.4\mu_0^2$ for analogs with isospin 5/2 and 3/2, respectively.

Extensive experimental material is available for $p_{3/2}-p_{3/2}$ analog–antianalog transitions. The data can be divided into three groups: 1) for nuclei of the *sd* shell up to ^{40}Ca; 2) for nuclei in which the excess neutrons occupy the $f_{7/2}$ shell; and 3) for nuclei in which the $f_{7/2}$ shell is filled and the excess neutrons fill the $p_{3/2}$, $p_{1/2}$, and $f_{5/2}$ shells. According to estimates made by Eq. (53), for all the regions the analog–antianalog transitions of $p_{3/2}-p_{3/2}$ type must be strong and have $B(M1)\approx 2\mu_0^2$.

In the first group—nuclei of the *sd* shell—these transitions are observed in ^{35}Cl, ^{39}K, and ^{41}K. The intensity of the $p_{3/2}-p_{3/2}$ transitions in ^{35}Cl and ^{41}K is about $1\mu_0^2$; in the case of ^{39}K the transition is somewhat hindered: $B(M1)\approx 0.15\mu_0^2$. In nuclei of the $f_{7/2}$ shell there are data on $p_{3/2}-p_{3/2}$ analog–antianalog transitions for ^{43,45,47,49}Sc, ^{47,49,51}V, ^{51}Mn, and ^{57}Co. In all cases the transition is strongly hindered. In ^{45}Sc, the

transition is so weak that it is not observed at all; in other nuclei its value is between 0.0016 and $0.032\mu_0^2$. In the isotope ^{57}Co, in which the excess neutrons fill the $f_{7/2}$ shell, the transition intensity is somewhat higher: $0.046\mu_0^2$. In the third group, the situation with the $p_{3/2}$–$p_{3/2}$ transition is complicated. In the two nuclei in which the excess neutrons begin to populate the $p_{3/2}$ shell, ^{55}Mn and ^{61}Cu, the intensity of the transition is fairly high: $0.32\mu_0^2$ for ^{55}Mn and $0.24\mu_0^2$ for ^{61}Cu. In the ^{63}Cu nucleus, in which the neutrons have completely filled the $p_{3/2}$ shell, the transition intensity is low: $0.0077\mu_0^2$.

There are few data on transitions of the $p_{1/2}$–$p_{1/2}$ type. In nuclei of the $f_{7/2}$ shell, such a transition is known only in ^{53}Mn. It is hindered and agrees with the predictions of Eq. (53). The same can be said of $p_{1/2}$–$p_{1/2}$ transitions in ^{61,63}Cu isotopes.

One observes $f_{5/2}$–$f_{5/2}$ analog–antianalog transitions in ^{51}V, ^{55}Co, and the isotopes ^{61,63}Cu. These transitions are also strongly hindered compared, for example, with the $f_{7/2}$–$f_{7/2}$ transitions. In the copper isotopes the transitions are weak and agree with the data of Table 7.

The $g_{9/2}$–$g_{9/2}$ analog–antianalog transitions are again strong. Experimental data are available for ^{59,61,63}Cu and ^{65,67}Ga. The transition intensities are of the order $1\mu_0^2$, decreasing slowly with increasing A to $0.10\mu_0^2$ for ^{67}Ga. Estimates in accordance with (53) give $B(M1)\sim 1$ Weisskopf unit.

Note that the general nature of the decay of $p_{3/2}$, $p_{1/2}$, and $f_{5/2}$ analogs in nuclei of the $f_{7/2}$ and fp shells is quite different from the decay of analogs in the sd shell. Whereas the analogs in the sd shell decay basically by one strong transition to the antianalog, in the sd shell one observes strong population of many states, including highly excited ones. The nature of the decay of $g_{9/2}$ analogs is again simple, i.e., there is one strong transition to the antianalog.

Thus, in the cases when the simplest theory predicts hindrance of the analog–antianalog transition, this does occur. The situation is worse when the theory predicts strong $M1$ transitions with strength of the order of one Weisskopf unit. Agreement with theory is observed for $f_{7/2}$–$f_{7/2}$ analog–antianalog transitions in nuclei with $A = 27$–37, to a lesser extent for $s_{1/2}$–$s_{1/2}$ transitions in the same region, and also for some $g_{9/2}$–$g_{9/2}$ transitions in the region $A = 59$–67. The $d_{5/2}$–$d_{5/2}$ transitions in the region $A = 19$–31 are hindered on the average by an order of magnitude.

An interesting situation is observed for $p_{3/2}$–$p_{3/2}$ transitions. For nuclei of the $f_{7/2}$ shell, the $p_{3/2}$–$p_{3/2}$ transition is observed to be strongly hindered.

In Ref. 72, theoretical estimates in accordance with Eq. (53) were compared with experiment for $f_{7/2}$–$f_{7/2}$ transitions in ^{31}P, ^{35}Cl, ^{37}Cl and $p_{3/2}$–$p_{3/2}$ transitions in ^{35}Cl and ^{49}Sc. The last case of very strong discrepancy is not explained. For ^{35}Cl and ^{37}Cl the agreement between theory and experiment is very good. For ^{31}P, the experimental value of $B(M1)$ was found to be more than four times less than the theoretical value. An attempt was made to explain this discrepancy by the influence of a core-polarization state. The $7/2^-$ states in ^{31}P can have the following configurations: $[(s^2_{1/2})_{01}f_{7/2}]_{7/2\,3/2}$, $[(s^2_{1/2})_{01}f_{7/2}]_{7/2\,1/2}$, and $[(s^2_{1/2})_{10}f_{7/2}]_{7/2\,1/2}$. Here, we have used the notation $[(s^2_{1/2})_{J_0T_0}f_{7/2}]_{JT}$, where J_0 and T_0 are the spin and isospin of the pair of nucleons above the inert ^{28}Si core; J and T are the spin and isospin of the $7/2^-$ state. The first configuration corresponds to an analog state; the second, to an antianalog; and the third, to a core-polarization state. Without allowance for the residual interaction, the probabilities of $M1$ transitions from the analog to the antianalog and to a core-polarization state are approximately equal and amount to about 2 Weisskopf units. Allowance for the residual interaction, for which a modified surface δ interaction was used,[85] leads to a mixing of the antianalog and the core-polarization state, so that the transition to the antianalog is enhanced to about 4 Weisskopf units, while the transition to the core-polarization state is reduced to about 0.1 Weisskopf units. The influence of the core is appreciable since a $s_{1/2}$–$s_{1/2}$ transition does occur that is not hindered in accordance with (52).

In the case of ^{35}Cl and ^{37}Cl there is in fact no influence of the core since the possible configurations for the $7/2^-$ states include a $d_{3/2}$ state: $[(d^n_{3/2})_{J_0T_0}f_{7/2}]_{JT}$. Transitions of the type $[d^2_{01}f]_{T=3/2}-[d^2_{01}f]_{T=1/2}$ are $f_{7/2}$–$f_{7/2}$ transitions, whereas $[d^2_{01}f]_{T=3/2}-[d^2_{10}f]_{T=1/2}$ hindered $d_{3/2}$–$d_{3/2}$ transitions.

Thus, in Ref. 72 Maripuu succeeded in explaining the strong $M1$ transitions in ^{35}Cl and ^{37}Cl, but not the transition in ^{31}P nor the importance of the core-polarization states. In Ref. 61, the calculations were made somewhat more precise. Analog–antianalog transitions in ^{35,37}Cl and ^{39}K were calculated.

The configuration space was made somewhat larger by the inclusion of the states $[(d^n_{3/2})_{J_0T_0}p_{3/2}]_{JT}$ and $[(d^n_{3/2})_{J_0T_0}f_{7/2}]_{JT}$ for (J_0T_0) equal to $(0,1)$, $(1,0)$, $(1,1)$, $(2,1)$, $(0,2)$, $(3,0)$, $(3,1)$. The results for ^{35,37}Cl were not very different from the simpler calculations. The calculated value for ^{39}K was an order of magnitude greater than the experimental. Similar calculations were made in Refs. 48 and 85.

Note that in all these cases a study was made of the effect of distribution of the strength of the antianalog state over several states due to the interaction of the antianalog state with configuration states. It was this distribution that gave the distribution of the strength of the $M1$ transition from the analog since the transition is due solely to the odd particle. Transitions between core states do not contribute since the neutron excess occupies the $d_{3/2}$ shell in these nuclei. The strongest hindrance, of the $p_{3/2}$ analog–antianalog transition in ^{49}Sc, remained unexplained.

Soon after this there appeared new data[24] on ^{51}V, in which the analog–antianalog transition is also observed to be hindered. Apparently, the most complete explanation of this fact was given by the calculations of Ikeda in 1969 for the decay of the $p_{3/2}$ analog in ^{51}V. The results of this calculation were partly used in Ref. 24.

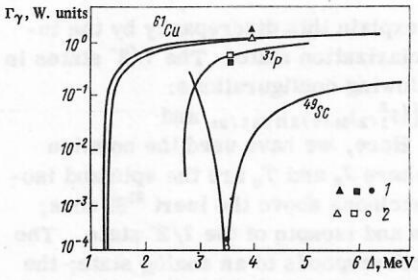

FIG. 12. Partial width of $M1$ transition to the antianalog state as a function of Δ for the nuclei ^{31}P, ^{49}Sc, and ^{61}Cu (Ref. 29). Δ is the distance between the antianalog state and the core-polarization state; 1) the experimental data; 2) theoretical data with allowance for core polarization. The two curves for ^{61}Cu correspond to different potentials.

The calculation was made with a residual interaction of the type $G_0\Sigma_{ij}\tau_i\tau_j + G_1\Sigma_{ij}\tau_i\tau_j\sigma_i\sigma_j$. The configuration space included $f_{7/2}$, $p_{3/2}$, $p_{1/2}$, and $f_{5/2}$ states. Allowance was made for the interaction of antianalog $p_{3/2}$ and $p_{1/2}$ states, core-polarization states, and spin-flip states. The result was a strong hindrance of the analog–antianalog transition. This model best reflects the basic characteristics of the γ decay of analogs.

The strong hindrance of the $p_{3/2}$ analog–antianalog transition in nuclei of the $f_{7/2}$ shell was also studied in Refs. 87 and 88. In Ref. 87, Maripuu considered the mixing of the antianalog state and core-polarization states. He showed that the amplitudes of the pure, unperturbed antianalog state and the amplitudes of core-polarization states enter the wave function of the antianalog state with opposite sign if the mixing is due to a short-range interaction whose strength is greater in the triplet than in the singlet state. The hindrance is large if the odd particle and the particle in the neutron excess occupy $j_>$ states, and it is small if the odd particle is in the $j_>$ state and the excess neutrons occupy the $j_<$ shell. The first case corresponds to the decay of $p_{3/2}$ analogs in nuclei of the $f_{7/2}$ shell; the second, to the decay of $f_{7/2}$ analogs in the upper part of the sd shell. Actual calculations were made for the $p_{3/2}$ analog–antianalog transition in ^{49}Sc. Residual interactions of two types were used: the effective interaction of Kuo and Brown[89] and an effective surface δ interaction.[85] The intensity of the analog–antianalog transition in the first case was found to be 10^{-4} Weisskopf units, and in the second case 10^{-2} Weisskopf units, i.e., the result depends rather strongly on the type of forces used.

In Ref. 88, Hirata considered $p_{3/2}$ analog–antianalog transitions in ^{49}Sc and ^{51}V. The basis function included the following configurations: $|p^n_{3/2}(f^p_{7/2}f^{n-1}_{7/2})_J;\ 3/2\ 7/2\rangle$, where $J=0, 1, 2, 3$, and also configurations of the type $|p^n_{3/2}(f^p_{5/2}f^{n-1}_{7/2})_{1+};\ 3/2\ 7/2\rangle$. He only considered states with spin $3/2^-$. He used the interaction of Kuo and Brown.[89] For the transition in ^{49}Sc he obtained the result $B(M1) = 1.2\cdot10^{-3}$ Weisskopf units. In the case of ^{51}V, the amplitude of the admixture of core-polarization states was treated as a free parameter. Depending on the parameter, one can obtain $B(M1)$ values for the analog–antianalog transition from 1 Weisskopf unit to 10^{-4} Weisskopf units. The minimal value, 10^{-4} Weisskopf units, is obtained with an amplitude of about -0.45.

We mention also Ref. 90, in which Maripuu studied the $g_{9/2}$ analog–antianalog transition in ^{59}Cu. He showed that in this case the transition is not hindered. It would seem that this contradicts his rule of Ref. 87 that the hindrance of the probability of a $j=l+1/2-j=l+1/2$ transition is strong if the excess neutrons occupy $j=l+1/2$ states. In ^{59}Cu, the excess neutrons occupy the $p_{3/2}$ orbit. We recall that the case of ^{31}P, in which the excess particles occupy the $s_{1/2}$ orbit, also remained obscure. These problems were resolved in Ref. 29 by Aleshin, who calculated the strength function of γ transitions from analogs with allowance for the Kuo–Brown residual interaction.[89] The configuration space included the antianalog state, core-polarization states, and spin-flip states. Calculations were made for the nuclei ^{31}P ($f_{7/2}$), ^{37}Cl ($f_{7/2}$), ^{49}Sc ($p_{3/2}$), and ^{61}Cu ($g_{9/2}$). For the analog–antianalog transitions the calculated values were near the experimental.

Following Ref. 29, let us consider the reasons for the strong hindrance of the transition in ^{49}Sc and the weak hindrance in ^{31}P and ^{61}Cu. After the inclusion of the residual interaction, the antianalog state and the core-polarization state go over into $\Psi_{\bar{A}}$ and Ψ_K states:

$$\left.\begin{aligned}\Psi_{\bar{A}} &= \alpha\bar{A} + \beta K;\\ \Psi_K &= -\beta\bar{A} + \alpha K,\end{aligned}\right\} \tag{54}$$

where $\alpha^2+\beta^2=1$. For the amplitudes β and α one can obtain the relation

$$\beta/\alpha = [(\Delta^2_{K\bar{A}} - 4V^2_{\bar{A}K})^{1/2} - \Delta_{K\bar{A}}]/2V_{\bar{A}K}. \tag{55}$$

where $\Delta_{K\bar{A}} = E_K - E_{\bar{A}}$ is the difference between the energies of the core-polarization state and the antianalog state:

$$V_{\bar{A}K} = \langle\bar{A}|V^{\text{res}}|K\rangle. \tag{56}$$

The probability of a transition to the $\Psi_{\bar{A}}$ state is

$$B(\Psi_{\bar{A}}) = (\alpha B^{1/2}_{\bar{A}} + \beta B^{1/2}_K)^2, \tag{57}$$

where $B_{\bar{A}}$ and B_K are the probabilities of transitions to the pure antianalog state and the pure core-polarization state. The values of $V_{\bar{A}K}$ were obtained from the Kuo–Brown matrix elements. The signs of α and β were opposite, this leading to a hindrance of the analog–antianalog transition. The amount of hindrance depends on α and β and the relative values of $B_{\bar{A}}$ and B_K.

The probability of a transition to the antianalog for the nuclei ^{61}Cu ($g_{9/2}$), ^{31}P ($f_{7/2}$), and ^{49}Sc ($p_{3/2}$) is shown as a function of $\Delta_{\bar{A}K}$ in Fig. 12; $\Delta_{\bar{A}K}$ are approximately the same for the three nuclei (3.5–4 MeV). However, the nature of the dependence of $B(\Psi_{\bar{A}}$ on $\Delta_{\bar{A}K}$ is different for the cases ^{31}P and ^{61}Cu, on the one hand, and ^{49}Sc on the other. The case of ^{49}Sc is distinguished because $B_{\bar{A}} < B_K$ for this nucleus, whereas $B_{\bar{A}} > B_K$ for ^{31}P and ^{61}Cu.

6. CORE-POLARIZATION STATES

The importance of these states in the investigation of the γ decay of analogs was manifested particularly

clearly when nuclei of the $f_{7/2}$ shell were investigated. As can be seen from what we have said above, the strong hindrance of the analog–antianalog transition can be explained by the admixture of core-polarization states to the antianalog. From the theoretical point of view, allowance for states of this type is completely justified since the probabilities of transitions from the analog to the pure antianalog state and a pure core-polarization state are comparable. From the experimental point of view, the study of core-polarization states is more difficult than that of analog–antianalog transitions. These states lie about 1–2 MeV higher in excitation energy than the antianalog. For the study of these highly excited states one faces the problem of the general shortage of experimental data on the energies, quantum numbers, and state population probabilities in different nuclear reactions. In addition, a relatively simple nuclear excitation such as a core-polarization state at a large height will be distributed over states lying near one another, and a phenomenon of the strength-function type is exhibited. Note, finally, that the experimental difficulties are appreciably aggravated when one investigates the γ decay of analogs for highly excited states.

Apparently, the first nucleus in which core-polarization states were discovered in the γ decay of analogs and correctly interpreted was ^{51}V (Ref. 24). Subsequently, a careful study was made of one of the clearest cases: the population of core-polarization states as a result of the decay of the analog in ^{49}Sc (Ref. 49). There are now quite a number of experimental data available. Note that this region has attracted the attention of many experimental groups, and data on it are accumulating rapidly.

The wave function of a core-polarization state can be written in the form

$$\Psi_K = |[j_{n1}(j_p j_{n-1})_I] JM\rangle. \tag{58}$$

We shall consider only the case when the proton particle and the neutron hole are coupled to angular momentum $I=1^+$ and $j_p=j_n$. This state has definite isospin $T=T_0-1$, where T_0 is the isospin of the analog. The probability of a transition from the analog to a pure core-polarization state has the following form for the analog of the one-particle neutron state $|j_{n1}\rangle$:

$$B(M1, A-K) = \sum_{M'\mu} |\langle [j'_{n1}(j'_p j'_{n-1})_{1^+}] J'M' | m(M1) | j_{n1} m_{n1}\rangle^2| = \frac{3}{4\pi}\mu_-^2 \frac{2J'+1}{3(2j_{n1}+1)2T_0}\langle j'_p \| \sigma \| j'_n\rangle^2 \left(1+\frac{gl}{\mu_-}k\right)^2 \cdot \delta_{j_{n1}j'_{n1}}, \tag{59}$$

where

$$k = \begin{cases} +l & \text{for } j'_p = l+1/2, \quad j'_n = l+1/2; \\ -1/2 & j'_p = l\mp 1/2, \quad j'_n = l\pm 1/2; \\ -(l+1) & j'_p = l-1/2, \quad j'_n = l-1/2. \end{cases}$$

If one considers the one-neutron parent state $|j_{n1}\rangle$ and the γ decay of the analog of this state, then three core-polarization states will be populated by $M1$ transitions. Their spins are $J=j_{n1}+1$, j_{n1}, $j_{n1}-1$. In the absence of interaction, the energies of these states are the same: The difference between their energies and the energy of the antianalog state is approximately equal to the pairing energy of the excess neutrons. A residual interaction may strongly change this estimate. Note that a core → core transition takes place without a change in the the state of the odd particle.

The probability of a transition to a core-polarization state is comparable to the probability of a transition to the antianalog state. The total probability of decay of the analog is distributed between the transitions to the antianalog and the core-polarization states. In some nuclei, for example, ^{35,37}Cl, the transition to the antianalog is predominant. It is difficult to look for core-polarization states in these nuclei. Conversely, in nuclei of the $f_{7/2}$ shell, the transition to the antianalog is hindered, and transitions to core-polarization states must be clearly manifested. As can be seen from (59), the transition probability does not depend on the state occupied by the odd particle, but is determined by the states occupied by the excess neutrons. The transitions must be strong if the excess neutrons occupy the states with $j_n=l+1/2$, and weak if $j_n=l-1/2$. Note that residual interactions strongly distort this simple picture since there is then an admixture of the antianalog state and a spin-flip state.

Experimental data on the population of the core-polarization states in the case of γ decay of analogs are collected in Table 9. The strength functions for $M1$ transitions from analog states are given in Fig. 13. The data are represented in the form of the distribution of the probability of $B(M1)$ transitions from the analog to low-lying states of the nucleus as a function of the excitation energy of these states. It can be seen that in the majority of cases strong $M1$ transitions to highly excited states are observed. These states are interpreted as core-polarization states. The antianalog state is always lower, and its identification is based on the data for the spectroscopic factors from transfer reactions for one particle. As a rule, the highly excited states that are strongly populated in the γ decay of analogs have a small value of the spectroscopic factor. On the other hand, as was shown above, an antianalog state with a large spectroscopic factor is very strongly populated in nuclei of the $f_{7/2}$ shell. Therefore, the appearance of a maximum in the strength function of a γ transition from an analog cannot be explained by fragmentation of the one-particle strength. The natural explanation is to take into account a new degree of freedom—core-polarization states. One can then understand why such a maximum is not observed in the nuclei of the upper half of the *sd* shell, in which the neutron excess occupies the $d_{3/2}$ state. Core polarization states in some nuclei may lie too near the analog, so that they are hard to observe in the γ decay of the analog.

The maximum in the strength function is expressed differently for different nuclei. The effect is most clearly observed for the decay of $p_{3/2}$ analogs in Sc and V isotopes. It is possible that the effects of unclosed shells lead to a "spreading" of the strength of a core-polarization state over many states of the nucleus. In the strength function, one can therefore expect a more

TABLE 9. Core-polarization (c.p.) states.

Nucleus	J^π, T_A	E_p, MeV	E^*, MeV	Level of parent nucleus, MeV	Energy region of c.p. states, MeV	$\sum B(M1)$, μ_0^2 for c.p. states	Literature
^{43}Sc	3/2−, 3/2	1.242	6.142	^{43}Ca, 2.05	3.2—3.9	0.17	[77]
^{45}Sc	3/2−, 5/2	1.2511	8.113	^{45}Ca, 1.43	3.8—4.7	2.1	[55]
		1.2676	8.130				
^{47}Sc	3/2−, 7/2	1.866	10.310	^{47}Ca, 2.016	5.2—7.0	~0.35	[91]
^{47}V	3/2−, 3/2	1.549	6.685	^{47}Ti, 2.545	3.0—5.2	0.72	[56]
		1.565	6.700				
^{49}Sc	3/2−, 9/2	1.9590	11.541	^{49}Ca, 0	6.3—7.2	4.8	[49]
		1.9641	11.546				
		1.9742	11.557				
^{49}V	3/2−, 5/2	1.007	7.742	^{49}Ti, 1.384	3.7—4.6	1.2	[79]
		1.013	7.748				
^{51}V	3/2−, 7/2	1.368	9.3881	^{51}Ti, 0	4.6—6.1	1.3	[24]
^{51}V	5/2−, 7/2	3.598	11.615	^{51}Ti, 2.136	4.5—4.9	0.03	[80]
^{51}Mn	3/2−, 3/2	1.059	6.3087	^{51}Cr, 1.899	2.8—3.9	0.04	[81]
		1.071	6.3198				
^{53}Mn	1/2−, 5/2	1.006	7.550	^{53}Cr, 0.56	2.9—3.2	0.75	[82]
^{55}Co	5/2−, 3/2	1.887	6.916	^{55}Fe, 2.144	3.7—4.7	0.23	[58]
^{57}Co	3/2−, 5/2	1.248	7.254	^{57}Fe, 0.014	3.2—3.9	~0.14	[83]
		1.262	7.268				
		1.268	7.274				
^{61}Cu	3/2−, 5/2	1.588	6.364	^{61}Ni, 0	2.5—3.1	1.0	[51]
		1.599	6.375				
		1.605	6.380				
		1.620	6.395				
^{61}Cu	5/2−, 5/2	1.674	6.449	^{61}Ni, 0.067	2.2—3.0	0.12	[52]
^{61}Cu	1/2−, 5/2	1.856	6.624	^{61}Ni, 0.282	2.7—3.3	0.46	[52]
		1.873	6.642				
^{63}Cu	1/2−, 7/2	2.481	8.569	^{63}Ni, 0	3.0—3.8	0.28	[53]
^{63}Cu	5/2−, 7/2	2.546	8.631	^{63}Ni, 0.088	2.5—3.4	0.07	[53]
		2.556	8.641				
^{63}Cu	3/2−, 7/2	2.659	8.743	^{63}Ni, 0.158	3.0—4.2	0.17	[53]

or less clearly expressed maximum at some mean energy corresponding to the predicted position for the core-polarization states.

The probability of an $M1$ transition from the analog to these states is determined by (59). However, when allowance is made for residual interactions there is an appreciable admixture of the antianalog state, which enhances the $M1$ transition. On the other hand, an admixture of spin-flip states leads[29] to a reduction in the transition probability. Thus, the main experimental quantities that characterize core-polarization states are the energy of the states and the probability of transition to them from the analog.

The first calculations predicting the position of core-polarization states and the probability of transition to these states from the analog were made by Ikeda in 1969. He calculated the strength function of γ transitions from the $p_{3/2}$ analog in ^{51}V in connection with the experimental results of Ref. 24. In the calculations, he used a residual interaction in the form

$$H_{\text{res}} = G_0 \sum_{ij} \tau_i \tau_j + G_1 \sum_{ij} \tau_i \tau_j \sigma_i \sigma_j. \qquad (60)$$

He found that, besides the lowest one-particle $p_{3/2}$ and $p_{1/2}$ states, states at a height of 4.5–5.0 MeV with basic configuration of the type $|p^n_{3/2}(f^p_{7/2}f^{n-1}_{7/2})_{1^+}\rangle$ must also be populated. At a distance of about 2–4 MeV above the analog state there are states having a basic configuration of the type $|p^n_{3/2}(f^p_{5/2}f^{n-1}_{7/2})_{1^+}\rangle$ and $|p^n_{1/2}(f^p_{5/2}f^{n-1}_{7/2})_{1^+}\rangle$. These states form the so-called giant Gamow–Teller resonance.

The same model was used in Ref. 49 to calculate the strength function of γ transitions from the $p_{3/2}$ analog in ^{49}Sc. The results of the calculation are shown in Fig. 14. As in the case of ^{51}V, the strength function contains two maxima. The lower corresponds to core-polarization states and is detected experimentally; the upper corresponds to spin-flip states. Note that the calculated value of the sum of $B(M1)$ to core-polarization states is about $10\mu_0^2$; the experimental value is $(4.8 \pm 1.5)\mu_0^2$ (Ref. 49).

In Ref. 29, Aleshin calculated the strength functions of γ transitions from analogs in ^{31}P ($f_{7/2}$), ^{49}Sc ($p_{3/2}$), and ^{61}Cu ($g_{9/2}$). He used the Kuo–Brown effective interaction for ^{31}P and ^{49}Sc. The configurations used in the calculations are shown in Fig. 15. The results of the calculations are shown in Fig. 16. It can be seen that for all the investigated cases there is, between the antianalog and the analog state, a group of states to which the γ decay must be fairly strong. The basic configuration of these states are core-polarization states.

7. GAMOW–TELLER GIANT RESONANCE

Proceeding systematically with our study of the problem of the γ decay of analog resonances, we find that it is necessary to study the strength function of γ transitions associated with an analog state. In other words, we must study the distribution over the excitation energy of the states Ψ_f for which the matrix element $\langle \Psi_f | m(M1) \Psi_A \rangle$ is nonzero. If these states are below the analog, we must consider transitions from the analog to these states. If they are above it, we must consider transitions from them to the analog.

In the foregoing sections we have analyzed the importance of antianalog states and core-polarization states. These states are always below the analogs. It only remains to consider a configuration that is very important for this problem—a spin-flip state. Unperturbed spin-flip states have energies near the analog or even above it. The wave function of a spin-flip state is similar to (58) except that the j_p and j_{n-1} orbits are different: $j_p = l + 1/2$ and $j_{n-1} = l - 1/2$. The transition probability is

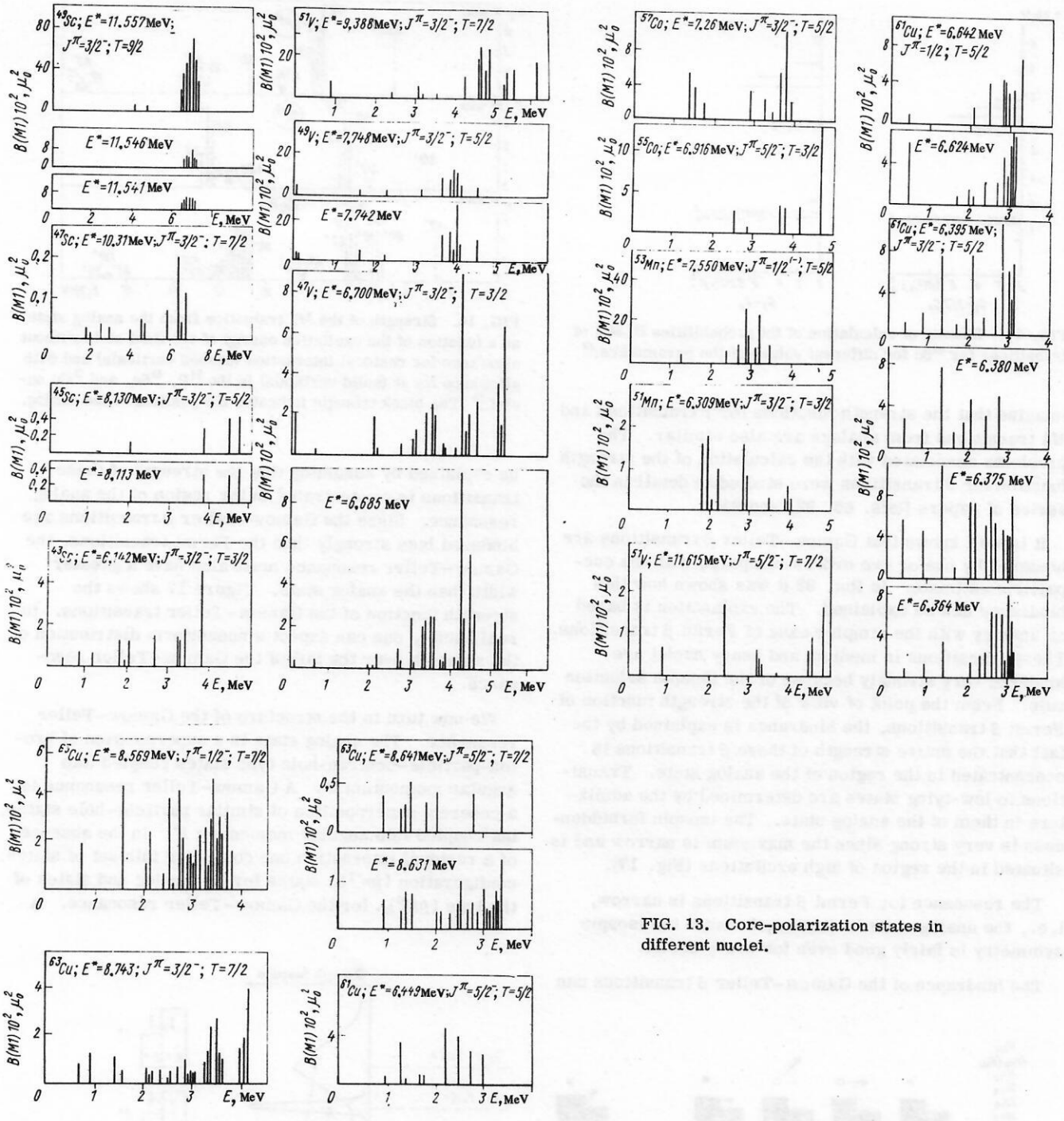

FIG. 13. Core-polarization states in different nuclei.

$$B(M1)=\frac{3}{4\pi}\mu_-^2\frac{(2J'+1)(2T_0-1)}{3(j_{n1}+1)(2T_0+1)^2}\langle j'_p\|\sigma\|j'_n\rangle^2\left(1+\frac{g_l}{\mu_-}k\right)\cdot\delta_{j_{n1}j'_{n1}}, \quad (61)$$

where

$$k=\begin{cases} +l & \text{for } j'_p=l+1/2, \quad j'_n=l+1/2; \\ -1/2 & j'_p=l\mp 1/2, \quad j'_n=l\pm 1/2; \\ -(l+1) & j'_p=l-1/2, \quad j'_n=l-1/2. \end{cases}$$

The extra isospin factor compared with (59) takes into account the circumstance that a spin-flip configuration does not have a definite isospin.

Allowance for the residual interaction means that transitions to spin-flip states are enhanced compared with the unperturbed value. There is a redistribution of the strength of the transition from the antianalog state to a core-polarization state and from the latter to a spin-flip state. There appears a state that is rather strongly collectivized, and it carries the main strength of the $M1$ transition from the analog.

One can arrive at the idea of the existence of a collective $(pn^{-1})_{1^+}$ state carrying the main strength of the $M1$ transitions from the analog by analyzing the similarity of the operators of the Gamow–Teller β transition and of an $M1$ transition from the analog, as was done by Gaarde *et al.*[24] The data presented above indicate that there is a certain similarity between β transitions and $M1$ transitions from analogs. One could

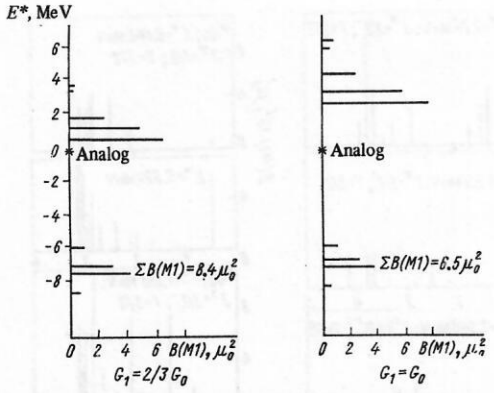

FIG. 14. Results of calculation of the probabilities $B(M1)$ of transitions for ^{49}Sc for different values of the parameters.[49]

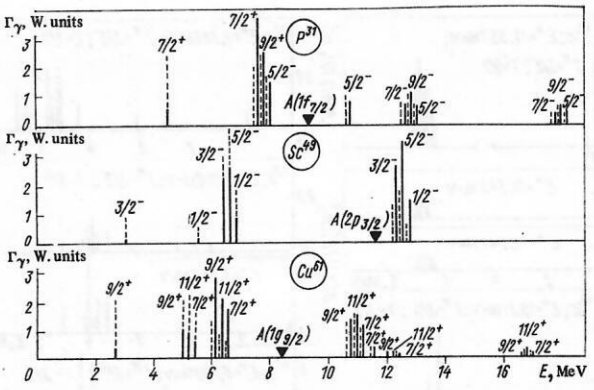

FIG. 16. Strength of the $M1$ transition from the analog state as a function of the excitation energy of the final state without allowance for residual interaction (dashed verticals) and with allowance for it (solid verticals) in the ^{31}P, ^{49}Sc, and ^{61}Cu nuclei.[29] The black triangle indicates the position of the analog.

imagine that the strength functions for β transitions and $M1$ transitions from analogs are also similar. The problems associated with the calculation of the strength function for β transitions were studied in detail in the series of papers Refs. 65, 92, and 94.

It is well known that Gamow–Teller β transitions are hindered by one or two orders compared with the one-particle estimate. In Ref. 92 it was shown how this hindrance can be explained. The explanation is based on analogy with the simpler case of Fermi β transitions. These transitions in medium and heavy nuclei are hindered very strongly because of the isospin selection rule. From the point of view of the strength function of Fermi β transitions, the hindrance is explained by the fact that the entire strength of these β transitions is concentrated in the region of the analog state. Transitions to low-lying states are determined by the admixture in them of the analog state. The isospin forbiddenness is very strong since the maximum is narrow and is situated in the region of high excitations (Fig. 17).

The resonance for Fermi β transitions is narrow, i.e., the analog state is narrow, because the isospin symmetry is fairly good even for heavy nuclei.

The hindrance of the Gamow–Teller β transitions can be explained by assuming that the strength of these transitions is concentrated in the region of the analog resonance. Since the Gamow–Teller β transitions are hindered less strongly than the Fermi transitions, the Gamow–Teller resonance must also have a greater width than the analog state. Figure 17 shows the strength function of the Gamow–Teller transitions. In real nuclei, one can expect a nonuniform distribution of the strength over the tail of the Gamow–Teller resonance.

We now turn to the structure of the Gamow–Teller resonance. The analog state is a superposition of proton-particle–neutron-hole type states coupled into angular momentum 0^+. A Gamow–Teller resonance is a coherent superposition of similar particle–hole states, but coupled into angular momentum 1^+. In the absence of a residual interaction one considers this set of states: configuration $(pn^{-1})_{0^+}$ states for the analog and states of the type $(pn^{-1})_{1^+}$ for the Gamow–Teller resonance. A

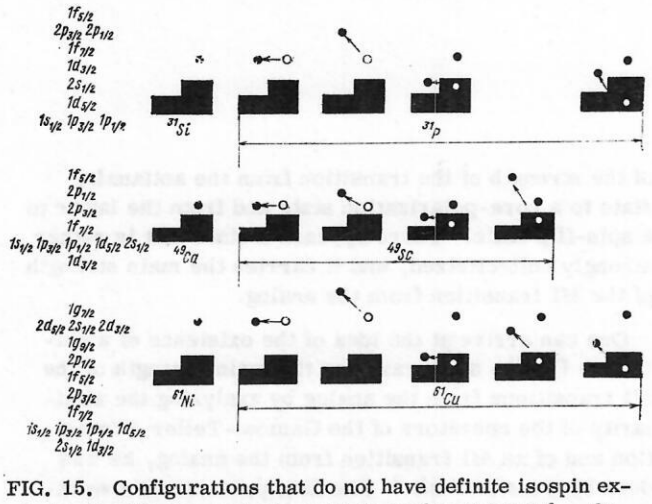

FIG. 15. Configurations that do not have definite isospin excited in the $M1$ decay of one-particle analog states $1f_{7/2}$, $2p_{3/2}$, $1g_{9/2}$ in the ^{31}P, ^{49}Sc, ^{61}Cu nuclei.[29]

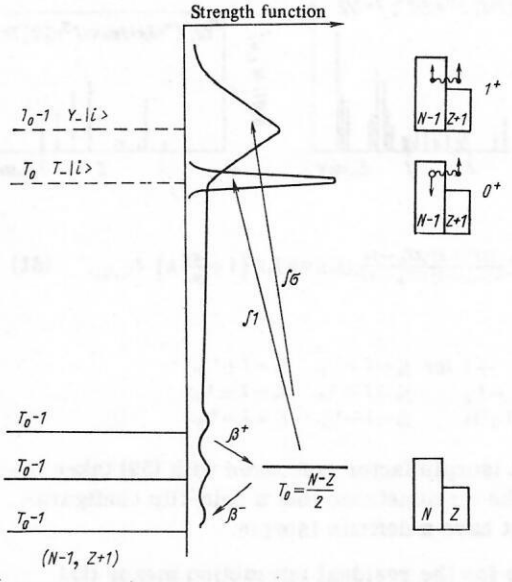

FIG. 17. Strength function for Fermi and Gamow–Teller β transitions.

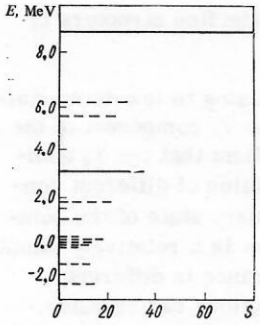

FIG. 18. Distribution of the strength of the Gamow–Teller transition for ^{208}Bi (Ref. 65).

repulsive residual interaction results in the appearance of one completely coherent collective state—a (pn^{-1}) analog in the first case and a giant Gamow–Teller resonance in the second. In Refs. 65 and 94, this model was developed in more detail.

Correlations of proton-neutron-hole pairs (pn^{-1}) in heavy nuclei were studied in Ref. 65. The normalized wave function of the unperturbed $(pn^{-1})_J$ state for an odd–odd nucleus $(N-1,\ Z+1)$ can be written in the form

$$|\Phi_{JM}(ac)\rangle = \sum_{m_\alpha m_\gamma} (-)^{j_c-m_\gamma} (j_a m_a j_c - m_\gamma | JM)\, a_\alpha^+ b_\gamma |\Psi_0\rangle \equiv A_{JM}^+(ac)|\Psi_0\rangle, \quad (62)$$

where $|\Psi_0\rangle$ is the ground state of the even–even nucleus; a_α^+ and b_γ are operators of creation of a proton and a neutron hole. The Hamiltonian of the system can be split into three parts in the form of normal products of creation and annihilation operators:

$$\mathcal{H} = U + \mathcal{H}_0 + \mathcal{H}_I, \quad (63)$$

where

$$U = \langle\Psi_0|\mathcal{H}|\Psi_0\rangle \quad (64)$$

is the energy of the vacuum;

$$\mathcal{H}_0 = \sum_\alpha \varepsilon_\alpha^p : a_\alpha^+ a_\alpha : + \sum_\gamma \varepsilon_c^n : b_\gamma b_\gamma : \quad (65)$$

is the sum of the one-particle and hole energies:

$$\mathcal{H}_I = \frac{1}{2} \sum_{\alpha\beta\gamma\delta} \langle\alpha\beta|V_{\gamma\delta}\rangle : c_\alpha^+ c_\beta^+ c_\delta c_\gamma : \quad (66)$$

is the residual interaction;

$$\langle\alpha\beta|V_{\gamma\delta}\rangle = \int \varphi_\alpha^*(1)\,\varphi_\beta^*(2)\,V_{12}\varphi_\gamma(1)\,\varphi_\delta(2)\,d\tau_1\,d\tau_2$$

are the operators $c^+ = (a^+$ or $b^+)$ and $c = (a$ or $b)$.

Let $|\Psi_{JM}\rangle$ be an excited state of the nucleus $(N-1,\ Z+1)$ with energy E_J:

$$\mathcal{H}|\Psi_{JM}\rangle = E_J|\Psi_{JM}\rangle. \quad (67)$$

For the amplitudes in the expansion of this function with respect to the functions $|\Phi_{JM}(ac)\rangle$:

$$\langle\Psi_{JM}|\Phi_{JM}(ac)\rangle = \xi_J(ac) \quad (68)$$

one can obtain the following equation of motion:

$$(E_J - U)\,\xi_J(ac) = \langle\Psi_{JM}|[\mathcal{H}, A_{JM}^+(ac)]|\Psi_0\rangle = (\varepsilon_a^p + \varepsilon_c^n)\,\xi_J(ac) + \sum_{db} F(db, ac : J)\,\xi_J(ab) + \langle\Psi_{JM}|X_{ac}|\Psi_0\rangle, \quad (69)$$

where

$$F(ac, db : J) = D(ac, db : J) + E(ac, db : J); \quad (70)$$

$$\left.\begin{matrix} D \\ E \end{matrix}\right\} \sum_{m_\alpha m_\beta m_\gamma m_\delta} (-)^{j_c - m_\gamma} (j_a m_\alpha j_c - m_\gamma | JM)\,(-)^{j_b - m_b} \times (j_d m_\delta j_b - m_\beta | JM) \left\{ \begin{matrix} -\langle\alpha\beta|V|\delta\gamma\rangle; \\ \langle\alpha\beta|V|\gamma\delta\rangle, \end{matrix}\right. \quad (71)$$

and X contains only terms with the product of four operators (c^+c^+cc). Ignoring this term, we obtain

$$\varepsilon_J \xi_J(ac) = (\varepsilon_a^p + \varepsilon_c^n)\,\xi_J(ac) + \sum_{bd} F(db,\ ac:\ J)\,\xi_J(db). \quad (72)$$

From this we can obtain the energy of the states ε_J^n and the amplitude $\xi_J^n(ac)$. For the state $|\Psi_{JM}^n\rangle$ we can then write

$$|\Psi_{JM}^n\rangle = \sum_{ac} \xi_J(ac)\,|\Phi_{JM}^n(ac)\rangle \equiv \sum_{ac} \xi_J^n(ac)\,A_{JM}^+(ac)\,|\Psi_0\rangle. \quad (73)$$

The residual interaction was chosen in the form

$$V_{12} = \left[\frac{1}{16}(3v_t - v_s)\,\tau_1\tau_2 + \frac{1}{16}(v_t + v_s)\,(\tau_1\tau_2)\,(\sigma_1\sigma_2)\right]\delta(r_{12}). \quad (74)$$

It was shown that with this interaction one obtains two collective coherent states: an analog state for (pn^{-1}) pairs with spin 0^+ and a Gamow–Teller resonance for pairs (pn^{-1}) with spin 1^+. Numerical calculations were made for the nucleus ^{208}Bi (Fig. 18). The Gamow–Teller strength is distributed mainly between the two states. For the upper, completely coherent state the main contribution comes from spin-flip configurations; for the lower, from core-polarization configurations.

In Ref. 94, Fujita and Ikeda formulate a model with pairing, including residual (pn^{-1}) interactions. They consider two extreme cases of residual neutron–proton interaction: short-range δ forces and long-range forces $V_{p,n} = k\,\Sigma_{ij}\,\tau_{i+}\tau_{j-}\sigma_i\sigma_j$, where the radial dependence is replaced by a constant. In both the first and the second case there is a collective state which expresses the main strength of the Gamow–Teller β transition. In Ref. 94 they also note that the existence of a Gamow–Teller giant resonance is intimately related to the question of the validity of supermultiplet symmetry in medium and heavy nuclei. It is well known that the existence of analog states indicates the possibility of using the isospin quantum number to classify nuclear states. This means that the isospin structure is valid even for heavy nuclei. If a Gamow–Teller resonance is found, this will imply the validity of supermultiplet structure. From the point of view of the symmetry in spin and isospin space, the nuclear Hamiltonian can be split into three parts:

$$\mathcal{H} = \mathcal{H}_0 + \mathcal{H}^{(2)} = \mathcal{H}^{(0)} + \mathcal{H}^{(1)} + \mathcal{H}^{(2)}, \quad (75)$$

where $\mathcal{H}_0$ is the charge-independent part; $\mathcal{H}^{(0)}$ is the spin- or isospin-independent part; $\mathcal{H}^{(1)}$ is the spin- or isospin-dependent part; and $\mathcal{H}^{(2)}$ is the charge-dependent part. This is expressed by the properties

$$[\mathcal{H}^{(0)}, T_\pm] = [\mathcal{H}^{(0)}, Y_\pm] = 0; \quad (76)$$

$$[\mathcal{H}^{(1)}, T_{\pm}] = 0. \quad (77)$$

Therefore, if some state is an eigenfunction independent of the spin and isospin of the part of the Hamiltonian $\mathcal{H}^{(0)}$ and $\mathcal{H}^{(0)}|n^{(0)}\rangle = E_n^{(0)}|n^0\rangle$, then the functions $T_{\pm}|n^0\rangle$ and $Y_{\pm}|n^0\rangle$ are also eigenfunctions of the same Hamiltonian. These states exhibit degeneracy with respect to the energy and belong to one Wigner supermultiplet. The Coulomb interaction forms the main part of the charge-dependent interaction $\mathcal{H}^{(2)}$. Despite its strength in heavy nuclei, the analog state is fairly narrow, and the isospin remains a good quantum number. Apparently, the main interaction breaking supermultiplet symmetry is the spin–orbit interaction in $\mathcal{H}^{(1)}$.

A systematic study of Gamow–Teller resonance was undertaken in Ref. 66. The methods of the theory of finite Fermi systems were used to solve the equations for the effective Gamow–Teller field. These calculations were made for a large number of nuclei from ^{72}As to ^{140}Pr. The position of the collective 1^+ state and the matrix elements of the Gamow–Teller transition between this state and the parent state were determined. The Gamow–Teller resonance is 3–6 MeV above the analog state and is characterized by a strong ($M_{GT}^2 \sim (N-Z)$) β transition to the parent state. The numerical calculations also revealed other collective states at lower excitation energies and characterized by $M_{GT}^2 \approx 1$. The quasiclassical solution of the microscopic equations made it possible to represent the results more lucidly. It was found that there are three types of collective states: ω_+, corresponding to a Gamow–Teller resonance with main contribution from (pn^{-1}) transitions from the lower component of the spin-orbit doublet to the upper component; ω_0, with main contribution from j–$j(pn^{-1})$ transitions (which correspond to core-polarization states); and also ω_-, with main contribution from transitions from the upper component of the spin-orbit doublet to the lower. This state appears only in nuclei with large $N-Z$.

In Ref. 66, Gaponov and Lyutostanskiĭ analyzed the question of the possible description of a Gamow–Teller resonance from the point of view of supermultiplet symmetry. They showed that the parent 0^+, the analog 0^+, and the Gamow–Teller 1^+ states belong to one Wigner supermultiplet (P, P', P'') with quantum numbers (T_0, 0, 0).

8. GAMMA DECAY OF FINE-STRUCTURE COMPONENTS OF ANALOGS

The majority of analog resonances are split and fragmented into several components, which are clearly revealed in experiments with high resolution. These components are called the fine-structure components of the analog and are states of the compound nucleus modulated by the analog configuration. The fine structure arises as a result of the mixing of the analog $T_>$ state proper and the $T_<$ levels of the compound nucleus. As a result, the wave function of each component of the analog's fine structure can be represented as a sum of $T_>$ and $T_<$ components. A measure of the contribution of the $T_>$ component is Γ_p, which can be determined from the elastic scattering of protons through the analog. More detailed information about the fine structure of analogs can be found in Ref. 3.

Gamma transitions from the analog to low-lying states may be due to either the $T_>$ or the $T_<$ component of the analog. It is natural to assume first that the $T_<$ component is a very complicated function of different configurations of the type of an ordinary state of the compound nucleus. The $T_>$ component is a relatively simple configuration about whose appearance in different nuclear processes definite predictions can be made. The various effects discussed above refer solely to the $T_>$ component of the analog, and the contribution of the $T_<$ component is usually ignored. This is evidently a satisfactory approximation in the cases when the analog is only slightly split or when one is studying the strongest strongest components of the fine structure, in which the $T_>$ component makes the main contribution. But in the cases when one observes a fairly well developed fine structure the contribution of the $T_<$ component is very important.

When analogs decay, transitions are observed to many low-lying states. It may happen that transitions to certain states are determined by the $T_>$ component and to others by the $T_<$ component of the analog. It is to be expected that the strongest transitions are determined by the $T_>$ component; in the case of weak transitions the probability of a contribution of the $T_<$ component is high. This assumption is based on the intuitive idea that the $T_<$ component is complicated and populates more or less uniformly all the levels of the nucleus. The γ decay widths of such a $T_<$ component must satisfy the Porter–Thomas distribution.

Gaarde *et al.*[49] analyzed qualitatively the contribution of the $T_>$ and $T_<$ components to the transitions. The $p_{3/2}$ analog in ^{49}Sc has a developed fine structure of eight components. The γ decay spectra of the three strongest of them were measured. The values of Γ_p were also determined. If the transition is determined by the $T_>$ component, the partial γ widths must be proportional to the corresponding values of Γ_p. Transitions to core-polarization states are determined by the $T_>$ component; transitions to antianalog states, by the $T_<$ component. More precisely, transitions to the antianalog are determined by a mixture of the $T_>$ and $T_<$ components, which compensate each other.

A completely new field of investigations is opened up if the quantitative methods of studying the effects of intermediate structures are applied to study of the fine structure of analogs. Intermediate structures are a fairly general phenomenon in nuclear physics. Searches for different intermediate structures attract the attention of many investigators. Particularly many searches have been made for intermediate structures in, for example, (n, γ) reactions with neutrons.[95]

The various methods for analyzing correlations developed in these investigations enable one to draw certain conclusions about the existence of intermediate structures, doorway states, etc. Traditionally, analog states are regarded as the clearest example of intermediate structure, and, from this point of view, an

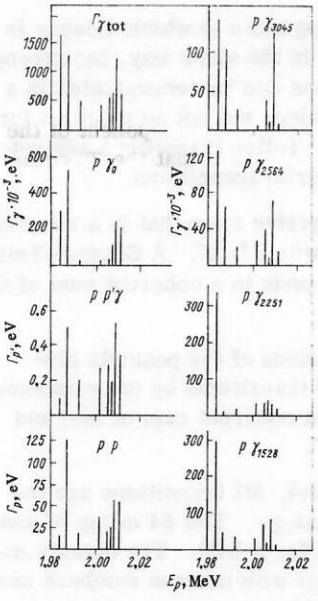

FIG. 19. Partial widths for the fine-structure components of the $p_{3/2}$ resonance in ^{55}Mn (Ref. 50).

analog state is a common doorway state for different reaction channels. The existing experimental data in no way contradict these assertions, though direct experimental proofs are virtually nonexistent. Correlation analysis, which is widely used to analyze reactions with neutrons, has not been applied until recently to the analysis of data on analogs.

The first applications of correlation analysis to analogs, made in Refs. 50 and 64, made it possible to obtain interesting data about the structure of the $T_<$ component of an analog. In Ref. 64, Kraft *et al.* measured the γ spectra from three components of the $p_{3/2}$ analog in ^{61}Cu. The Γ_p values for these resonances are unknown, so that one cannot make a correlation analysis of Γ_p and Γ_{γ_i}. Such an analysis would enable one to determine the partial γ transition for which the $T_>$ component is important. In other words, one could establish the transitions for which the $T_>$ component of the analog is a common doorway state. However, if it is assumed that the transition to some state is determined by the $T_>$ component of the analog, then, comparing the behavior of the intensities of the γ's on the transition from resonance to resonance, one could hope to obtain some definite results. The strongest transition in the decay of the $p_{3/2}$ analog in ^{61}Cu is the transition to the antianalog, which is the ground state. It is natural to assume that it is determined by the $T_>$ component of the analog.

To determine which component of the analog determines the transitions to other states, one can compare the intensities of γ transitions for these states with the transition to the ground state for different resonances.

Quantitatively, it is convenient to introduce a correlation coefficient ρ_j defined by

$$\rho_j = \frac{\sum_i (\Gamma^0_{\gamma_i} - \overline{\Gamma}^0_{\gamma_i})(\Gamma^j_{\gamma_i} - \overline{\Gamma}^j_{\gamma_i})}{\sqrt{\sum_i (\Gamma^0_{\gamma_i} - \overline{\Gamma}^0_{\gamma_i})^2 \sum_i (\Gamma^j_{\gamma_i} - \overline{\Gamma}^j_{\gamma_i})^2}} \left(1 - \frac{1}{2}\frac{\sum_i \varepsilon_i^2}{\sum_i (\Gamma_{\gamma_i} - \overline{\Gamma}_{\gamma_i})^2}\right). \quad (78)$$

Here, Γ^γ_0 and Γ^j_γ are the γ widths of transitions to the ground state (Γ^0_γ) and to the level j (Γ^j_γ); $\overline{\Gamma}^0_\gamma$ and $\overline{\Gamma}^j_\gamma$ are the means over the resonances; the summation over i is the summation over the resonances; ε is the error in Γ^j_γ. The usual form of the linear correlation coefficient contains only the first factor. The second factor was proposed by Lane[95] in order to take into account the errors in the measurements of Γ^j_γ.

If one observes a direct proportionality between the probability of transitions to the ground state and to level j for all resonances, then $\rho_j = +1$. If there is no correlation, $\rho_j = 0$.

If the transition to level j is determined by the $T_>$ component, one can expect $\rho_j \approx 1$. If the transition is determined by the $T_<$ component, at the first glance it appears that ρ_j must be equal to zero since the $T_<$ component contains a large collection of different configurations and the final result for the transition probability cannot be predicted. The experimental values of ρ_j for the correlations between transitions to the ground state and level j were found to be negative and have values near -1, i. e., one observes anticorrelations between transitions to the ground state, on the one hand, and transitions to the $p_{1/2}$ and $f_{5/2}$ states, on the other, and correlations between transitions to the $p_{1/2}$ and $f_{5/2}$ levels. This result can be understood as follows. Transitions to the $p_{1/2}$ and $f_{5/2}$ states are determined by the $T_<$ component of the analog, but this component does not have a complicated structure, so that the decay exhibits as simple a configuration as the analog. In other words, when analogs decay two doorway states are manifested: One is the $T_>$ component of the analog and the second is the $T_<$ component with as a simple a structure as the analog's.

In Ref. 50, a many-channel investigation was made of the fine structure of the $p_{3/2}$ analog in ^{55}Mn. Measurements were made of the elastic and inelastic scattering of protons with a high resolution, and also of the γ decay of eight components of the fine structure. The results are shown in Fig. 19, which represents the partial particle and γ widths for eight resonances of the fine structure. The results of the correlation analysis are given in Table 10.

As in the case of ^{61}Cu, anticorrelations are observed for transitions to excited levels with respect to transitions to the ground state. For transitions to excited states, stable correlations are noted. Peters, Bilpuch, and Mitchell,[50] like Kraft *et al.*,[64] conclude that there is a second doorway state apart from the analog in the fine-structure components.

TABLE 10. Results of correlation analysis.

Gamma widths	p, p	p, $p_1\gamma$	p, γ_0	p, γ_{1528}	p, γ_{2251}	p, γ_{2564}	p, γ_{3045}	p, γ_{tot}
p, p	1	0,79	0,73	—0.37	—0.47	0,02	0.18	0.26
p, p_1	—	1	0,45	—0.42	—0.61	0,00	0.25	0.16
p, γ_0	—	—	1	0.30	0.19	0.57	0.67	0.81
p, γ_{1528}	—	—	—	1	0.96	0,90	0.74	0.75
p, γ_{2251}	—	—	—	—	1	0.76	0.54	0.63
p, γ_{2564}	—	—	—	—	—	1	0.93	0.90
p, γ_{3045}	—	—	—	—	—	—	1	0.94
p, γ_{tot}	—	—	—	—	—	—	—	1

In Refs. 50 and 64 no assumptions are made about the physical nature of the second doorway state. To solve this very interesting problem, it is evidently necessary to bear in mind that, in the theory of analog resonances, configurations of the type of antianalog states or configuration states are regarded as one of the main sources of mixing. It is possible that a configuration this type, playing the role of a hallway state, is manifested in the γ decay of the fine-structure components. Detailed study of this question is very interesting and important for the study of the effects of mixing of $T_>$ and $T_<$ states in the theory of analog resonances.

9. $E1$ TRANSITIONS FROM AN ANALOG AND FIRST-FORBIDDEN β DECAY

If an $M1$ transition from an isobaric analog state is analogous to a Gamow–Teller analog β transition, a first-forbidden β decay is analogous to an $E1$ transition with $\Delta T = 1$. However, whereas as in the first case the β-transition probability is determined by a single matrix element, six matrix elements can contribute to the probability of a first-forbidden β transition: $\int \lambda_5$, $\int \boldsymbol{\alpha}$, $\int i\mathbf{r}$, $\int \boldsymbol{\sigma}\mathbf{r}$, $\int \boldsymbol{\sigma}\times\mathbf{r}$ and $\int iB_{ij}$.

The probability of an $E1$ γ decay is characterized by $B(E1)$, which is equal to

$$B(E1) = \sum |\langle f | \mathcal{M}(E1) | i \rangle|^2, \tag{79}$$

where the value of the operator $\mathcal{M}$ is determined by

$$\mathcal{M}(E1) = (e_p - e_n) r Y^1_\mu. \tag{80}$$

Comparing this expression with the form of the matrix element $\int i\mathbf{r}$ of β decay, we can see that they are similar, so that

$$\left| \int \mathrm{ir} \right| = [2(T+1)(4\pi/3)]^{1/2} |M^\gamma_{JSA}|. \tag{81}$$

(if T is a good quantum number).

It is a very difficult problem to determine individual matrix elements in a first-forbidden β decay. They can be found, and then only under definite conditions, by combining the results of measurements of β–γ directional correlations, the circularly polarized β–γ correlation, and the profile of the β spectrum for known spins of the nuclear levels participating in the decay.

On the basis of the similarity between the matrix elements $\int i\mathbf{r}^6$ and $|M^\gamma_{JSA}|$, Fujita[96] suggested that one could obtain information about first-forbidden β decay by studying $E1$ γ transitions from an isobaric analog state. This information is of interest for the following reason.

Comparison of the probabilities of Gamow–Teller β transitions with the one-particle estimate shows that they are hindered by one or two orders of magnitude. This hindrance was explained in Refs. 94 and 97 by Fujita and Ikeda, who introduced the concept of the strength function for Gamow–Teller β transitions.

These transitions are analyzed by analogy with the analysis of T-forbidden Fermi β transitions. The small value of the matrix elements of the latter is explained by the existence of an analog state to which β decay is energetically impossible. In the same way, the strength of Gamow–Teller transitions can be concentrated in a definite region near the analog, but not so much as for the analog because Gamow–Teller transitions are not forbidden so strongly as Fermi transitions.

An analog state is a collective state that is a coherent superposition of $\bar{n}p$ states with $J^\pi = 0^+$. A Gamow–Teller giant resonance corresponds to a coherent sum of $\bar{n}p$ states with $J^\pi = 1^+$.

In Ref. 98, a study was made of the possible hindrance of first-forbidden β transitions by the existence of an $E1$ giant resonance—a coherent sum of $(\bar{n}n)$ and $(\bar{p}p)$ excitations with $J^\pi = 1^-$.

In the region of light nuclei, $M1$ transitions are the principal decay mode of analogs. The $E1$ decay of analogs begins to predominate for $A \gtrsim 90$. The objects investigated are usually nuclei with nucleon numbers near $N = 50$, 82, 126 and $Z = 82$, whose states can be described as one-particle or one-hole to a good approximation.

For the excitation of analog resonances one uses $p\gamma$, γp, and $ee'p$ reactions, from the analysis of which one can obtain information about the strengths of the $E1$ transitions from the analog. For the radiative capture of a proton into an analog level the γ width is determined from $\sigma(p\gamma)$, the reaction cross section. In the case of the γp process, the photoabsorption cross section is almost equal to $\sigma(\gamma p)$ since neutron emission from the isobaric analog state is forbidden by isospin. The $ee'p$ reaction under definite conditions, namely, when the momentum transfer is equal to the momentum in the photoreaction, is analogous to the photoreaction. Thus, the radiative width of the isobaric analog state can be determined in the $ee'p$ process in the same way as in the γp process. Recently, the $ee'p$ reaction has been used to study analog states since it is more convenient from the point of view of control, determination of the dose of the incident beam, etc., than the γp reaction. The position of isobaric analog states is determined from the excitation function of the corresponding reaction; a criterion of correct identification is provided by the energy position and the resonance nature.

In the considered region of nuclei, it is very difficult to determine widths of γ transitions from analog levels by analyzing reaction cross sections. This is because the analog levels are in an energy region near a giant dipole resonance. To obtain the correct strength of $E1$ transitions from an analog, it is necessary to take into account the interference effects between the isobaric analog state and the giant dipole resonance.

When $E1$ transitions from an isobaric analog state are studied, one compares the experimental γ widths of these transitions with the predictions made in different models and with the corresponding quantities obtained for the first-forbidden analog β transitions.

Let us consider the nuclei near ^{208}Pb. The ^{208}Pb nucleus is unique in being the only heavy nucleus in which

both the proton and the neutron shell are closed. The large energy gap between the last filled shell and the next shell (3–4 MeV) leads to the assumption of a closed shell configuration for the ground state of ^{208}Pb and simple particle-hole configurations for some of the low-lying states. It has been shown that the ground and low-lying states in ^{209}Pb are comparatively pure one-neutron states. Hence, their analogs in ^{209}Bi must be strongly manifested in the excitation function in the $p\gamma$ reaction, and the strengths of the transitions from these states to the one-proton final states of ^{209}Bi can be readily calculated from a simple one-particle shell model.

One can also point out a further feature of the isobaric analog states in the region of Pb. In this region, all the low-lying isobaric analog states lie appreciably higher (in excitation energy) than the principal part of the giant dipole resonance, in contrast to the region of small A.

A study was made of $E1$ transitions from the isobaric analog states in ^{209}Bi in Refs. 99 and 100. In the former, the isobaric analog states in ^{209}Bi were obtained in the reaction ^{208}Pb$(p\gamma)$ with $E_p = 8.8–18.0$ MeV. The profile of the observed isobaric analog states was asymmetric because of interference with the giant dipole resonance. To obtain the cross section due to the isobaric analog states, the interference was analyzed in the framework of S-matrix theory with allowance for the amplitudes in the entrance and exit channels for the isobaric analog states and the giant dipole resonance. The result of this analysis is ambiguous, and depends on the choice of the phase difference $\Delta\varphi$ (~ 0 or $\sim 90°$) between the isobaric analog states and the giant dipole resonance. For $\Delta\varphi \sim 0$, the radiative widths Γ_γ are significantly hindered compared with the one-particle widths; for $\Delta\varphi \approx 90°$, they are enhanced. One can choose between these two possible values for $\Delta\varphi$ by taking into account: 1) the scheme of the $p\gamma$ reactions in the region of medium A, where the isobaric analog states are found near or below the giant dipole resonance. Measurements in this region indicate that $\Delta\varphi \approx 0°$; 2) the theoretical calculations made by Ejiri[101] for $E1$ transitions from isobaric analog states for $A \approx 140$, which indicate a hindrance of the transition strength due to collective effects; 3) comparison of the measured $E1$ amplitude with the experimental estimates of the intensities of analog β decays in the region of Pb (Ref. 102). These factors force one to take $\Delta\varphi \approx 0°$.

In Ref. 100, Shoda *et al.* investigated $E1$ transitions from isobaric analog states in the nuclei ^{207}Pb and ^{209}Bi using the $ee'p$ reaction. In ^{209}Bi, they studied $E1$ transitions from the analogs to the ground and excited states of ^{209}Pb and the ground state of ^{209}Bi. In two cases out of three hindrance of the $E1$ transition was observed and the results were similar to those of Ref. 99. In some investigations, nuclei near the shell $N = 50$ have been investigated.

In Ref. 103, Hasinoff *et al.* studied the γ decay of analog states in ^{88}Sr. Calculations were made in Refs. 68 and 104, allowance being made for not only $1p–1h$ configurations but also $2p–2h$ excitations. Alongside the ordinary giant dipole resonance, a concentration of the electric dipole strength with $T_>$ was noted in the region of higher excitation energies. An $E1$ decay from several analog resonances was observed in the reaction ^{88}Sr$(p\gamma)^{89}$Y in Refs. 105–107. The transitions from the analogs were appreciably weaker than the one-particle transitions (by $\sim 10–22$ times). The resonances lie lower than the giant dipole resonance and are not part of the coherent strength of the $T_>$ states.

In Ref. 103, $E1$ transitions from resonances were studied for the nucleus ^{90}Zr. Calculations were made in Ref. 104 with shell wave functions and a realistic two-body interaction.

The third region of nuclei to which much attention is devoted in the study of $E1$ transitions from analogs is the region $A \sim 140$. The $E1$ strength in ^{142}Nd was investigated in Ref. 108. An appreciable part of the $E1$ strength is in the highest $T_>$ level of ^{142}Nd. In Ref. 109, experimental data on the $E1$ radiative widths of isobaric analog states in the nuclei ^{139}Ba, ^{141}Ce, ^{148}Pm, and also ^{207,209}Pb were considered from the point of view of different models. Fujita, Hirata, and Shoda[109] succeeded in explaining the experimental fact that $\langle i\mathbf{r}\rangle$ is approximately independent of the type of transition, i.e., it is approximately the same for transitions with and without spin flip. The energies and the radiative widths for an 1^- isobaric analog state were found in Ref. 110 in the $ee'p$ reaction in the nuclei ^{138}Ba, ^{140}Ce, ^{142}Nd, and ^{144}Sm.

The matrix elements of the β decay of ^{139}Ba, ^{141}Ce, and ^{148}Pm were studied by means of the $ee'p$ reaction by Shoda *et al.*[111] The experimental data were compared with a theory based on the shell model with jj coupling. Good agreement between the experiment and the theory was obtained for ^{141}Ce. The $E1$ transition from the analog and the first-forbidden β transition of ^{141}Ce were compared in Ref. 112. The strength of the $E1$ transition from the $f_{7/2}$ analog to the ground state of ^{141}Pr was measured in the reaction ^{140}Ce$(p\gamma)^{141}$Pr.

It was found that the transition is hindered relative to the one-particle estimate by about five times. Such hindrance was also found for medium nuclei,[106,113] and it can be explained by the existence of a collective state.

10. SOME QUESTIONS OF EXPERIMENTAL TECHNIQUE

We have seen that in investigation of the γ decay of analog resonances a number of problems arise that require knowledge of the reduced probabilities of transitions from the analog to the levels of the investigated nucleus. To obtain these values, it is necessary to identify the analog, study its decay scheme, determine the absolute widths of the transitions, and establish their multipolarities.

The analog resonance can be identified in a $p\gamma$ reaction as follows. Its approximate position is determined by the energy scheme of the reaction shown in Fig. 20. This shows the ground states of three nuclei: The first two are the target nucleus ${}_zA_N(T_0, T_0)$, and the compound nucleus ${}_{z+1}(A+1)_N$, in which the isospin and the projection of the ground state have the quantum numbers $(T_0 - 1/2,\ T_0 - 1/2)$. In the same nucleus there are analog resonances with quantum numbers $(T_0 + 1/2,\ T_0$

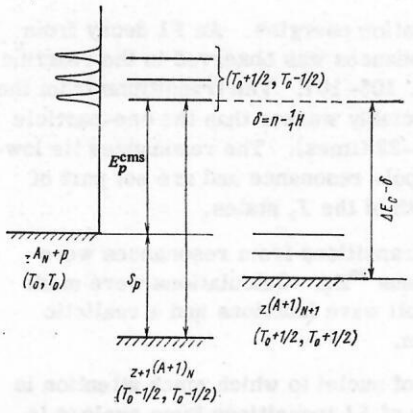

FIG. 20. Energy scheme of analog resonances in the $p\gamma$ reaction.

$-1/2$); these are analogs of low-lying states of the nucleus $_z(A+1)_{N+1}(T_0+1/2,\ T_0+1/2)$.

By definition, the analog states have the same nuclear interaction energy and differ by the Coulomb energy ΔE_c and the mass difference of the neutron and the hydrogen atom, so that

$$_{z+1}(A+1)^*_N - {}_z(A+1)_{N+1} = \Delta E_c - \delta.$$

It can be seen from Fig. 20 that the excitation energy of the analog resonance in the compound nucleus is $E^* = E_p^{cms} + S_p$, where E_p^{cms} is the energy of the protons in the center of mass system in which the analog is observed; S_p is the binding energy of the proton in the compound nucleus. Since the indeterminacy of ΔE_c is 40–50 keV, and sometimes 100 keV, the position of the analog in the investigated nucleus is predicted with the same degree of uncertainty. If the analog has not been noted in any other reactions in this nucleus, it is difficult to find it in a range of about 100 keV in the $p\gamma$ reaction, since other nonanalog resonances can be excited with comparable intensity in this reaction. As a rule, however, the position of the analog in the nuclei in which it is studied in the $p\gamma$ reaction can be established from the excitation function in the elastic scattering of protons, which is often measured at the same time as the excitation function of the $p\gamma$ reaction. The elastic scattering of protons is selective for analog resonances, and in this reaction they are excited with much greater probability than other resonances of the compound nucleus. Thus, the pp reaction enables one to establish the energy position of the analog to within 2–3 keV, and sometimes better.

It must however be pointed out that the analogs obtained in a given nucleus by the capture of a proton with large angular momentum l_p need not be observed in the pp reaction because of the large centrifugal barrier, especially if the energy of the protons corresponding to the analog is low.

Other reactions in which analogs can be reliably identified are the $(^3He, d)$ or (d, n) proton transfer reactions, whose cross sections for analogs are usually much larger than for neighboring nonanalog levels. In these reactions, the position of the analogs can be established to within 7–15 keV.

The excitation function in the $p\gamma$ reaction can be measured by means of an NaI(Tl) crystal. The discrimination threshold is set in such a way as to lower the background without loss of essential information about the decay of the analog. As a rule, the threshold is chosen in such a way that the energy of the γ's observed by the detector is approximately equal to half the analog energy: $E^*/2$. The decay scheme of the analog is not known in advance. Usually, there are transitions to the lower levels of the nucleus and transitions to highly excited states. The energy of the γ's corresponding to direct transitions from the analog to the lower levels is greater than $E^*/2$. Thus, these γ's are observed by the detector, whereas the γ's of the background are cut off. Direct transitions to the high levels of the nucleus may also be cut off (if $E_\gamma < E^*/2$), but one will then detect γ's resulting from transitions from these high levels downward.

To investigate the decay of analogs in the $p\gamma$ reaction, it is necessary to choose the target thickness appropriately. The choice of the thickness is governed by the distance between the levels of the nucleus in the investigated excitation region. The thickness of the target must be such that the energy loss of protons of the given energy in it is appreciably less than the distance between neighboring levels. On the other hand, there is a lower limit for the target thickness. It is determined by the resolution of the system which accelerates the protons. If the resolution is ΔE keV, the target thickness must naturally be of the same order. For nuclei with $A \sim 60$ and $E_p \sim 1.5$–2.5 MeV, and in the region of excitation energies of 6–7 MeV, it is convenient to use a target about 10–20 $\mu g/cm^2$ thick when the proton beam has a resolution of 1–2 keV.

The excitation function measured in the reaction $^{60}Ni(p\gamma)^{61}Cu$ with a target 10 $\mu g/cm^2$ thick is shown in Fig. 21 (Ref. 51). The peaks in Fig. 21 correspond to the split $p_{3/2}$ analog in ^{61}Cu. The numbers next to the peaks are the proton energies corresponding to the fine-structure components of the analog. The background visible

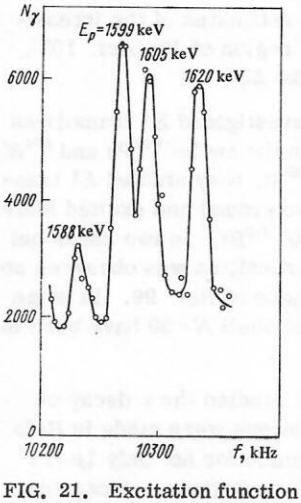

FIG. 21. Excitation function in the reaction $^{60}Ni(p\gamma)^{61}Cu$ (Ref. 51). E_p is the proton energy corresponding to the fine-structure components of the analog.

in Fig. 21 is mainly due to γ's produced in reactions of the protons with impurities of light elements contained in the target or the Faraday cup. The most characteristic line, which is almost always present in the γ spectra, is the ^{16}O line with energy 6129 keV obtained from the reaction $^{19}F(p, \alpha)^{16}O$.

After the excitation function has been measured and the analog identified, one turns to the construction of its decay scheme. The γ spectra are measured by means of large Ge(Li) detectors. The energy calibration in the region up to 3 MeV does not present difficulties. At higher energies, a convenient reference is the impurity line at 6129 keV mentioned above. The most energetic line in the investigated spectrum is due to the γ transition from the analog to the ground state of the nucleus. Usually, this transition is rather pronounced. Since the energy of the protons corresponding to excitation of the analog is known, so is the energy of this γ transition. Using the energies of the photopeak and of the single and double escape peaks for each known transition, one can construct a calibrated curve in the whole energy range.

When γ spectra are identified, one must separate out the direct γ transitions from the analog from other γ transitions. The direct transitions from the analog can be readily distinguished from the other γ's which are due to decay of levels if the analog resonance has a number of fine-structure components. An example of such a resonance is shown in Fig. 21. In this case, the direct γ transitions for the different components of the analog are shifted in energy by amounts ΔE corresponding to the energy distances between the components, whereas the decay γ's are unchanged in all the spectra. The lines observed in the spectrum are arranged in the decay scheme of the analog in the usual manner with allowance for the energy balance and the balance of the intensities.

The absolute values of the radiative widths Γ_γ are usually determined by the "thick-target" method. In this method, one measures the yield of γ's at the resonance energy, and this in the case of a thick target corresponds to a step in the excitation function of the $p\gamma$ reaction. The target thickness is such that the energy loss of the protons in the target at the given E_p appreciably exceeds the width of the resonance. The use of thin targets to measure the absolute widths is assumed to be a less reliable method, since these targets undergo significant changes during proton bombardment.[114]

For a thick target, the observed yield of γ's is related to the integrated reaction cross section by

$$\int \sigma\, dE = ASY/QN, \tag{82}$$

where A is the mass number of the target; S is the stopping power of the material of the target measured in eV per g/cm^2; Q is the number of protons incident on the target; N is Avogadro's number; Y is the yield of γ's of given energy; and σ is the cross section determined by the Breit–Wigner dispersion formula for the $p\gamma$ reaction:

$$\sigma = g\pi\lambda^2\Gamma_p\Gamma_\gamma/[(E-E_R)^2+{}^1/_4(\Gamma_p+\Gamma_\gamma)^2]. \tag{83}$$

Here, $g=(2J_R+1)/[(2j+1)(2J_M+1)]$ (J_R is the spin of the resonance; j is the spin of the incident particle; J_M is the spin of the target nucleus); λ is the wavelength of incident proton; E_R is the proton energy at resonance; Γ_p and Γ_γ are the proton and the γ width, respectively.

Integrating the cross section over the energy, we obtain

$$\int \sigma\, dE = 2g\pi^2\lambda^2\Gamma_p\Gamma_\gamma/(\Gamma_p+\Gamma_\gamma). \tag{84}$$

If $\Gamma_p \gg \Gamma_\gamma$, then

$$\int \sigma\, dE = 2g\pi^2\lambda^2\Gamma_\gamma. \tag{85}$$

Using this equation, we can determine the absolute γ width from the experimental value of $\int\sigma dE$ for the given resonance.

The determination of $\int\sigma dE$ requires knowledge of the isotopic composition of the target, the stopping power of the material of the target, the proton charge incident on the target, and the efficiency of the γ detector.

As we have already mentioned, the excitation functions are measured with NaI(Tl) scintillation detectors, whose absolute efficiencies can be assumed known. To determine the partial γ widths it is necessary to use γ spectra measured by Ge(Li) detectors with known relative efficiency. One first calibrates the Ge(Li) detector absolutely for a given energy of the γ's.

The determination of the $B(M(E), \lambda)$ values requires data on the multipolarities of the γ transitions. These data can be obtained from measurements of the angular distribution of the γ's relative to the direction of the incident protons. The correlation function $W(\theta)$ is a series in Legendre polynomials whose coefficients are obtained by analyzing the measured angular distribution by the method of least squares:

$$W(\theta) = \sum_k a_k P_k(\cos\theta). \tag{86}$$

If the reaction proceeds through an isolated resonance level, the parity of the radiation is strictly determined. Therefore, k is even and in the angular distribution there is symmetry of the backward and forward directions, i.e., the angular distribution curve is symmetric about $\theta = 90°$.

Because multipoles of order higher than $L=2$ seldom arise, the series (86) seldom contains values greater than $k=4$. Most often, one encounters an $M1+E2$ mixture of multipoles. In this case,

$$W(\theta) = a_0 + a_2 P_2(\cos\theta) + a_4 P_4(\cos\theta).$$

The coefficients a_0, a_2, and a_4 are functions of the spins of the target nucleus, of the resonance level of the compound nucleus, and of the final state; functions of the orbital angular momenta of the incident proton and the emitted γ; and, finally, functions of the mixing parameters δ and δ_1. The former, δ, is the amplitude of the ratio of the mixing of the multipoles of the emitted gammas: $\delta = \langle L+1\rangle/\langle L\rangle$. The latter, δ_1, is the amplitude of the ratio of the mixture of the orbital angular

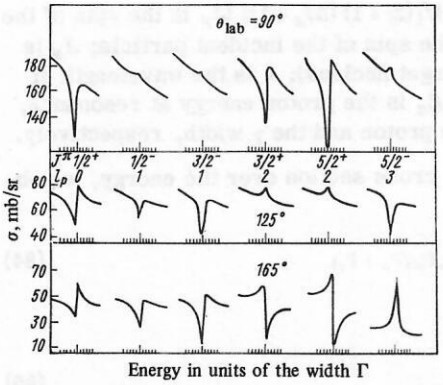

FIG. 22. Excitation function in the pp reaction for different J, l_p, and scattering angles.[115]

momenta of the incident protons: $\delta_1 = \langle l_1 + 2 \rangle / \langle l_1 \rangle$. The spin of the target nucleus is usually known. If the spin of the resonance or the final state is not determined, a measurement of the angular distribution can be used to determine it. For this, one must find the best possible sets of the parameters a_2/a_0 and a_4/a_0 for each allowed value of the spin and the values of the mixing parameters δ and δ_1. Then, if these sets for all values of the spin except one lie outside the allowed region of the measured values of the parameters, that spin is established. However, cases that can be distinguished as readily as this in such a procedure are not encountered all that often. Usually, there are a fair number of arbitrary parameters that enable one to satisfy several possible values of the spin.

As a rule, in study of the γ decay of analogs in the $p\gamma$ reaction the spin of the resonance is known from proton elastic scattering. The form of the pp scattering cross section depends strongly on the transferred angular momentum l_p and for one and the same value of this quantity the profile is different for different scattering angles. Studying the excitation function of the pp reaction at different angles, one can determine l_p uniquely. This is illustrated in Fig. 22 (Ref. 115). It can be seen that there is a possibility of determining not only l_p but also the spin J^π of the resonance. The profile of the reaction cross sections does not depend so strongly on the spin as on l_p. Therefore, in the most difficult cases polarization measurements are required for a unique determination of J^π.

In the cases when the spin of the resonance and the spin of the final state to which the γ decay takes place are known, δ can be readily determined from the angular distribution of the γ's. For $J^\pi_{res} = 3/2$ one can frequently restrict oneself to measuring the spectra at two angles: 0 and 90°. Knowing δ, one can determine the partial probabilities for each multipolarity.

An exception occurs in the cases when the spin of the resonance is 0 or 1/2, and in these cases the γ's from transitions from the resonance to any levels of the nucleus are isotropic.

Note also that for δ one always obtains two values, from which one must be chosen. For the choice, one invokes theoretical estimates of the probabilities of the corresponding transitions or a comparison with the probabilities of pure transitions of the given multipolarity in the investigated region.

We have shown above how interesting is the information obtained from the γ decay of the fine-structure components of analog resonances. To obtain this information one requires a high resolution to measure the energy of the protons in the pp and $p\gamma$ reactions. The first experiments with very high resolution (about 250 eV) were described in Refs. 116 and 117, although the existence of fine structure had been noted earlier.[118] In Refs. 116 and 117, high resolution was achieved by stabilization of the proton beam. The scheme for stabilizing the Van de Graaff proton beam—it was used in both investigations—is shown in Fig. 23 (Ref. 119).

The proton beam, after passing through the analyzing magnet, was split into two parts. The main part was focused onto the target, while the lesser part was deflected and directed through a system of slits into another, correcting magnet. The distance to this magnet was chosen to be fairly long so that the measurement of the position of the beam associated with the change in the energy of the protons significantly influenced the path of the particles in the magnet. After they had left the magnet, the protons were directed onto a wedge-shaped foil. At the energy chosen for the protons, the beam struck the middle of the wedge. If the proton energy was increased, the beam passed nearer the edge of the wedge; if it was decreased, nearer to the base of the wedge. Thus, the effect of the wedge was that even a slight change of the proton energy before the wedge resulted in a large change after it (a change in the energy in the beam by 100 eV led to a change by 50 keV after passage through the wedge). The protons were then observed by a detector, from which a pulse was transmitted to a system that developed a feedback signal. When the proton energy deviated from the chosen value, a voltage proportional to the deviation appeared at the output of this system. Simultaneously, a signal was sent to the target, creating around it a decelerating or accelerating field depending on whether the proton energy had increased or decreased. With the use of this system, the energy spread in the proton beam was 200–300 eV.

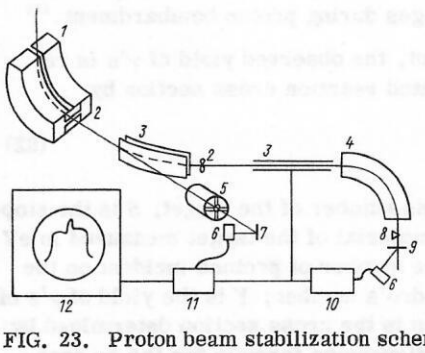

FIG. 23. Proton beam stabilization scheme. 1) Deflecting magnet; 2) slits; 3) deflecting plates; 4) correcting magnet; 5) quadrupole lenses; 6) proton detectors; 7) target; 8) wedge; 9) scattering foil; 10) "equalizer"; 11) gate circuit; 12) multichannel analyzer (Ref. 119).

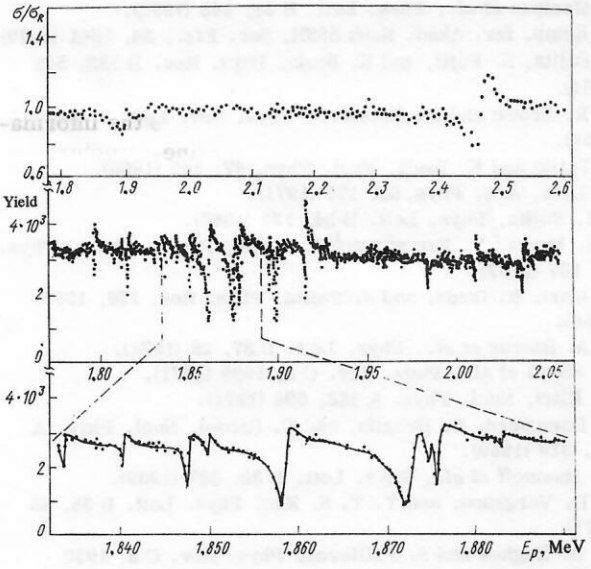

FIG. 24. Excitation function in the reaction ^{40}Ar(pp): σ/σ_R is the ratio of the measured cross section to the Rutherford cross section.[116]

Figure 24 shows the excitation functions of the ^{40}Ar(pp)^{40}Ar reaction measured with ordinary resolution (upper curve) and with resolution 250 eV. Below, a section of the spectrum of width of about 60 keV is shown in the neighborhood of the analog resonance. In the upper curve one can see two anomalies in the yield of protons at energies $E_p = 1.87$ and 2.45 MeV. These anomalies correspond to the excitation of resonances in ^{41}K, which are analogs of the two excited states of ^{41}Ar. In the lower curves one can see that each analog resonance consists of many narrow resonances, which have been called the fine structure.[116,117]

Simultaneous investigation of the pp and $p\gamma$ reactions for a split analog enables one to draw conclusions about the relative contributions of the $T_>$ and $T_<$ components to the analog resonance. Therefore, experiments with high resolution are very promising.

[1]S. S. Hanna, In: Isospin in Nucl. Phys. (ed. D. Wilkinson), North-Holland, Amsterdam (1969), p. 593.
[2]Yu. V. Naumov and O. E. Kraft, Izospin v Yadernoĭ Fizike, (Isospin in Nuclear Physics), Nauka, Moscow–Leningrad (1972).
[3]Yu. V. Naumov, Izv. Akad. Nauk SSSR, Ser. Fiz., **38**, 1617 (1974).
[4]J. Cerny, Ann. Rev. Nucl. Sci. **18**, 27 (1968).
[5]T. K. Koh *et al.*, Phys. Rev. C **7**, 50 (1973).
[6]S. Maripuu and B. H. Eildenthal, Phys. Lett. B **38**, 464 (1972).
[7]J. Szücs *et al.*, Nucl. Phys. A **212**, 293 (1973).
[8]J. C. Hardy, H. Brunnader, and J. Cerny, Phys. Rev. C **1**, 561 (1970).
[9]K. A. Snover *et al.*, Phys. Rev. Lett. **22**, 239 (1969).
[10]N. A. Jelley, Phys. Lett. B **40**, 200 (1972).
[11]E. G. Adelberger and D. P. Balamuth, Phys. Rev. Lett. **27**, 1597 (1971).
[12]J. Vernotte *et al.*, Phys. Rev. C **8**, 178 (1973).
[13]E. G. Adelberger, Phys. Rev. Lett. **29**, 883 (1972).
[14]J. J. Simpson, W. R. Dixon, and R. S. Storey, Phys. Rev. Lett. **29**, 1472 (1972).
[15]G. W. Hoffmann *et al.*, Phys. Rev. Lett. **28**, 41 (1972).
[16]C. J. Batty *et al.*, Phys. Lett. **19**, 33 (1965).
[17]B. Ya. Guzhovskiĭ *et al.*, Izv. Akad. Nauk SSSR, Ser. Fiz. **31**, 1679 (1967).
[18]H. M. Kuan *et al.*, Phys. Lett. B. **25**, 217 (1967).
[19]G. L. Latshaw, Bull. Amer. Phys. Soc. **13**, 883 (1968).
[20]D. W. Heikkinen *et al.*, Bull. Amer. Phys. Soc. **13**, 884 (1968).
[21]S. Gales *et al.*, Compt. Rend. Acad. Sci. **271**, 970 (1970).
[22]S. J. Skorka, J. Hertel, and T. W. Retz-Schmidt, Nucl. Data A **2**, No. 5, 347 (1966).
[23]D. F. H. Start *et al.*, Nucl. Phys. A **206**, 207 (1973).
[24]C. Gaarde *et al.*, Nucl. Phys. A **143**, 497 (1970).
[25]S. Maripuu, Nucl. Phys. A **153**, 183 (1970).
[26]H. V. Klapdor, K. Buchholz, and F. Kästner, Z. Phys. **238**, 11 (1970).
[27]E. Osnes and C. S. Warke, Nucl. Phys. A **154**, 331 (1970).
[28]J. Fujita and K. Ikeda, Progr. Theoret. Phys. **35**, 622 (1966).
[29]V. P. Aleshin, Candidate's Dissertation [in Russian], Kiev (1972).
[30]J. H. Aitken *et al.*, Phys. Lett. B **30**, 473 (1969).
[31]A. Arima *et al.*, Nucl. Phys. A **170**, 273 (1971).
[32]M. R. Gunye and C. S. Warke, Phys. Rev. C **5**, 1860 (1972).
[33]K. Ananthanarayanan, Nucl. Phys. A **159**, 45 (1970).
[34]R. C. Bearse *et al.*, Phys. Rev. C **1**, 608 (1970).
[35]N. Shikazono and Y. Kawarasaki, Nucl. Phys. A **188**, 461 (1972).
[36]G. C. Morrison *et al.*, Phys. Rev. **174**, 1366 (1968).
[37]A. D. W. Jones *et al.*, Phys. Rev. C **1**, 1000 (1970).
[38]P. W. M. Glaudemans, P. M. Endt, and A. E. L. Dieperink, Ann. Phys. **63**, 134 (1971).
[39]P. W. M. Glaudemans *et al.*, Phys. Lett. B **28**, 645 (1969).
[40]F. Ajzenberg-Selove, Nucl. Phys. A **190**, 1 (1972).
[41]J. D. Pearson and R. H. Spear, Nucl. Phys. **54**, 434 (1969).
[42]N. Shikazono and Y. Kawarasaki, Phys. Lett. B **32**, 473 (1970).
[43]R. W. Kavanagh, Nucl. Phys. A **129**, 172 (1969).
[44]D. H. Youngblood *et al.*, Phys. Rev. **164**, 1370 (1967).
[45]E. F. Kennedy, D. H. Youngblood, and A. E. Blaugrund, Phys. Rev. **158**, 897 (1967).
[46]M. A. Eswaran, M. Ismail, and N. L. Ragoowansi, Phys. Rev. C **5**, 1270 (1972).
[47]D. Evers and W. Stocker, Phys. Lett. B **33**, 559 (1970).
[48]G. I. Harris and J. J. Perrizo, Phys. Rev. C **2**, 1347 (1970).
[49]C. Gaarde *et al.*, Nucl. Phys. **184**, 241 (1972).
[50]W. C. Peters, E. G. Bilpuch, and G. E. Mitchell, Nucl. Phys. A **207**, 626 (1973).
[51]O. E. Kraft, Yu. V. Naumov, and I. V. Sizov, Soobshcheniya (Communications), JINR, R15-8201 (1974); Yad. Fiz. **20**, 1081 (1974) [Sov. J. Nucl. Phys. **20**, 567 (1975)].
[52]O. E. Kraft, Yu. V. Naumov, and I. V. Sizov, Soobshcheniya (Communications), JINR, R15-8202 (1974); Yad. Fiz. **21**, 919 (1975) [Sov. J. Nucl. Phys. **21**, 472 (1975)].
[53]O. E. Kraft *et al.*, Programma i Tezisy Dokladov XXV Soveshchaniya po Yadernoĭ Spektroskopii i Strukture Atomnogo Yadra (Program and Abstracts of Papers at 25th Conference on Nuclear Spectroscopy and Nuclear Structure), Nauka, Leningrad (1975); Izv. Akad. Nauk SSSR, Ser. Fiz., **39**, 1268 (1975).
[54]P. M. Endt and C. Van der Leun, Nucl. Phys. **214**, 1 (1973).
[55]G. Bergdolt and A. M. Bergdolt, Nucl. Phys. A **211**, 486 (1973).
[56]M. Schrader, K. Buchholz, and H. V. Klapdor, Nucl. Phys. A **213**, 173 (1973).
[57]N. H. Prochnow *et al.*, Nucl. Phys. A **199**, 571 (1973).
[58]D. J. Martin *et al.*, Nucl. Phys. A **187**, 337 (1972).
[59]J. R. Leslie, D. J. Martin, and W. McLatchie, Phys. Lett. B **36**, 76 (1971).
[60]W. C. Peters, E. G. Bilpuch, and G. E. Mitchell, Phys. Lett. B **42**, 422 (1972).

[61]S. Maripuu and G. A. Hokken, Nucl. Phys. A **141**, 481 (1970).
[62]L. W. Fagg *et al.*, Phys. Rev. **171**, 1250 (1968).
[63]B. Lawergren, I. J. Taylor, and M. Nessin, Phys. Rev. C **1**, 994 (1970).
[64]O. E. Kraft *et al.*, Soobshcheniya (Communications), JINR R15-7072 (1973).
[65]K. Ikeda, Progr. Theor. Phys. **31**, 434 (1964).
[66]Yu. V. Gaponov and Yu. S. Lyutostanskiĭ, Yad. Fiz. **19**, 62 (1974) [Sov. J. Nucl. Phys. **19**, 33 (1974)].
[67]J. D. Vergados and T. T. S. Kuo, Nucl. Phys. A **168**, 225 (1971).
[68]B. Goulard, T. A. Hughes, and S. Fallieros, Phys. Rev. **176**, 1345 (1968).
[69]A. Mekjian and W. M. MacDonald, Nucl. Phys. A **121**, 385 (1968).
[70]A. M. Lane and J. M. Soper, Nucl. Phys. **37**, 663 (1962).
[71]D. Robson, Phys. Rev. B **137**, 535 (1965).
[72]S. Maripuu, Nucl. Phys. A **123**, 357 (1969).
[73]C. Van der Leun, D. M. Sheppard, and P. M. Endt, Nucl. Phys. A **100**, 316, 333 (1967).
[74]F. W. Prosser and G. I. Harris, Phys. Rev. C **4**, 1611 (1971).
[75]S. Maripuu, Nucl. Phys. A **151**, 465.
[76]E. G. Kopanets *et al.*, Izv. Akad. Nauk SSSR, Ser. Fiz., **35**, 1676 (1971).
[77]K. Goode, K. Kemp, and Yu. Naumov, Izv. Akad. Nauk SSSR, Ser. Fiz., **35**, 687 (1971).
[78]G. B. Vingiani, G. Chilosi, and C. Rossi-Alvarez, Phys. Lett. B **34**, 597 (1971).
[79]H. V. Klapdor, Nucl. Phys. A **134**, 419 (1969).
[80]H. G. Price, Nucl. Phys. A **165**, 593 (1971).
[81]M. Schrader, K. Buchholz, and H. V. Klapdor, Nucl. Phys. A **223**, 365 (1974).
[82]S. Maripuu, Nucl. Phys. A **149**, 593 (1970).
[83]H. V. Klapdor, Phys. Lett. B **35**, 405 (1971).
[84]I. Szentpétery and J. Szücs, Phys. Rev. Lett. **28**, 378 (1972).
[85]P. W. M. Glaudemans *et al.*, Nucl. Phys. A **102**, 593 (1967).
[86]R. K. Bansal, Phys. Rev. **153**, 1084 (1967).
[87]S. Maripuu, Phys. Lett. B **31**, 181 (1970).
[88]M. Hirata, Phys. Lett. B **32**, 656 (1970).
[89]T. T. S. Kuo and G. E. Brown, Nucl. Phys. A **114**, 241 (1968).
[90]S. Maripuu *et al.*, Phys. Lett. B **41**, 148 (1972).
[91]K. Kemp, Izv. Akad. Nauk SSSR, Ser. Fiz., **34**, 1641 (1970).
[92]J. Fujita, S. Fujii, and K. Ikeda, Phys. Rev. B **133**, 549 (1964).
[93]G. E. Brown and M. Bolsterli, Phys. Rev. Lett. **3**, 472 (1959).
[94]J. Fujita and K. Ikeda, Nucl. Phys. **67**, 145 (1965).
[95]A. Lane, Ann. Phys. **63**, 171 (1971).
[96]J. I. Fujita, Phys. Lett. B **24**, 123 (1967).
[97]J. I. Fujita, Y. Futami, and K. Ikeda, Progr. Theor. Phys. **38**, 107 (1967).
[98]H. Ejiri, K. Ikeda, and J. Fujita, Phys. Rev. **176**, 1277 (1968).
[99]K. A. Snover *et al.*, Phys. Lett. B **37**, 29 (1971).
[100]K. Shoda *et al.*, Phys. Rev. C **3**, 1999 (1971).
[101]H. Ejiri, Nucl. Phys. A **166**, 594 (1971).
[102]J. Damgaard, R. Broglia, and C. Riedel, Nucl. Phys. A **135**, 310 (1969).
[103]M. Hasinoff *et al.*, Phys. Lett. B **30**, 337 (1969).
[104]J. D. Vergados, and T. T. S. Kuo, Phys. Lett. B **35**, 93 (1971).
[105]T. A. Hughes and S. Fallieros, Phys. Rev. C **3**, 1950 (1971).
[106]S. M. Shafroth and G. J. F. Legge, Nucl. Phys. **107**, 181 (1968).
[107]P. Richard *et al.*, Phys. Lett. B **29**, 649 (1969).
[108]M. Hasinoff *et al.*, Nucl. Phys. A **195**, 78 (1972).
[109]J. I. Fujita, M. Hirata, and K. Shoda, Phys. Lett. B **33**, 550 (1970).
[110]K. Shoda *et al.*, Phys. Rev. C **4**, 1842 (1971).
[111]K. Shoda *et al.*, Phys. Rev. C **3**, 2006 (1971).
[112]H. Ejiri *et al.*, Nucl. Phys. A **128**, 388 (1969).
[113]J. L. Black and N. W. Tanner, Phys. Lett. **11**, 135 (1964).
[114]W. A. Fowler, C. C. Lauritsen and T. Lauritsen, Rev. Mod. Phys. **20**, 236 (1948).
[115]G. Vourvopoulos and J. D. Fox, Phys. Rev. **141**, 1180 (1966).
[116]G. A. Keyworth *et al.*, Phys. Lett. **20**, 281 (1966).
[117]G. A. Keyworth *et al.*, Nucl. Phys. **89**, 590 (1966).
[118]P. Richard *et al.*, Phys. Rev. Lett. **13**, 343 (1964).
[119]C. Gaarde, K. Kemp, and T. Nielsen, Nucl. Phys. A **118**, 641 (1968).

Translated by Julian B. Barbour